SYNCHROPHASOR BASED OUT-OF-STEP PROTECTION IN MODERN POWERGRID

by

Mahaboob Subhan Shaik

A thesis submitted to the faculty of
The University of North Carolina at Charlotte
in partial fulfillment of the requirements
for the degree of Master of Science in
Electrical Engineering

Charlotte

2017

Approved by:

_____
Dr. Sukumar Kamalasadan

_____
Dr. Badrul Chowdhury

_____
Dr. Valentina Cecchi

ABSTRACT

MAHABOOB SUBHAN SHAIK. Synchrophasor based out-of-step protection in modern power grid. (Under the direction of DR. SUKUMAR KAMALASADAN)

Power systems are continually subjected to wide range of disturbances and they must adjust to these changes and continue to operate satisfactorily. Small disturbance instability and transient instability are major threats to power system security which can cause out of step conditions. The majority of out-of-step protection systems installed throughout the world use local measurements that is voltage and current measurements at one end of transmission line. The disadvantage of this scheme is its inability to have knowledge about the other parts of the complex power network. Even though, the out-of-step tripping system is well designed and appropriately set, it still has a number of disadvantages in minimizing the effects of the disturbance. In this context, there is a need for Special Protection Schemes (SPS) which receive the data from more than one locations and process the decisions in wide area orientation. More recent technological advancements in microprocessor based relays, combined with GPS receivers for synchronization and accurate time stamping, are providing synchronized measurements called synchrophasors. In this thesis an out-of-step detection algorithm is proposed using system total transient energy based on the synchrophasor data obtained from phasor measurement units. Conventional out-of-step detection techniques are discussed and compared with proposed algorithm. The main advantage of the proposed method is that, it detects unstable swings faster than conventional methods. Further, a method for power system stabilizer (PSS) design is discussed and the performance of the performance of out-of-step protection with PSS is studied.

ACKNOWLEDGEMENTS

This thesis would not have been possible without the constant support and prayers of my wife, in-laws and my parents. They have supported me financially and helped me remain calm all throughout my thesis work.

I would like to express my utmost gratitude to my advisor, Dr. Sukumar Kamalasadan for his guidance and support during these two years of my master's studies. His patience and constant encouragement even when I was getting stuck in a problem have really helped me to go through this process and learn to think through the problem.

I sincerely thank the committee members Dr. Valentina Cecchi and Dr. Badrul Chowdhury for taking time to be on my committee and assess my work.

I am thankful to my colleagues and friends for their love and support.

Finally, I would like to thank all the professors and staff at the University of North Carolina At Charlotte who have contributed in enriching my knowledge.

TABLE OF CONTENTS

LIST OF TABLES

LIST OF FIGURES

CHAPTER 1 : INTRODUCTION

Electrical Energy is generated, transmitted and distributed by electric power systems, which are vital infrastructure whose contribution is critical to the economy of a nation. A power system is a multi-variable complex electrical network with a number of generators, load points, buses and interconnecting transmission lines. Today the power system is spread out geographically in large area and the equipment complexities are increased. Providing un-interrupted supply of electrical energy to meet the load demand is complex technical challenge. Consequently, the safe, secure and reliable operation of the power system has been a major concern throughout the years and it will get more complicated in years to come.

Study of power system security and reliability requires the proper assessment of system conditions and stability during small and severe disturbances. At steady state, a power system has characteristics of constant voltage, frequency and the power angle for all the synchronous generators. But the load on a power system is never a constant and hence the disturbances are always present. Moreover, due to deregulation of electrical energy markets, power systems are being operated closer to their maximum loadability. Expansion of transmission networks to face the future demand growth suffers hindrances due to the environmental constraints. As a result, power systems are more vulnerable to severe disturbances like faults and lightning strokes on critical pieces of equipment. In

the next section, a general overview of the power system and the issues associated with the power system operation are discussed.

1.1. Power System Structure

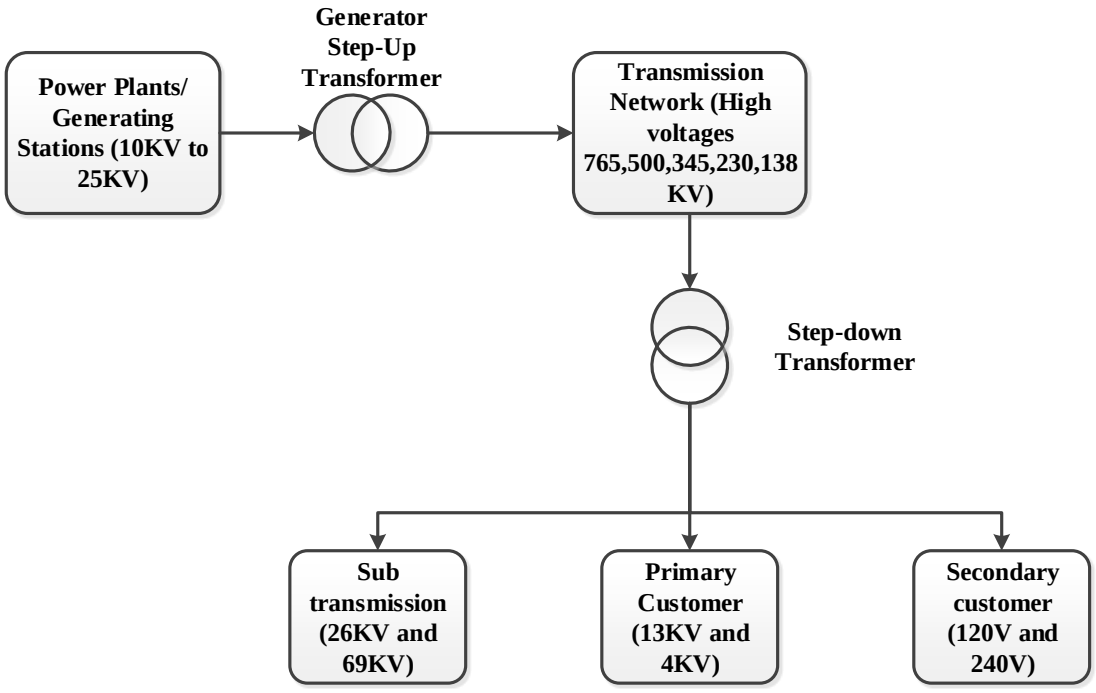

FIGURE 1.1: Structure of power system

As shown in the figure 1.1, a typical power system consists of generation units, transmission networks, distribution networks and loads. The electric power is generated by synchronous generators located in the power plants. The voltage of the generated power ranges from 10KV to 25KV. This voltage is then stepped up to higher voltages ranging from 138KV to 765KV using step-up transformers. The electric power is transmitted through the transmission network. At HV-MV substations, the voltages are

stepped down to lower levels. There the electric energy is distributed through primary and secondary distribution feeders depending on the customer energy needs. Industrial customers that require large amount of power are connected to primary feeders while domestic users are connected to secondary feeders.

The main aim of a power system is to generate the active power to meet the load demand at every instant of time. The active power transfer between two points is given by the equation

$$P_{12} = V_1 V_2 Y_{12} \sin(\delta_1 - \delta_2) \qquad (1.1)$$

Where V_1 and V_2 are the voltages at the two points, $(\delta_1 - \delta_2)$ is the phase angle difference, Y_{12} is the admittance between the two points.

From the equation (1.1), the voltage and the phase angle are the critical parameters on which the transfer of active power depends. Moreover, the loads in the power system are designed to operate at a particular frequency therefore maintaining the frequency is also an important aspect for the successful power system operation.

A disturbance in power system is the result of either change in the load demand or any abnormal condition such as short circuit or lightning strike. A synchronous generator produces active power at a constant frequency if the generated active power matches the load demand. Any change in the load makes the generator to accelerate or decelerate, and as a result the frequency may increase or decrease. Automatic generator control (AGC) schemes are used to adjust the generation to the load demand in the real time. These adjustments require larger time frames as the time constants of the turbine and governors

control are large. On the other hand, abnormal conditions such as faults are the severe disturbances and need to be identified and isolated as soon as possible for the secure operation of the power system. In the next section, the definition of power system reliability, stability and quality are discussed followed by the classification of power system operating states.

1.2. Reliability of Power System

A power system is said to be reliable when it is able to meet the power system load demand with an acceptable continuity of service at specified frequency and voltage quality. Reliability can be sub-divided into three components, namely, stability, quality and security.

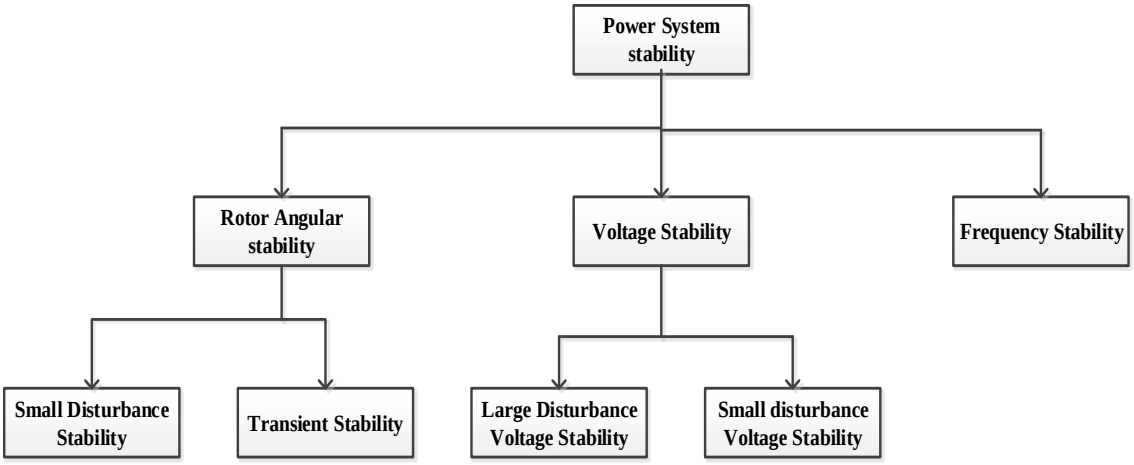

FIGURE 1.2: Classification of power system stability

Power System Stability is defined as the ability of an electrical power system, for given operating conditions, to regain its state of operating equilibrium after being subjected to a physical disturbance, with the system variables bounded, so that the entire

system remains intact and the service remains uninterrupted. Figure 1.2 shows the classification of power system stability based on the physical parameter that cause instability. In terms of duration of study, stability can also be classified as short term stability and long term stability. Rotor Angular stability refers to the ability of synchronous generator in an interconnected system to remain in synchronism after being subjected to disturbances. It depends on the machine's ability to maintain equilibrium between electromagnetic torque and mechanical torque of each synchronous machine in the system. When the disturbances are small, the study is referred as small signal stability. The component models can be linearized with respect to initial equilibrium point and system can be studied using Eigen value analysis.

Quality is the ability of the power system to maintain continuity of power with desired frequency and voltage. Security is defined as the ability of the system to cope with any abnormal disturbances such as short circuits or unwanted relay trips following loss of major components. The power system planners and the control center operators execute N-1 security level. Specifically, this function checks whether system has enough reserve margins in generation and transmission to withstand the loss of single equipment subject to equality and inequality constraints.

1.3. Power System Operating States

For the purpose of analyzing power system security and designing appropriate control and protection schemes, the system operating conditions can be classified into five different states, namely normal, emergency, alert, in extremis, and restorative state. Figure 1.3 depicts the five operating states along with possible state transitions.

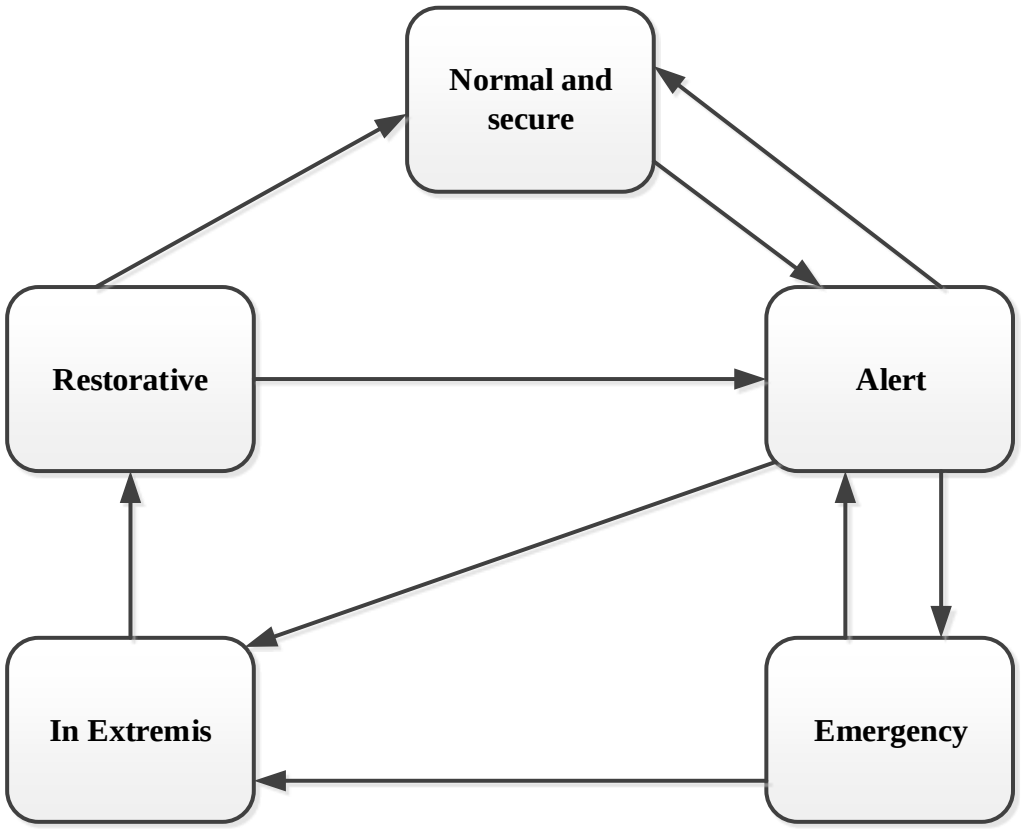

FIGURE 1.3: Operating states and transitions

Normal and secure state:

During the normal operating state, both equality and inequality constraints are satisfied. Equality constraints refer to the balance between the generated power and load demand while inequality constraints state the limits of some system variables such as currents, voltages and frequency. A system which is in the normal state can be secure or insecure. In secure case, the system is capable to withstand a single contingency without violating any equality and inequality constraints. In the insecure case, the system is unable to cope with contingencies.

Alert State:

In alert state, a power system is considered to be insecure. System operators must be alert and constantly keep monitoring equality and inequality constraints. However, in an event of any contingency, the lack of reserve margins may result in violation of some inequality constraints, inducing a transition of the system to emergency state. In that instance, some equipment may operate above their rated capabilities. If the severity of the disturbance is very high, the system may change its state directly to in extremis state.

Emergency State:

A power system enters into emergency state from alert state when a contingency occurs in the system. During emergency conditions, the voltage levels falls below the stability limits at various buses and the system components are overloaded, implying the inequality constraints are violated. The system can be restored back to the alert state by initiating effective control strategies such as fault clearing, fast valving, exciter control, generation tripping, and load shedding.

In extremis State:

When effective control measures are not applied to a system operating in emergency state, it will enter into in extremis state. Here both equality and inequality constraints are violated. In this state, the system may undergo cascading outages, which may result in the formation of disconnected islands while inducing major disruption in the service. Controlled system separation and load shedding are few actions that may be taken to prevent occurrence of major failures and ensure least disruption in service.

Restorative State:

This state indicates that control actions are being implemented, which aim at restoring the integrity of the power system. Depending on the existing operating conditions, the system may transit from this state to alert state or the normal state.

Fault identification and fault clearing during emergency state are performed by protection systems. A power system protection system is an auxiliary system which identifies the faults in the power system and isolates the faulted equipment as early as possible so that the remaining power system is intact. The protective devices receive the current and voltage data using measuring devices such as current transformers and voltage transformers. At the load centers, under voltage or over voltage relays are implemented to detect the abnormal conditions in voltages. At the generating plants, under or over frequency relays to detect the frequency variations. If the frequency measured is out of the operating limits the control measures such as load shedding or generator tripping will be implemented. All these schemes are local protection schemes but the stresses due to major disturbances are global in nature. So there is a need to design the global protective schemes which use the data from more locations and also act with wide area orientation. These schemes are also called as special protection schemes (SPS) or rapid action schemes (RAS). With the advent of phasor measurement units (PMUs), which provide highly accurate synchronized measurements, designing and implementation of special protection schemes became easier. Out-of-step protection scheme is one of the special protection schemes which got a wide attention in current research trends.

One of the major problems in power systems operation is the small signal oscillatory instability caused by insufficient damping. These oscillations are referred as power swings and are detected by the power swing blocking or out-of-step tripping function. In the literature, there are many conventional methods to detect the power swings and to differentiate between stable and unstable swings. But they are dependent on the network structure and the locally measured quantities because of which they suffer the inaccurate detection and operation. With special protection schemes using synchrophasors, the unstable swings can be detected fast and accurate.

1.4. Scope and Thesis Organization

The main objective of this thesis work is to develop a real time out-of-step detection algorithm for detection of unstable power swings using synchrophasor measurements in transmission systems. Furthermore, the behavior of out-of-step protection with power system stabilizer, is analyzed. The test system used for this purpose is Kundur two area system.

Chapter 2 is devoted to the literature review of power system protection and the theoretical background of distance protection and out of step protection on a transmission line. It contains the discussion about various types of distance relays and power swing detection methods. It also contains brief introduction about the real time transient stability assessment and its use in out of step detection.

Chapter 3 outlines design and hardware implementation of the conventional dual blinder based out of step protection and synchrophasor based out of step protection using the real time digital simulator (RTDS).

Chapter 4 is devoted to the transient energy function method to determine the stable and unstable power swings. The related mathematical formulation is discussed and the total energy of the system is computed using the Lyapunov function.

Chapter 5 deals with the synchrophasor based out of step protection integrated with power system stabilizer. It also contains the design methodology of power system stabilizer using Heffron-Phillips Model of the synchronous machine. Chapter 6 provides the conclusion of this research and possible future works.

CHAPTER 2 : LITERATURE REVIEW

In this chapter, basics of power system protection is discussed and the theoretical framework of distance protection and out of step protection is presented. Protective relays are used to detect abnormal system conditions that arise due to faults in the system by a continuous monitoring of various system variables such as voltages, power flows, power injections, and system frequency. Most protective relays are used to detect and disconnect an element of the power system that is functioning outside its normal range. Further, in section 2.3, different types of conventional out-of-step schemes are presented. In section 2.4, a brief overview of transient stability analysis methods and their feasibility for real time applications is discussed.

2.1. Overview of Power System Protection

A typical protective system consists of current and voltage transformers, protective relay, circuit breaker, control wiring or control schematic, communication system and co-ordination methodology with other relays, fuses and active controls. Protective relay is a piece of equipment whose function is to detect the abnormal system conditions or the defective apparatus and initiate the proper control response. The common control responses are trip commands to the circuit breaker, issuing alarms indications to the power system operator and in some cases closing commands to the circuit breaker.

In the old days, electromechanical relays are used in the protective systems. They consist of moving parts which operates on the electromagnetic forces due to the currents

and voltages. Because of the presence of moving mechanism, these relays are inaccurate in terms of both the operating quantity and the operating time. They are used for only one function. Then Solid state relays that use digital and analog circuitry came into the picture which can be used for multiple protection functions. But these relays cannot be re-programmed with changes in the network parameters and hence they are not flexible. With the advent of the microprocessor technology, the modern relays are the numerical in nature which consists of the analog to digital converters and the relay logic is implemented in the microprocessor. These are flexible and can be used for multiple protective functions.

The main characteristics of a protective relay are the speed, selectivity, sensitivity and the reliability. Speed is the ability of the relay to react quickly to the system abnormalities there by to minimize the system damage. Selectivity refers to the accurate identification of the abnormal zone and isolate so that the major portion of the system is intact. Sensitivity is the ability of the relay to detect the fault or abnormal condition very accurately. Faults are the rare events in the power system. A reliable protective relay should be operational for long time without acting, and in case of fault it should operate properly and appropriately.

There are different kinds of protection schemes implemented for different equipment in the power network. They are namely distance protection, differential protection, overcurrent, earth fault protection, over/under voltage protection, over/under frequency protection and out-of-step protection. When a fault occurs on a piece of equipment of a system, it is essential that it is detected by the associated protection relays and eliminated

via the opening of the circuit breakers under the relay supervision [1]. Following a fault, the electric power output of the generators varies while the mechanical input to the generators remains practically constant, inducing a change in the generator speed and thereby, a change in the frequency of the system. The effect of this frequency change depends on the fault duration and the clearing time [2]. The fault clearing time is the sum of the fault detection time, the signal transmission time and the time required by the circuit breakers to open.

Relays that are used in transmission line protection are of primary interest in this research work. These relays are used to clear the faults by controlling the opening and closing of circuit breakers when a fault occurs in the line. It is very essential that the relaying schemes employed is able to discriminate between normal loading conditions, swing conditions, out-of-step conditions and fault conditions [17], [18]. Tripping during stable power swings and faults due to improper functioning of relays may eventually lead to a total system collapse. Out-of-step relaying has been installed to perform tripping and blocking operations when out-of-step conditions are detected in the system. In the next sections, we discuss various types of distance relays, out-of-step schemes and their usage in performing blocking and tripping operations.

2.2. Distance Relays

Distance relays are the most effective and feasible protection scheme for transmission line protection compared to current actuated over current protection. The over current relays are principally depend on only one actuating quantity which is current. Parameters like line resistance, source impedance, type of fault, fault location affect the fault current

in the transmission line. This leads to unsatisfactory performance of the over current relay.

The basic principle of distance protection is to measure the impedance of the line using the current and voltage measurements available at relaying point and compare it with the predetermined impedance reach. If measured impedance is less than the reach impedance the relay senses a fault and give the trip command appropriately. Careful selection of the reach settings and tripping times for various zones of measurement enables correct co-ordination between distance relays on a power system. Basic distance protection comprise instantaneous directional zone 1 and one or more time delayed zones. The performance of a distance protection relay is based on the reach sensitivity and the operating time.

In current use, popular distance relays are impedance relays, reactance relays, mho relays. The characteristic of a distance relay is well understood by plotting positive sequence impedance (Z1) on the R-X plane. The relay operation takes place when the measured impedance falls within the relay characteristics, which depend on the parameter to which the distance relay is set to respond to. It is circular for impedance relays and horizontal for reactance relays. The flowing sub sections describe the operation principles of the three types of distance relays.

2.2.1. Impedance Relays:

In an impedance relay the operating torque is produced by current and restraining torque is produced by voltage. In other words, an impedance relay is voltage restrained over current relay. The torque equation is:

$$T = K_1 I^2 - K_2 V^2 - K_3 \qquad (2.1)$$

Where I and V are rms magnitudes of current and voltage and K3 is control spring effect. We let K3 zero and at the verge of operating, net torque is zero.

$$\frac{V}{I} = Z = \sqrt{\frac{K_1}{K_2}} = constant \qquad (2.2)$$

Figure 2.2 depicts the tripping characteristic of a simple impedance relay in RX plane. By default impedance is not directional but can be made directional by including directional element.

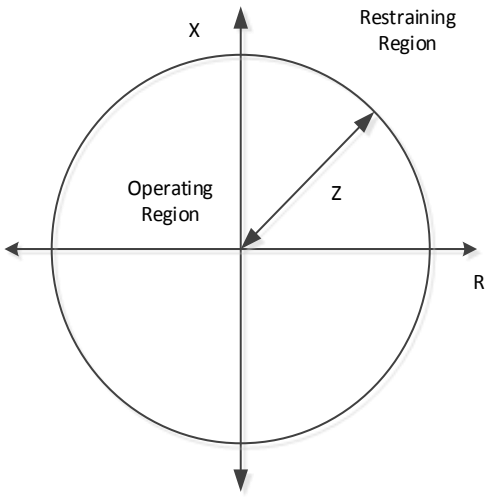

FIGURE 2.1: Impedance relay Characteristics

2.2.2. Mho Relays:

In Mho relay, the operating torque is produced by the volt-amperes element and the restraining torque is produced by voltage element. In other words, mho relay is voltage

controlled directional relay. Figure 2.3 shows characteristics of mho relay. The torque equation is

$$T = K_1 VI cos(\theta - \tau) - K_2 V^2 - K_3 \qquad (2.3)$$

Where I and V are rms magnitudes of current and voltage, θ is angle between I and V and τ is the angle of maximum torque.

At the verge of operating,

$$\frac{V}{I} = Z = \frac{K_1}{K_2}\cos(\theta - \tau) \qquad (2.4)$$

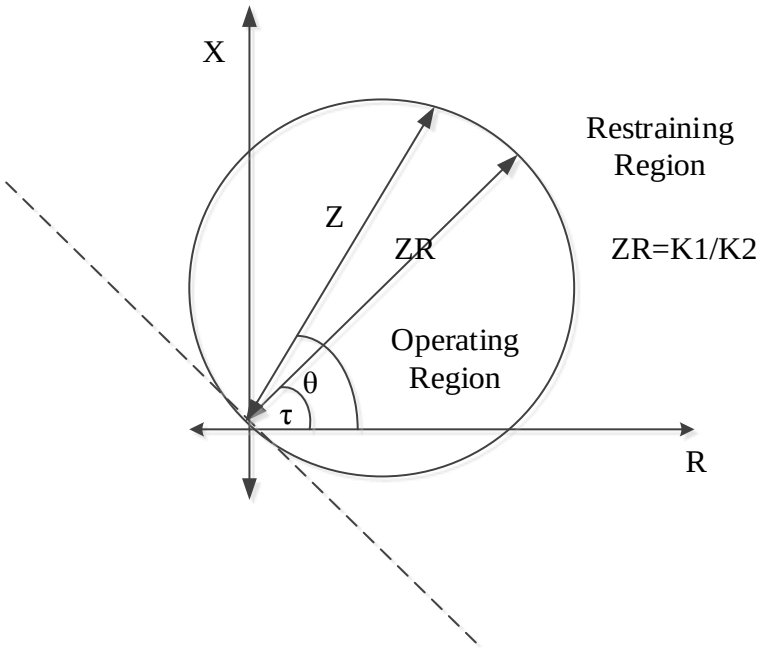

FIGURE 2.2: Mho relay characteristics

2.2.3. Reactance Relays:

In Mho relay, the operating torque is produced by the current element and the restraining torque is produced by current and voltage of the directional element. In other words, reactance relay is an over current relay with directional restraint. The directional element is so designed to give maximum torque angle of 90 degrees. Figure shows characteristics of reactance relay. The torque equation is

$$T = K_1 I^{2-} K_2 V I sin\theta - K_3 \qquad (2.5)$$

Where I and V are rms magnitudes of current and voltage, θ is angle between I and V.

At the verge of operating,

$$\frac{V}{I} sin\theta = Z sin\theta = X = \frac{K_1}{K_2} = constant \qquad (2.6)$$

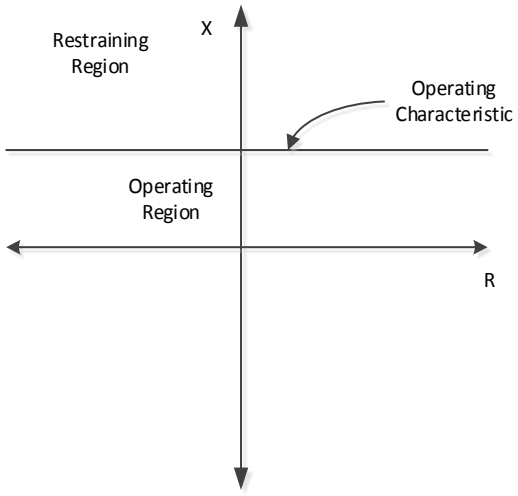

FIGURE 2.3: Reactance relay characteristics

2.2.4. Choice between Impedance, Mho and Reactance relays

Mho relays are best suited for phase fault detection in long transmission lines, especially where the severe switching surges may occur. These relays are the most selective of all the three types. In other words, when mho relay is adjusted to protect any given line, its operating characteristic occupy very less space in R-X plane, which means it will be least affected by abnormal conditions in the system other than the line faults. Operation of mho relays is affected by the arc resistance therefore they are suitable for long transmission lines. One more advantage of mho relay is that it inherently contains directionality, hence separate directional element is not needed [45].

The Reactance relays are best suited for ground fault detection because their operation is unaffected by the fault resistance. The ground faults involve variable arc resistance. The Impedance relay is better suited for moderate transmission lines. Arc resistance affect the impedance relay more than reactance type relay but less than the mho relay. Switching surges affect the impedance relay more than mho relay and less than the reactance type relay. The impedance relay is inherently non-directional and separate element is required to make it directional. The next section discuss about the zone adjustments in transmission line distance protection in microprocessor based numerical relays using mho characteristics.

2.2.5. Zones in Distance Protection

Numerical distance relays have a reach setting up to 80% of the protected line impedance for instantaneous zone 1 protection. The remaining 20% is safety margin and it ensures that there is no zone 1 over reaching the line due to errors in current and

voltage transformers and errors in the settings and relay measurements. Reach setting of zone 2 protection should cover 120% of the protected line impedance. It is common practice to set the zone 2 reach to be equal to the protected line + 50% of the adjacent shortest line. This ensures that the resulting zone2 reach does not extend beyond the zone 1 of the adjacent line protection. Zone 2 tripping is time delayed to ensure grading with the primary relaying applied to the adjacent circuits. Zone 3 reach should be set to at least 1.2 times the impedance presented to the relay for a fault at the remote end of the second line section. It should be time delayed to cover the zone 2 operating time plus circuit breaker tripping time. In modern digital or numerical relays zone 4 may be used as back up protection for local bus bar, by applying a reverse reach setting of the order of 25% of the zone 1 reach.

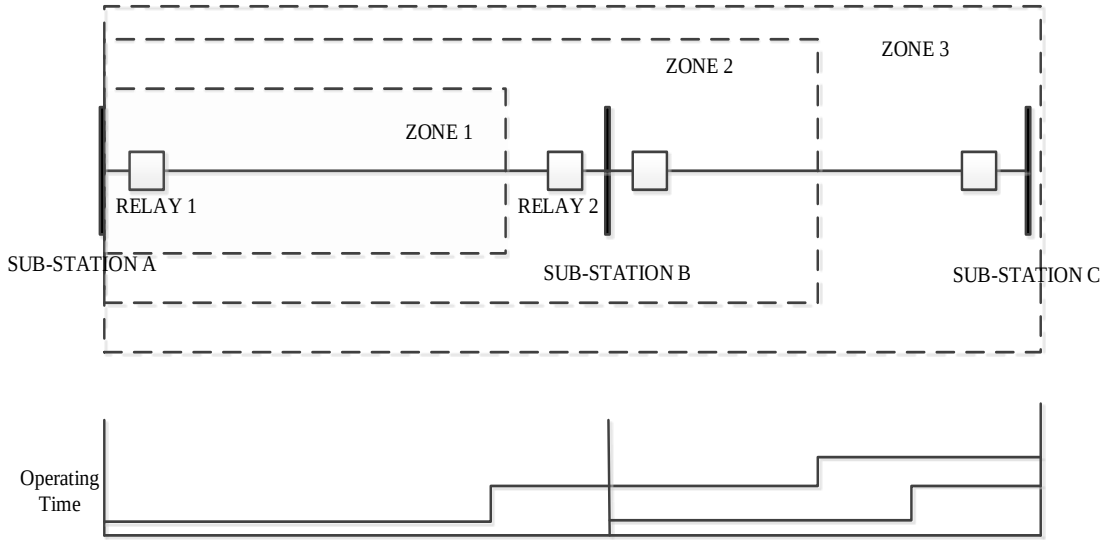

FIGURE 2.4: Zones of distance protection

2.3. Out-of-Step Protection

Power systems under steady state conditions operate very close to the nominal frequency and maintain the all bus voltages in between 0.95 to 1.05 per unit. A balance is established between generated and consumed active and reactive power and the system frequency normally varies less than +/- 0.02Hz. Any change in generation, load demand or the transmission network causes the change in power flow across the system until new equilibrium is reached. These changes occur continuously and are compensated by control systems. So they normally don't have any detrimental effect on the power grid or its protective systems.

Severe faults, switching of heavily loaded transmission lines or loss of excitation in large synchronous machines result in sudden changes to electrical power, whereas the mechanical power input to the generator remains constant. These disturbances cause oscillations in machine rotor angles and can result in severe power flow swings. This situation is called out-of-step (OOS) conditions. Large power swings can cause unwanted relay operations at different network locations, which can add up the severity and cause major outages and black outs.

During a system power swing event, a distance relay may detect the power swing as a phase fault if the positive sequence impedance locus enters into the operating characteristic of the relay. Let us take a look at the impedance measured by a distance relay during out-of-step condition.

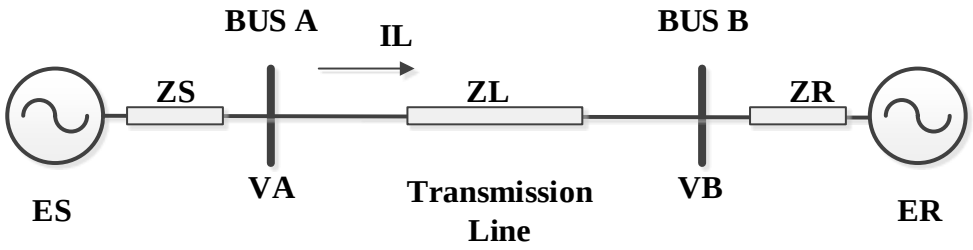

FIGURE 2.5: Two source equivalent power system

Considering a two machine system as shown in figure 2.5, the current IL at bus A is computed as

$$IL = \frac{ES - ER}{ZS + ZL + ZR} \qquad (2.6)$$

Where ZS is the equivalent source impedance, ZL is the line impedance and ZR is the equivalent impedance on the receiving end of the line.

The positive sequence impedance measured by the relay at bus A can be written as

$$Z1 = \frac{VA}{IL} = \frac{ES - IL * ZS}{IL} = \frac{ES * (ZS + ZL + ZR)}{ES - ER} - ZS \qquad (2.7)$$

Let us assume the phase difference between ES and ER is δ and the ratio of the two source voltage magnitudes is k.

$$\frac{ES}{ES - ER} = \frac{k[(k - cos\delta) - jsin\delta]}{(k - cos\delta)^2 + (sin\delta)^2} \qquad (2.8)$$

If the two source voltage magnitudes are equal then k=1 then above equation can be expressed as

$$\frac{ES}{ES-ER}=\frac{1}{2}\left(1-jcot\left(\frac{\delta}{2}\right)\right) \qquad (2.9)$$

Finally the impedance measured by the relay will be

$$Z1=\frac{VA}{IL}=\frac{(ZS+ZL+ZR)}{2}\left(1-jcot\left(\frac{\delta}{2}\right)\right)-ZS \qquad (2.10)$$

The trajectory of the measured impedance at the relay during a power swing when angle between the two source voltages varies, is shown in the figure 2.6. This trajectory is a straight line that intersect the line segment AB at middle point. This point is called electrical center of the swing. The angle between the two segments that connect P to points A and B is equal to the angle δ. When the angle is 180 degrees, the impedance is precisely at the location of electrical center.

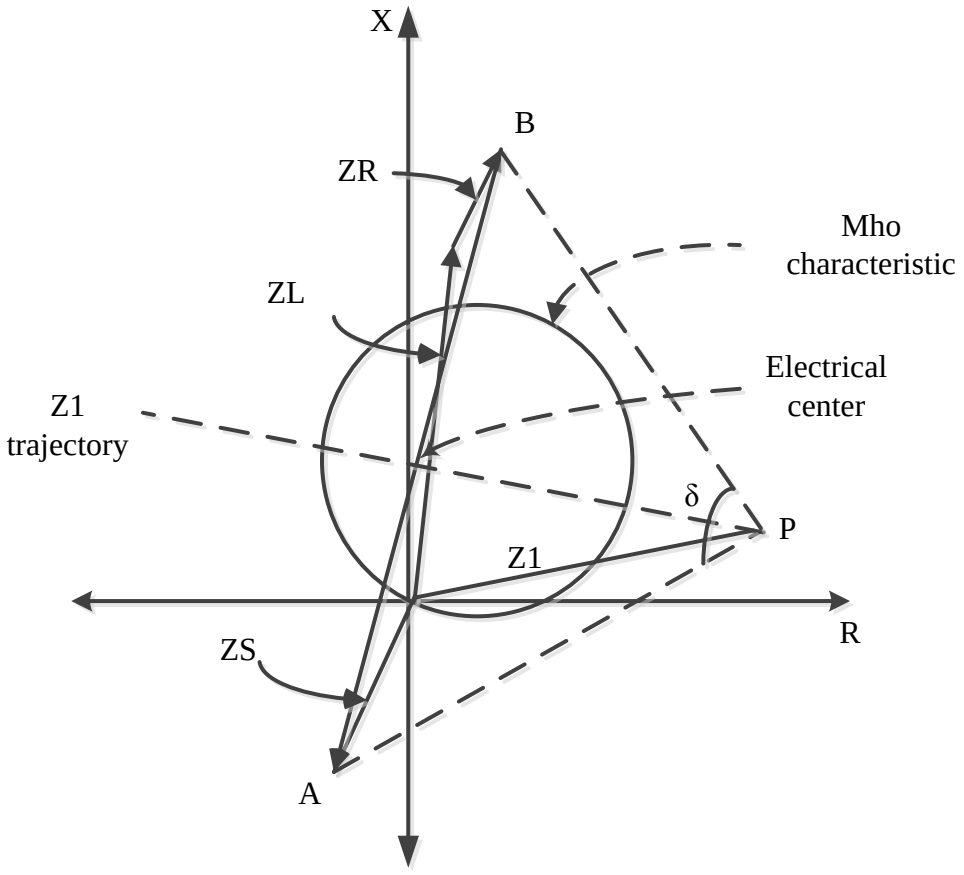

FIGURE 2.6: Impedance trajectory at the relay location during power swing.

From equation 2.7 the rate of change of positive sequence impedance can be expressed as

$$\frac{dZ1}{dt} = -j(ZS + ZL + ZR) * \frac{e^{-j\delta}}{(1 - e^{-j\delta})^2} * \frac{d\delta}{dt} \qquad (2.11)$$

Where $\frac{dZ1}{dt}$the time derivative of positive sequence impedance is measured by the relay and $\frac{d\delta}{dt}$ is the slip frequency ω.

$$(ZS + ZL + ZR) = ZT \qquad (2.12)$$

Using the trigonometric identity:

$$\left|1 - e^{-j\delta}\right| = 2\ sin\left(\frac{\delta}{2}\right) \qquad (2.13)$$

The rate of change of Z1 impedance is finally expressed as:

$$\left|\frac{dZ1}{dt}\right| = \frac{|ZT|}{4\ sin^2\left(\frac{\delta}{2}\right)}|\omega| \qquad (2.14)$$

Equation 2.14 expresses the fact that the rate of change of positive sequence impedance depends upon the source, line impedances and the slip frequency which in turn depends on the severity of the perturbation. As a consequence, any method that uses the Z1 impedance displacement speed complex R-X plane can be used to detect the power swing. It should be noted that, in reality, the two source magnitudes ES and ER are neither equal in magnitude and nor constant. So the locus of Z1 impedance will switch from one circle to other depending upon the instantaneous magnitude ratio [12].

The distance protection relays shouldn't trip unintentionally during dynamic system conditions such as stable or unstable power swings, and allow the power system to return to the stable operating condition. Power swing block (PSB) is available in numerical distance relays to prevent unwanted operation during power swings. It differentiate between faults and the power swings and block the distance elements during power swing. However, faults that occur during power swings should be detected and cleared with high degree of selectivity and dependability.

Unstable and large power swings cause separation of rotor angles between groups of generators and eventual loss of synchronism. This situation is called out of step condition. Uncontrolled tripping in these conditions may cause cascaded outages and black outs. Therefore controlled tripping of certain power system elements is necessary to prevents major outages and blackouts. This purpose can be achieved by Out of step trip (OST) function in distance relays. The main task of OST function is to differentiate between stable and unstable power swings and initiate the system separation at predetermined network locations in order to maintain power system stability and reliability. The following subsection discuss about the power swing detection schemes.

2.3.1. Power Swing Detection Methods:

a) Conventional rate of change of impedance [11]:

During normal system operating conditions, the measured impedance is the load impedance and its locus is far away from relay characteristics [11]. When a fault occurs the impedance point moves immediately into the relay operating characteristics whereas during power swing impedance point moves slowly on the impedance plane. The rate of change of impedance is measured by determining the elapsed time required by the impedance vector to pass through a zone limited by two additional concentric impedance characteristics.

The inner concentric zone setting should be larger than the largest tripping characteristic. The advantage is that the detection of power swing can be done before the impedance locus enters into the operating characteristic. The main settings in this method are the delta impedance and the timer. Extensive stability studies required to find the

correct settings. The disadvantage is that the outer zone limits the maximum load carried by the transmission line. This is called load encroachment.

b) Blinder schemes [16] [17]:

Dual blinder scheme:

The two blinder scheme works on the same principle as the concentric characteristics scheme. The timer starts when the impedance vector crosses the outer blinder and stops when the inner blinder is crossed. If the measured time is greater than the delta time setting then power swing is detected. All the distance elements will be blocked. If an unstable power swing is detected, the mho element may be allowed to trip immediately or trip may be delayed until the swing passes through.

The advantage of this method is the power swing detection settings are independent of distance protection settings. However, finding the correct settings needs extensive stability studies.

Single blinder scheme:

A single blinder scheme uses only one set of blinder characteristics. In addition with an auxiliary logic it can be used for out of step trip function. However, it cannot distinguish between a fault and OOS condition until the fault has passed through second blinder in given time. This scheme can be used to prevent the automatic reclosing for a detected unstable power swing. The basic advantage of this scheme is the usage for load encroachment.

c) R- Rdot scheme [3, 14]:

To prevent severe voltage dips in the power system with uncontrolled loss of loads, out-of-step tripping initiation on major EHV interconnections is required before voltage at electrical center reaches a minimum value. This can be achieved by using the control algorithms that depend on rate of change of apparent resistance. The algorithms are

Conventional OST relay: $Y1 = (R - R1) \leq 0$ (2.3)

R-dot relay: $Y2 = (R - R1) + T1\frac{dR}{dt} \leq 0$ (2.4)

Where Y1 and Y2 are control outputs, R is apparent resistance measured by the relay and R1, T1 are relay settings.

d) Continuous impedance calculation [11]:

This method determines the power swing based on the continuous impedance calculation. For example, for each 3ms time step an impedance calculation is performed and compared with the impedance of previous step. If there is a deviation an out of step situation is assumed. The next step impedance is predicted base on the previous two values. If the prediction is correct, ten power swing is detected. There is no need for delta time and delta impedance settings in this method. However, if the changing impedance vector is faster than the relay processing speed the detection may be unsuccessful.

e) Swing center voltage and its rate of change [11]:

Swing center voltage (SCV) is defined as the voltage at the location of a two source equivalent system where the voltage value is zero when the angles between the two

sources are 180 degrees apart. When a two source system loses stability, the angle difference between the sources will increase as a function of time. The SCV can be expressed using the local available quantities as

$$SCV \approx |V_s|.cos\varphi \qquad (2.5)$$

Where $|V_s|$ is the magnitude of locally measured voltage, and φ is the angle difference between the V_s and local current. This can be expressed as

$$SCV = E1.cos\left(\frac{\delta}{2}\right) \qquad (2.6)$$

Where E1 is the positive sequence source voltage magnitude equal to ES, ER and δ is the phase angle difference between the two sources. The absolute value of SCV is maximum when δ is zero and this value will be minimum if δ is 180 degrees. Therefor by looking at the rate of change of swing center voltage, the power swing situation can be detected.

$$\frac{d(SCV)}{dt} = -\frac{E1}{2}\sin\left(\frac{\delta}{2}\right).\frac{d\delta}{dt} \qquad (2.7)$$

The main advantage of SCV method is that SCV is independent of the system source and line impedances, whereas all other quantities such as the resistance, real power and their rates of change depend on the system source impedances and other system parameters.

f) Synchrophasor based out of step relaying

With the advent of synchronized phase angle measurement also called as synchrophasor, the measurement of the phase angle of the bus voltages at different locations can be obtained in real time and these can be used to create a protection algorithm that detects power swings, instability conditions and also the remedial action schemes such as network separation and load shedding.

2.4. Real Time Transient Stability Assessment

This section presents a brief literature review on the real-time transient stability assessment (TSA) methodologies. More details on the fundamentals of power system transient stability can be found in [1]. The critical challenge in online transient stability assessment is the requirement for real-time operation with fast and precise calculations, without reducing the complexity and the dimensionality of the power system component models. Several approaches have been proposed in this direction to deal with this problem efficiently without compromising the accuracy of results.

The simplest method for stability analysis is known as equal area criterion. This method is based on graphical interpretation of energy stored in the rotating part as an aid to determine the machine's stability after a disturbance. This method is only applicable to one machine connected to infinite bus or a two machine system. For multi machine systems, the most commonly used tool for transient stability analysis is time domain dynamic simulations. All the power system components are modeled as a set of non-linear algebraic-differential equations and are solved using numerical integration methods. This method has a major advantage in terms of the accuracy of the results since

very detailed dynamic models can be used without simplifications. However, the major disadvantage is that it requires a lot of time and huge computational effort, which makes it unsuitable for the online applications. This method is used mainly for offline transient stability studies. Another disadvantage is that this method does not provide any control actions that could prevent power system instability.

The widely used approach for online transient stability analysis is direct methods. A direct method for transient stability analysis is defined as a method that is able to determine stability without completely integrating the differential equations that describe the system. The major advantage is that the computational effort is greatly reduced compared to the time domain simulations and can be suitable for online real-time applications. Moreover, they can provide stability regions around an operating point and enable sensitivity analysis [46]. Among the direct methods, Lyapunov's based direct method for stability analysis is mostly used. In this method, a Lyupanov-type function called transient energy function (TEF) is used in order to compute the region of stability around the post disturbance equilibrium point of the system. The assessment of stability of equilibrium point via the calculation of critical clearing times and critical energies is done by determining boundary of the region of stability. The challenge and the disadvantage of this method is the difficulty in determining the suitable Lyupanov function. Several different types of functions are proposed in the literature, either simplified or complex. The Lyupanov function should be a system level function that represents energy of the whole system. As a result, the inaccuracy in the existing power system component models is a barrier to the construction of an accurate Lyupanov function. The other challenge is that the energy function has to be constructed for the post

disturbance system configuration. This means that the post fault system has to be identified using the time-domain approaches. This task is highly challenging in larger systems, given the time limitations within which the computations have to be performed. The energy function based direct methods are applicable for only the first swing transient stability analysis. Moreover, the application of TEF methods also involves the simulation of the system in time domain for at least the fault period, so combinations of TEF methods with time domain analysis are commonly encountered in the literature. The computationally intensive part of the TEF methods is the calculation of the post-fault system equilibrium points. However, despite of the disadvantages, the direct methods are far more efficient and suitable for real time applications compared to the time domain analysis. The selection of the transient energy function and the background theory is detailed in chapter 4.

2.5. Summary

In this chapter, the overview about the power system protection and three different types of distance relays namely impedance relays, mho relays and reactance relays were described. The merits and demerits and possible applications of these relays were discussed. The identification of protective zones in numerical distance relays including the reach and time settings, was shown.

Further, the need for detection of power swing was explained and the relation between the rate of change of angular difference and the rate of change of positive sequence impedance measured by the relay, was established. Various types of power swing detection schemes were presented, in which the most popular scheme is the dual

blinder based detection scheme. Also, an overview of the real time transient stability assessment using direct methods is presented. The basic advantages and disadvantages are discussed. A more detailed discussion can be found in chapter-5. The following chapter discusses about the implementation of distance and out-of-step protection in SEL-421 relay and simulation using real time digital simulator (RTDS).

CHAPTER 3 : DESIGN AND IMPLEMENTATION METHODOLOGY FOR DISTANCE AND OUT-OF-STEP PROTECTION

This chapter presents the methodology of out-of-step protection scheme using dual blinder characteristic and using synchrophasor measurements. The dual blinder scheme is implemented in SEL-421 numerical protection relay and the synchrophasor based scheme is implemented in Real Time Digital Simulator. The test system used to compare these methods, is Kundur two area system and it is built in RTDS and validated using MATLAB Power System Analysis Toolbox (PSAT). The trip signal feedback from SEL-421 relay to RTDS is done by GOOSE communication and corresponding methodology is briefly discussed in section 3.3.1. This hardware in the loop setup is validated by performance comparison between RTDS in built distance protection component and SEL-421 distance function. We will start with general design and implementation methodology of out-of-step protection scheme.

3.1. Implementation Methodology

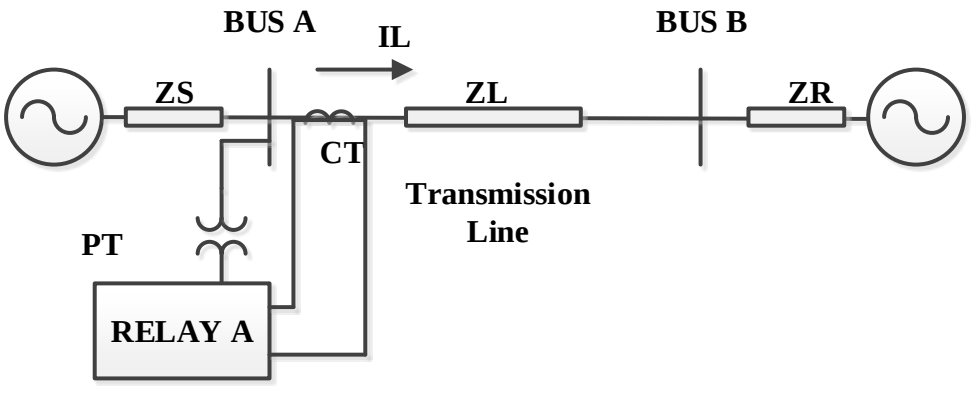

FIGURE 3.1: Two source equivalent of a power system with protection relay

Consider a two source equivalent of a power system as shown in figure 4.1. Relay A is the distance relay located at sending end of the transmission line. ZL is the positive sequence impedance of the line and ZS is the equivalent positive sequence impedance before the sending end of the line. ZR is the equivalent positive sequence impedance after the receiving end of the line. To implement the out-of-step protection scheme in Relay A, the distance protection zone reaches should be calculated.

Distance protection settings for Relay A:

Zone 1 Reach $Z1MP = 80\%\ of\ ZL = 0.8 * ZL$ (3.1)

Zone 2 Reach $Z2MP = 120\%\ of\ ZL = 1.2 * ZL$ (3.2)

3.1.1. Out-of-step Protection using Dual Blinder Characteristic:

Dual blinder scheme is the most common method in distance relays to detect power swings. In SEL-421 relay, this method uses two resistive blinders at each side of the relay distance zones, Resistive left Outer and inner blinders (RLO, RLI) and resistive right outer and inner blinders (RRO, RRI). The implementation requires two timers, namely, out-of-step blocking delay (OSBD) and out-of-step tripping delay (OSTD).

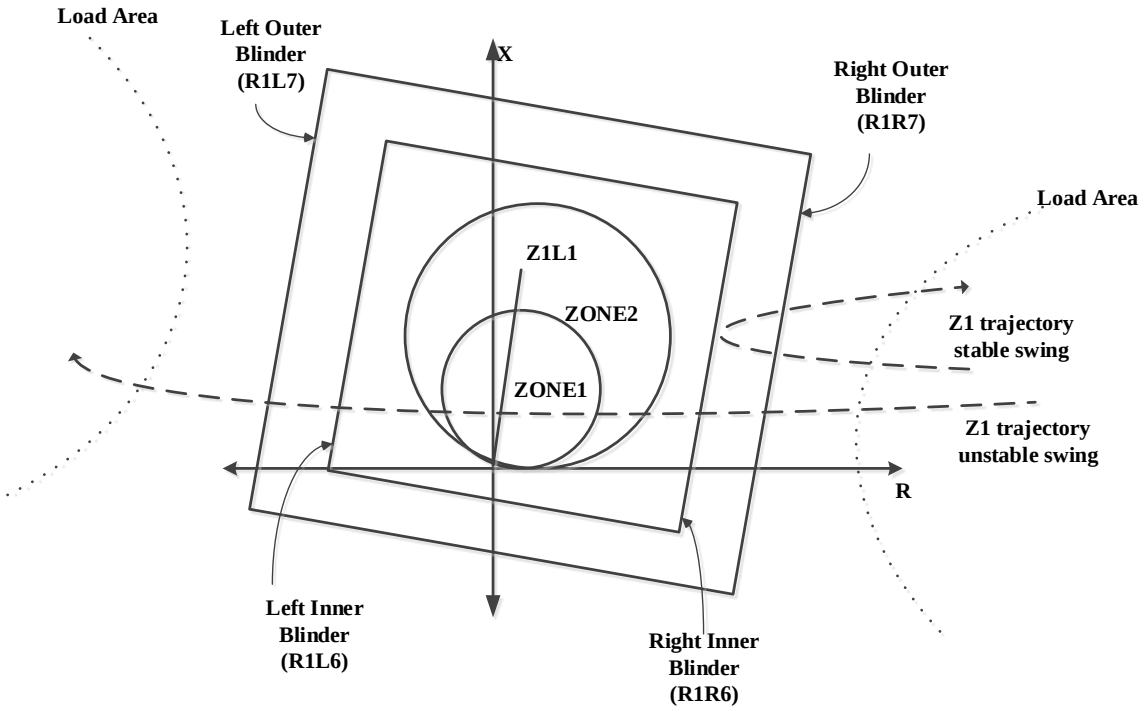

FIGURE 3.2: Out-of-step dual blinder characteristics

The inner resistive blinder must be placed outside the largest distance protection characteristic (zone) that is to be blocked. In addition, the outer resistive blinder must be place away from the load region to prevent PSB operation caused by heavy loads in the system. The timer starts when the impedance vector crosses the outer blinder and stops when the inner blinder is crossed. If the measured time is greater than the delta time setting then power swing is detected.

The above requirements are difficult to achieve in some application systems, depending on the relative line and source impedance magnitudes. If the line impedance is larger than the system impedance, the swing locus could enter zone2 and zone1 before the phase angle difference of voltage reaches 120 degrees that is even during the stable

power swing. It may be difficult to set the inner and outer blinders in this case. If the line is heavily loaded, the necessary PSB settings are so large that the load impedance may cause incorrect blocking. To overcome this problem, traditionally two methods are used. One is using lenticular distance characteristics and the other is using blinders that restricts the tripping area of mho elements. In modern numerical protection relays, there is load encroachment feature to deal with loading issues.

The blinder settings and the timer settings are not trivial to calculate and depending upon the system, it is necessary to run extensive stability studies to determine the fastest power swing and proper blinder resistance settings. The source impedances also vary constantly according to the network changes such as addition of generation, load shedding. Generally, very detailed system stability studies are necessary to consider all contingencies in determining the equivalent source impedance to set the power swing blocking function.

Calculations for blinder settings [44]:

Inner resistance blinder:

$$R1R6 = 1.2 * \frac{Z2MP}{2 * \sin(Z1ANG)} \quad (3.3)$$

Outer resistance blinder:

Let Maximum load current be $IL(\max)$ and corresponding line-neutral voltage beV_{LN}.

Minimum load impedance $ZL_{min} = \frac{V_{LN}}{IL(\max)}$

$$R1R7 = 0.9 * ZL_{min} * \cos\big(45 + (90 - Z1ANG)\big) \quad (3.4)$$

Inner reactance blinder:

$$X1T6 = 1.2 * Z2MP \quad (3.5)$$

Outer reactance blinder:

$$X1T7 = X1T6 + (R1R7 - R1R6) \quad (3.6)$$

OST DELAY:

Total transfer impedance $ZT = Z1S + Z1R + Z1L$

$$AngR6 = 2 * \text{atan}\left(\frac{\frac{ZT}{2}}{R1R6}\right) \quad (3.7)$$

$$AngR7 = 2 * \text{atan}\left(\frac{\frac{ZT}{2}}{R1R7}\right) \quad (3.8)$$

Let the fastest unstable swing frequency be f_{slip}.

$$OSTD = \frac{(AngR6 - AngR7) * f_{nom}}{360 * f_{slip}} \quad (3.9)$$

3.1.2. Out-of-step Protection using Synchrophasors

Synchrophasors, or synchronized phasor measurements, defined as the representation of power system voltage and current vector to an absolute time reference. This reference is provided in the form of a common timing signal by high-accuracy

clocks synchronized to coordinated universal time (UTC) such as global positioning system (GPS).

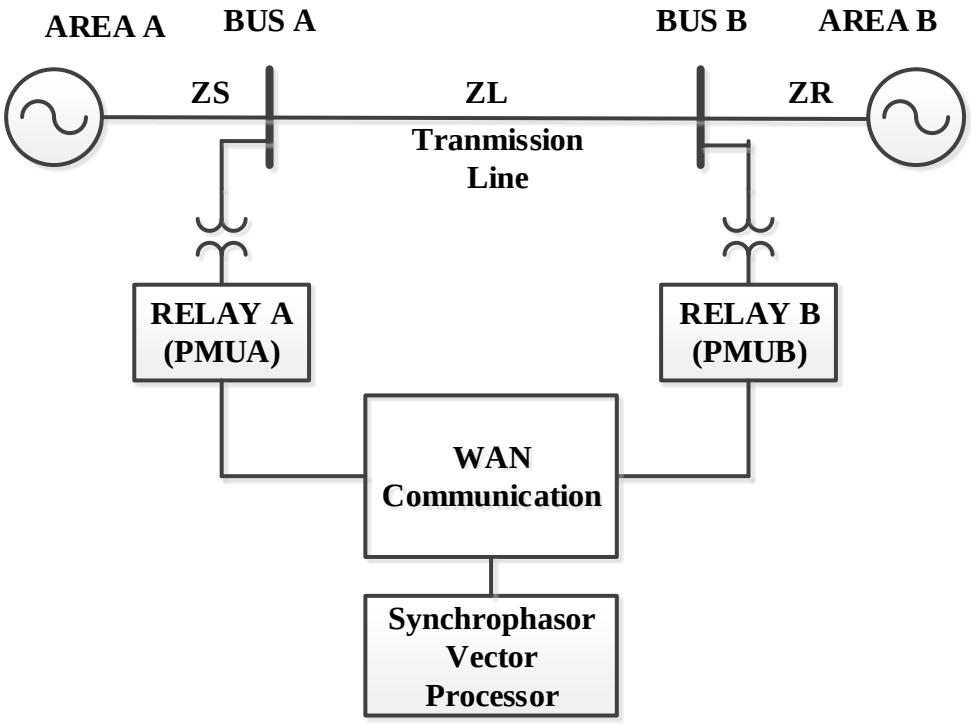

FIGURE 3.3: Two source equivalent of power system with PMUs

In a two area power system, the electrical center is a point that corresponds to the half of the total impedance between the two sources. The proposed algorithm requires that the electrical center is between the two relays that acquire the synchrophasor measurements. It uses the voltage synchrophasors from the buses at both ends of the line to calculate the angle difference (δ_k) between these voltages. The rate of change of δ_k is defined as slip frequency (S_k) given by equation 3.11 and the change of slip frequency with respect time is defined as the acceleration frequency (A_k) and is given by equation 3.12.

$$\delta_k = Angle(V_k^{PMUA}) - Angle(V_k^{PMUB}) \quad (3.10)$$

$$S_k = \frac{\delta_k - \delta_{k-1}}{t_k - t_{k-1}} \quad (3.11)$$

$$A_k = \frac{S_k - S_{k-1}}{t_k - t_{k-1}} \quad (3.12)$$

Where

$Angle(V_k^{PMUA})$: Positive sequence voltage angle measured by PMUA at kth instant.

$Angle(V_k^{PMUB})$: Positive sequence voltage angle measured by PMUB at kth instant.

S_k : slip frequency at kth processing instant.

A_k : Angle acceleration at kth processing instant.

$t_k - t_{k-1}$: Processing interval.

Figure 3.5 depicts the characteristic of out-of-step element that defines the region of stable operation. The slip frequency and acceleration are used to identify the unstable power swing conditions. The flow chart for the algorithm is shown in figure 3.4.

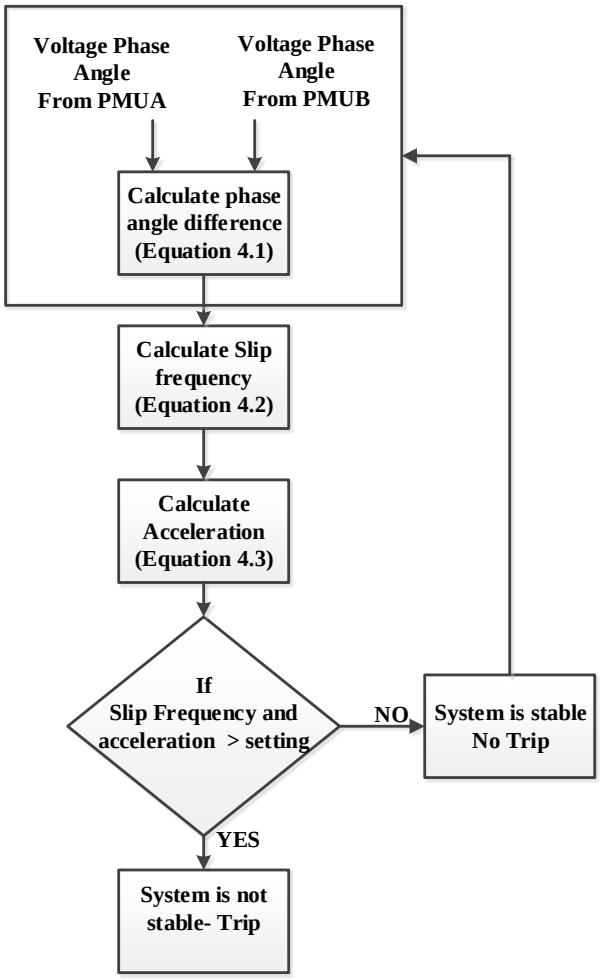

FIGURE 3.4: Synchrophasor based out-of-step detection flow-chart.

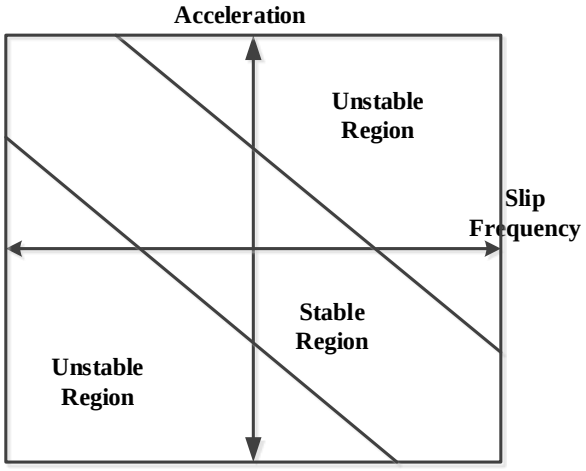

FIGURE 3.5: Synchrophasor based out-of-step element characteristic

3.2. Description of Kundur Two Area System

Kundur two area system is most suitable test system for the study of out-of-step protection because it consists of two areas which are connected by two weak tie lines. The electrical center of the system lies on the tie line. If a fault occurs on one of the tie-lines, the power swing will be created with swing center on the second tie-line. The out-of-step relay is implemented on this second tie line to observe the system stability.

The test system contains four generators in two symmetrical areas connected by two tie lines. Area 1 has the load of 967MW and generation of 1400MW. Area 2 has a load of 1767MW and generation of 1463MW. Each tie line is carrying approximately 200MW. The one line diagram is shown figure 3.6.

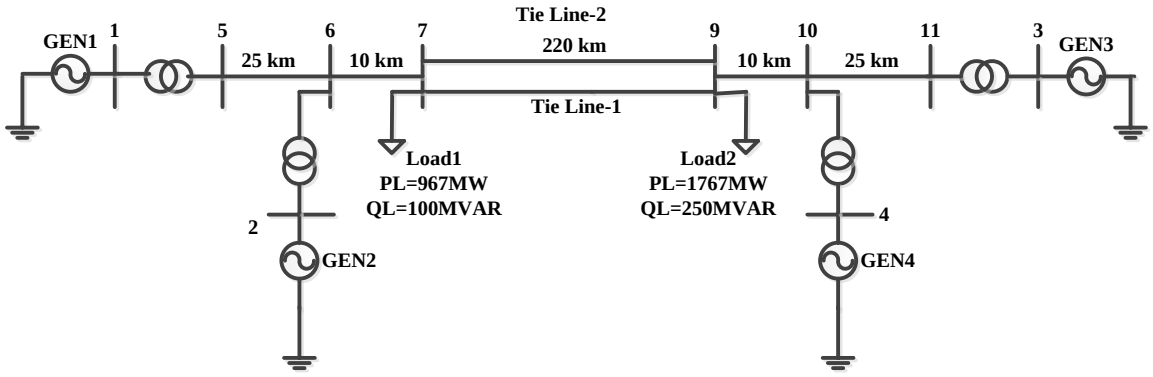

FIGURE 3.6: Kundur two area system one-line diagram

The system is simulated in real time digital simulator (RTDS RSCAD version : 4.006.2). The power flow study is done and the results are tabulated in table 3.1. To validate the results, the same test system is simulated in PSAT. The load flow results are

shown in table 3.2. The voltage profile comparison between the two software is shown in figure 3.7. The results of RTDS are close to the results of PSAT.

Table 3.1: RTDS load flow results of Kundur two area system

Bus No.	Voltage (p.u)	Angle (deg)	Pgen (MW)	Qgen (MVAR)	Pload (MW)	Qload (MVAR)
1	1.00	28.42323	700	165.8954	0	0
2	1.00	17.9484	700	298.4364	0	0
3	1.00	0	723.5095	158.1786	0	0
4	1.00	-11.0357	700	264.9216	0	0
5	0.97932	51.57996	0	0	0	0
6	0.95739	40.94757	0	0	0	0
7	0.93785	32.16020	0	0	967	100
8	0.91653	17.57083	0	0	0	0
9	0.94882	3.19324	0	0	1767	250
10	0.96293	12.00442	0	0	0	0
11	0.98107	22.93845	0	0	0	0

Table 3.2: PSAT load flow results of kundur two area system

Bus No.	Voltage (p.u)	Angle (deg)	Pgen (MW)	Qgen (MVAR)	Pload (MW)	Qload (MVAR)
1	1.00	27.8522	700	154.8148	0	0
2	1.00	17.4123	700	273.5515	0	0
3	1.00	0	722.2486	146.5128	0	0

4	1.00	-10.965	700	239.4671	0	0
5	0.98116	21.0232	0	0	0	0
6	0.96151	10.443	0	0	0	0
7	0.99497	1.7411	0	0	967	100
8	0.93142	-12.5803	0	0	0	0
9	0.95604	-26.6104	0	0	1767	250
10	0.96715	-17.8934	0	0	0	0
11	0.98298	-7.034	0	0	0	0

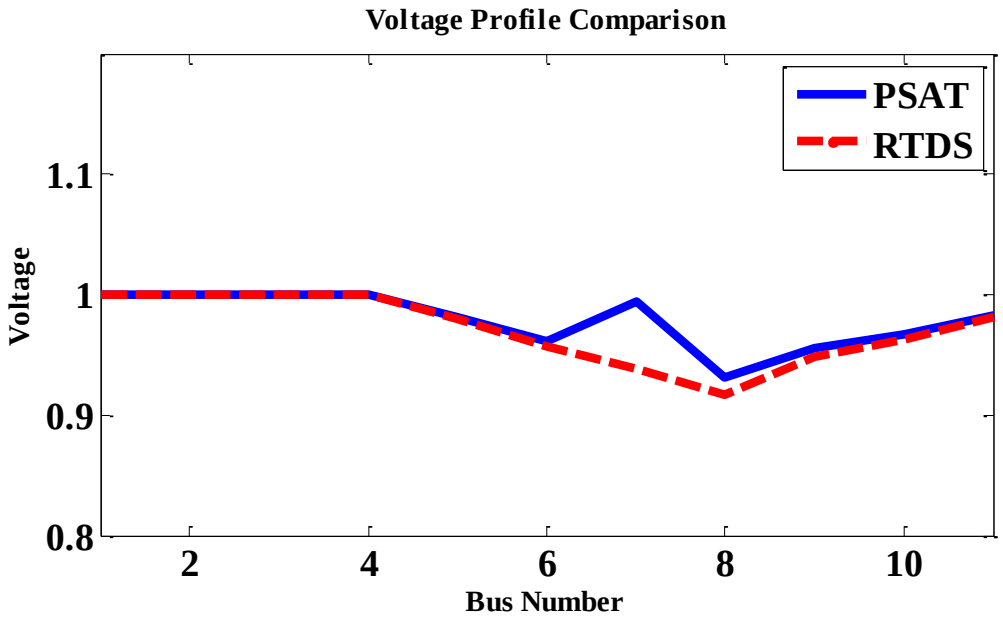

FIGURE 3.7: Kundur two area system voltage profile from PSAT and RTDS load flows

3.3. Real Time Test Platform

A real-time test platform is developed in the Duke Energy Smart Grid Laboratory within the Energy Production and Infrastructure Center (EPIC). The real-time platform is suitable for the design, testing, and validation of protective relays and wide area controllers. IEEE Standard C37.118 Synchrophasor communication protocol and IEC 61850 Generic Object Oriented Substation Event (GOOSE) protocols are implemented for wide-area communications. Figure 3.8 shows the test platform which consists of Real Time Digital Simulator (RTDS), multiple PMUs, a protocol gateway, and a MATLAB based controller. Since the platform allows one to use actual hardware for measurement, communications, protection, and control, it allows for the connection of all necessary external hardware. The simulations performed here are expected to be helpful in any state-of-the-art Smart Grid laboratory.

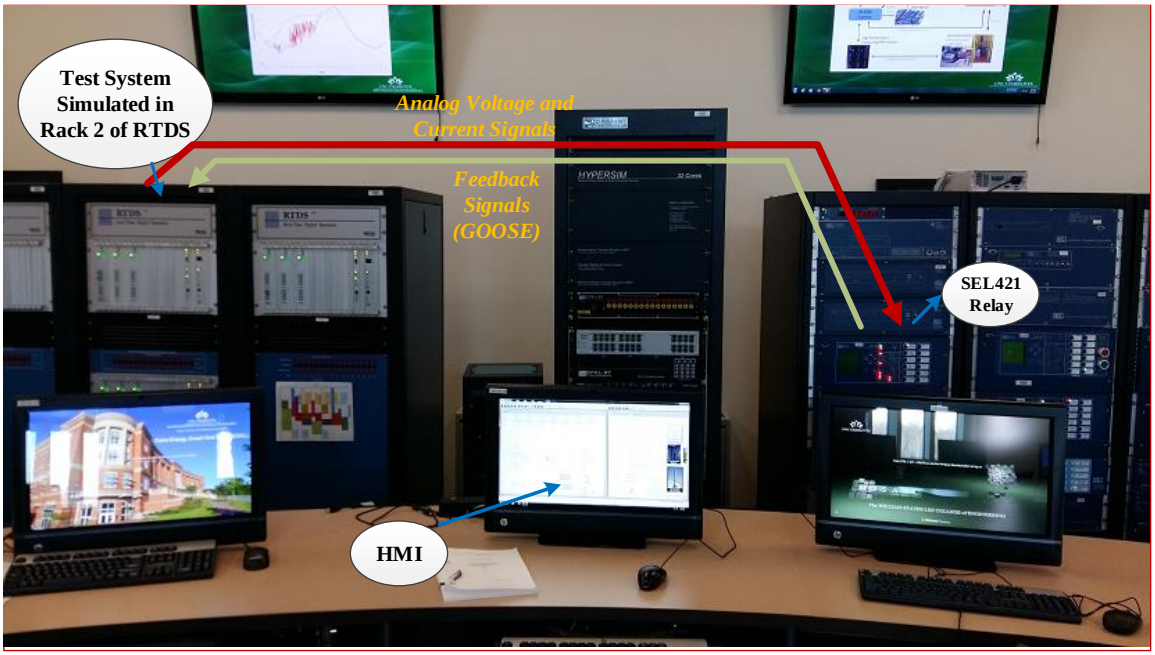

FIGURE 3.8: Real Time Test Platform

3.3.1. Implementation of Distance Protection

In the test system shown in figure 3.6, the distance protection is implemented on the tie line 1. The parameters of the transmission line are shown in the table 3.3.

Table 3.3: Line Parameters in Kundur two area system

Parameter	**Value**
Line length (km)	220
Positive sequence resistance	0.0001 p.u (0.0529 ohms/km)
Zero sequence resistance (p.u.)	0.0003 p.u (0.1587 ohm/km)
Positive sequence reactance (p.u.)	0.001 p.u. (0.529 ohms/km)
Zero sequence reactance (p.u.)	0.003 p.u (1.587 ohms/km)
Positive sequence impedance	116.96 /_84.29^0 ohms
Zero sequence impedance	350.88/_84.29^0 ohms

Based on the line parameters, the zone reach settings are calculated.

$$Z1MP = 0.8 * 116.96 = 93.568\ ohms$$

$$Z2MP = 1.2 * 116.96 = 140.352\ ohms$$

3.3.2. Hardware-in-the-Loop Setup with SEL- 421

In order to implement the distance protection using SEL 421 numerical relay we need to connect it to RTDS so that the currents and voltages of the line to be fed. This is done through GTAO card which interfaces the analog signal from the RTDS to the external devices. The GTAO card, shown in figure 4.8, consists of twelve 16bit analog output channels with an output range of +/- 10V. The primary values of line currents and

voltages are converted to the secondary values using CT and PT and given to GTAO card.

In SEL 421 relay the low level test interface connections are used for analog inputs. RTDS secondary values of voltage and current are scaled down in GTAO card and applied to this low level test interface. In SEL relay there are predefined scaling factors to scale up the input analog signals and by using proper CT and PT ratios in the relay the metering quantities are verified.

The trip commands and feedback signals from the relay are interfaced to RTDS by using GOOSE communication. To establish GOOSE, on RTDS side GTNET-GSE card is configured, which is used to interface a number of different network protocols with RTDS simulator. The GTNET card supports IEC-61850 GOOSE/GSSE, IEC-61850-9-2(sampled values), DNP3, PLAYBACK, IEEE C37.118 data stream output protocols. The configuration is shown in the figure 3.9. The feedback signals from the external device is to be mapped to the corresponding inputs of the GTNET card. This mapping is done in .SCD file, stands for substation configuration description file and is configured using AcSELerator Architect software.

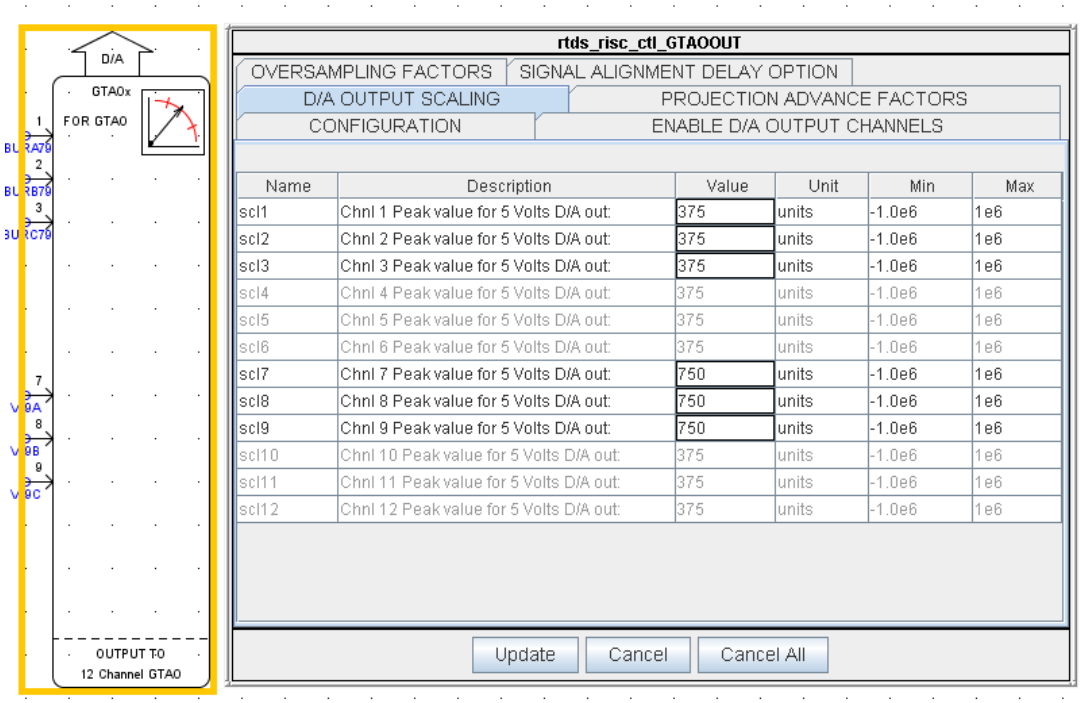

Name	Description	Value	Unit	Min	Max
scl1	Chnl 1 Peak value for 5 Volts D/A out:	375	units	-1.0e6	1e6
scl2	Chnl 2 Peak value for 5 Volts D/A out:	375	units	-1.0e6	1e6
scl3	Chnl 3 Peak value for 5 Volts D/A out:	375	units	-1.0e6	1e6
scl4	Chnl 4 Peak value for 5 Volts D/A out:	375	units	-1.0e6	1e6
scl5	Chnl 5 Peak value for 5 Volts D/A out:	375	units	-1.0e6	1e6
scl6	Chnl 6 Peak value for 5 Volts D/A out:	375	units	-1.0e6	1e6
scl7	Chnl 7 Peak value for 5 Volts D/A out:	750	units	-1.0e6	1e6
scl8	Chnl 8 Peak value for 5 Volts D/A out:	750	units	-1.0e6	1e6
scl9	Chnl 9 Peak value for 5 Volts D/A out:	750	units	-1.0e6	1e6
scl10	Chnl 10 Peak value for 5 Volts D/A out:	375	units	-1.0e6	1e6
scl11	Chnl 11 Peak value for 5 Volts D/A out:	375	units	-1.0e6	1e6
scl12	Chnl 12 Peak value for 5 Volts D/A out:	375	units	-1.0e6	1e6

FIGURE 3.9: RTDS – GTAO card configuration and scaling

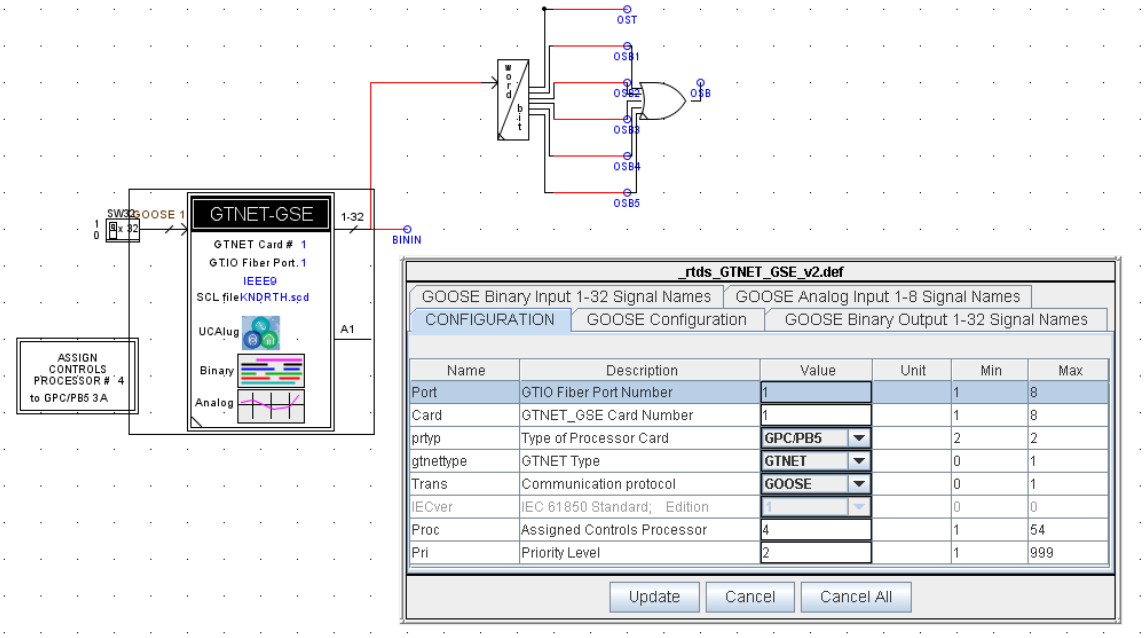

Name	Description	Value	Unit	Min	Max
Port	GTIO Fiber Port Number	1		1	8
Card	GTNET_GSE Card Number	1		1	8
prtyp	Type of Processor Card	GPC/PB5		2	2
gtnettype	GTNET Type	GTNET		0	1
Trans	Communication protocol	GOOSE		0	1
IECver	IEC 61850 Standard; Edition	1		0	0
Proc	Assigned Controls Processor	4		1	54
Pri	Priority Level	2		1	999

FIGURE 3.10: RTDS – GTNET card configuration

In the Project Editor, the correct version relay is imported and the GOOSE transmit dataset is changed as per the required feedback signals. These settings are downloaded into the relay and also the saved as .SCD file. This file is imported in RTDS GTNET card, and the corresponding signals are mapped as shown in the figure 3.11.

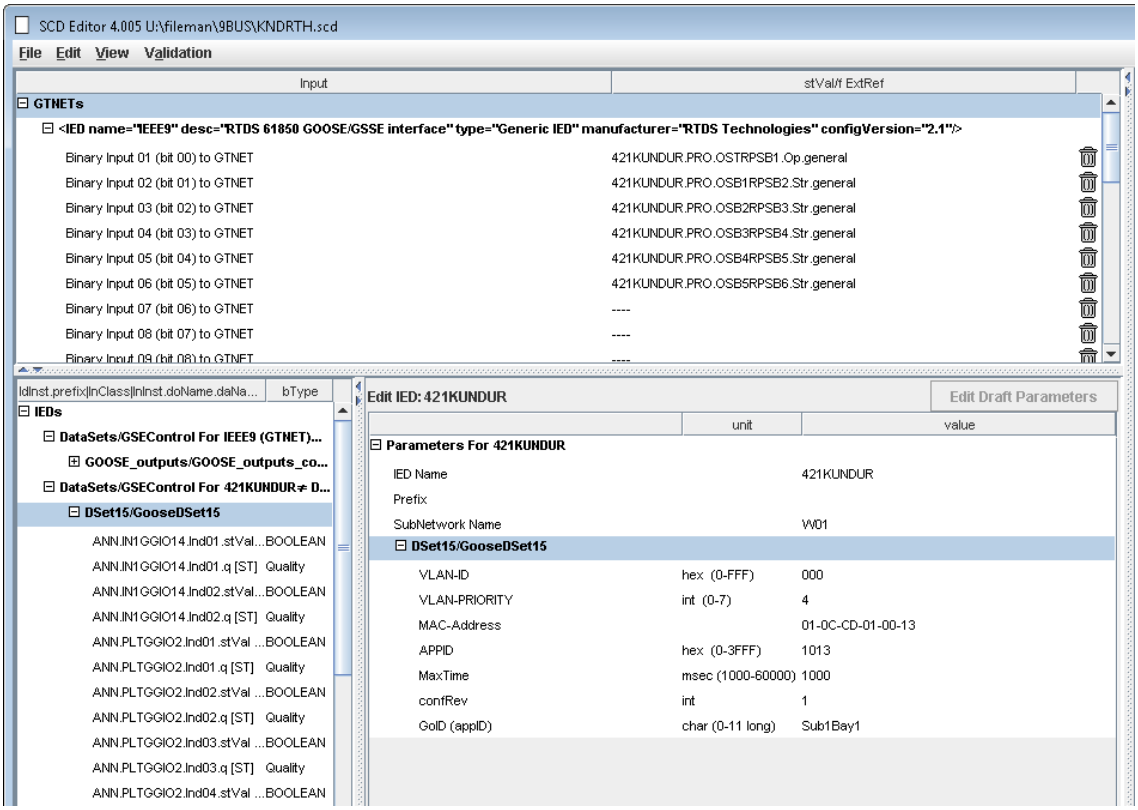

FIGURE 3.11: RTDS – GTNET SCD file digital signal mapping

The performance of SEL-421 relay including the GOOSE communication is verified by implementing the distance protection scheme using RTDS in built distance protection component (21), which is shown in figure 3.12.

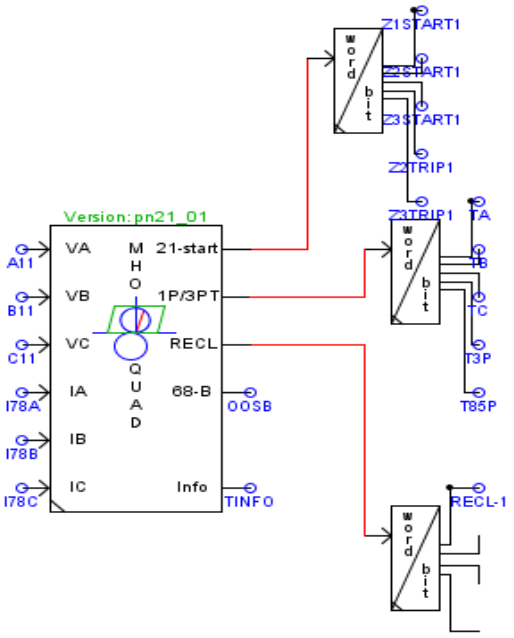

FIGURE 3.12: RTDS component of distance protection (21 element)

3.3.3. Case Studies

Different types of fault scenarios are simulated on the tie line 1 in the system shown in figure 3.6. The detected zones and the trip times are tabulate in the table 3.4. It is observed that the operated trip times are close and the performance of SEL-421 using hardware-in-the-loop setup is satisfactory. The plots of line voltage, line currents, and protection trips for case 2 are shown in figures 3.13 to 3.16.

Table 3.4: Simulated fault scenarios for distance protection

Case	Description	RTDS 21element		SEL-421 with GOOSE	
		Zone	Time (msec)	Zone	Time (msec)
Case-1	No fault	--	--	--	--
Case-2	L-G fault on Phase A in the middle of the tie-line 1	Zone 1	16	Zone 1	20.4
Case-3	L-L fault in the middle of the tie-line 1	Zone 1	18	Zone 1	22.2
Case-4	Three Phase fault in the middle of the tie-line 1	Zone 1	16.8	Zone 1	14.6
Case-5	L-G fault on Phase A near the end of the tie line 1	Zone 2	209.6	Zone 2	211.8
Case-6	L-L fault near the end of the tie line 1	Zone 2	208	Zone 2	209
Case-7	Three Phase fault near the end of the tie line 1	Zone 2	211.2	Zone 2	211

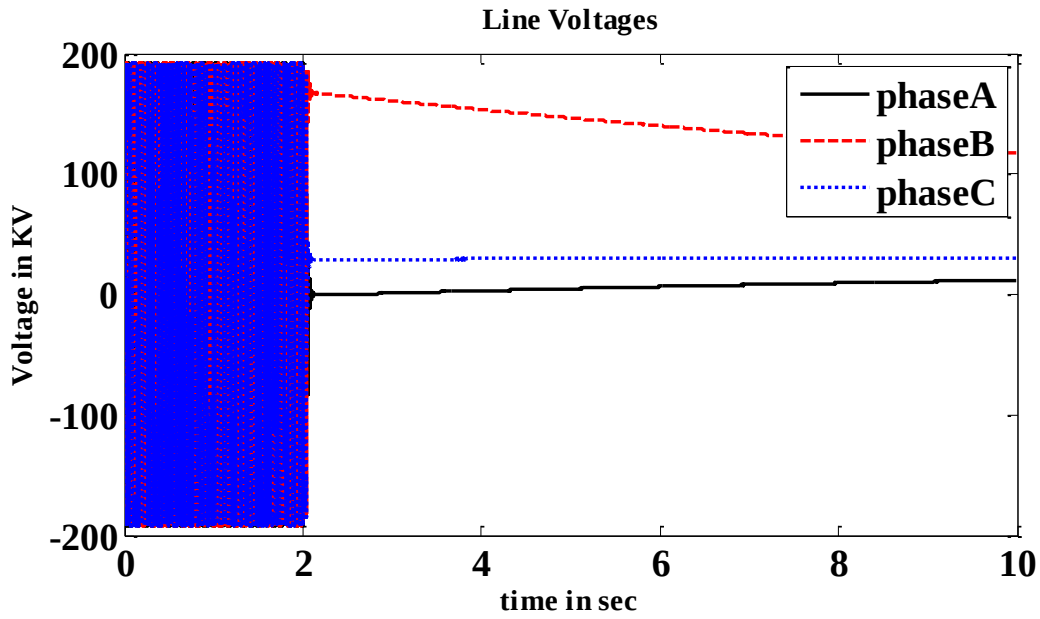

FIGURE 3.13: Line voltages in case 2 (L-G Fault on A phase)

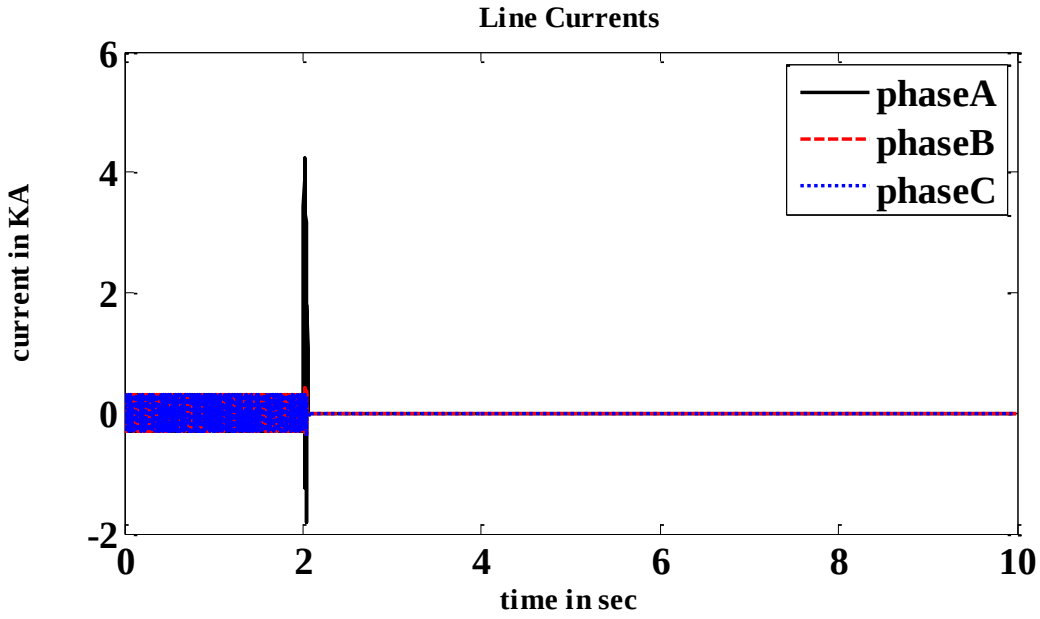

FIGURE 3.14: Line currents in case 2 (L-G Fault on A phase)

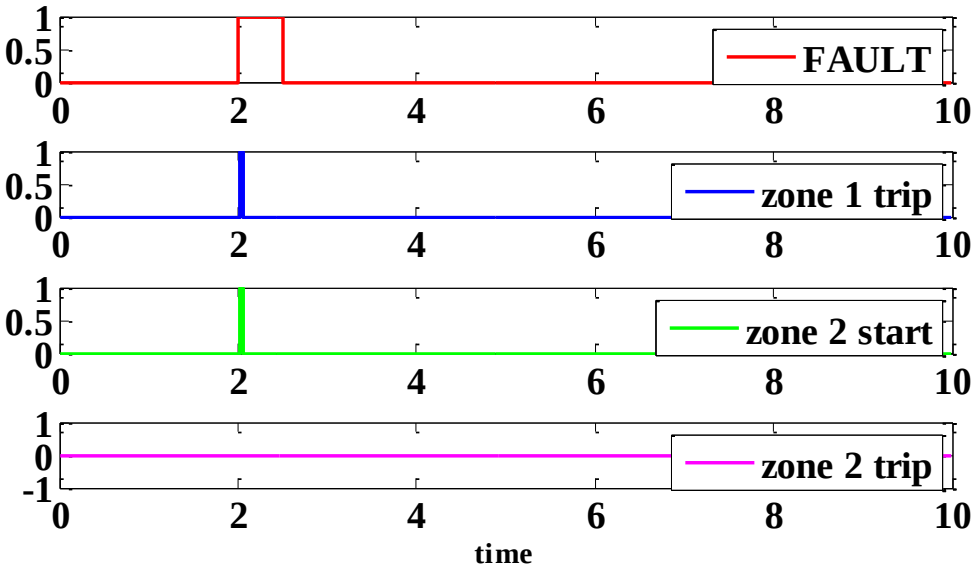

FIGURE 3.15: Protection trips in case 2 (L-G Fault on A phase)

3.4. Implementation of Out-of-step Protection using Dual Blinder Scheme

To simulate an out-of-step condition, the test setup is configured as shown in figure 3.16. Distance protection relays are implemented on the both ends of the tie-line 1 (Relay A, Relay B). These relays are the in-built RTDS distance elements. Out-of-step protection is implemented using SEL-421 numerical relay (Relay C) and it is situated on tie-line 2 at the bus 7 end. Relay A and Relay B are incorporated with auto reclose feature to get the tripped line back into the service after a specific set time. A three phase fault is injected in the middle of tie-line 1 and is cleared by Relay A and Relay B. The generated power swing is observed using Relay C using dual blinder scheme. The setting calculations are as follows:

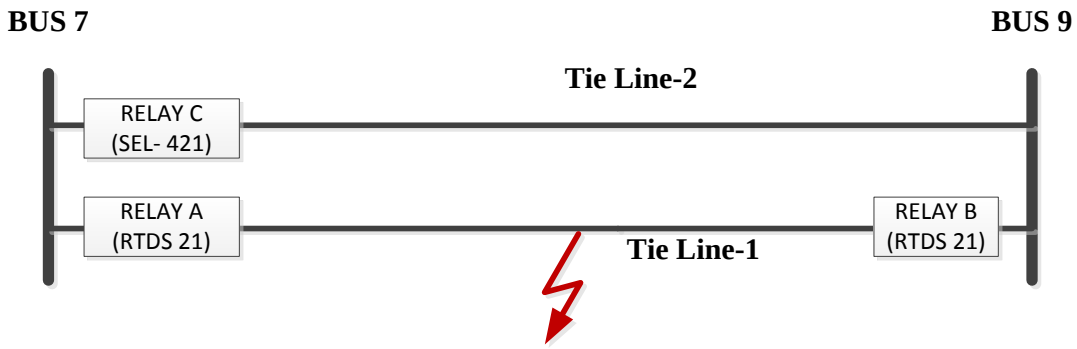

FIGURE 3.16: Test setup for out-of-step protection

Calculations for blinder settings:

$$\frac{CTR}{PTR} = \frac{500}{2000} = 0.25$$

Positive sequence impedance of line

$$Z1L1 = 116.96 \angle 84.29^0 primary = 29.24 \angle 84.29^0 \; secondary$$

Zone 2 Reach $Z2MP = 140.35 \; primary = 35.0875 \; ohms \; secondary$

Source Impedance $Z1S = \; 118.94 \; ohms \; primary = 29.375 \; ohms \; secondary$

Receiving end Impedance $Z1R = 114.84 \; ohms \; primary = 28.71 \; ohms \; secondary$

$$f_{nom} = 60 \; Hz$$

Inner resistance blinder $R1R6 = 21.157 \; ohms$

Maximum load current $IL(\max) = 536.4A\ primary = 1.0728A\ secondary$

Corresponding line-neutral voltage $V_{LN} = 132.79\ KV\ primary = 66.395V\ secondary$

Minimum load impedance $ZL_{min} = \frac{V_{LN}}{IL} = \frac{66.395}{1.0728} = 61.89\ ohms$

Outer resistance blinder $R1R7 = 35.27\ ohms$

Inner reactance blinder $X1T6 = 42.105\ ohms$

Outer reactance blinder $X1T7 = 56.218\ ohms$

OST DELAY:

Total transfer impedance $ZT = 87.685\ ohms$

$$AngR6 = 128.45^0$$

$$AngR7 = 102.37^0$$

For this test system fast unstable swing frequency $f_{slip} = 4Hz$

$$OSTD = \frac{(128.45 - 102.37) * 60}{360 * 4} = 1.0866\ cycles = 18.11\ msec$$

The nearest valid setting for OSTD is 1.125 cycle. The SEL-421 relay settings shown in figure 3.17.

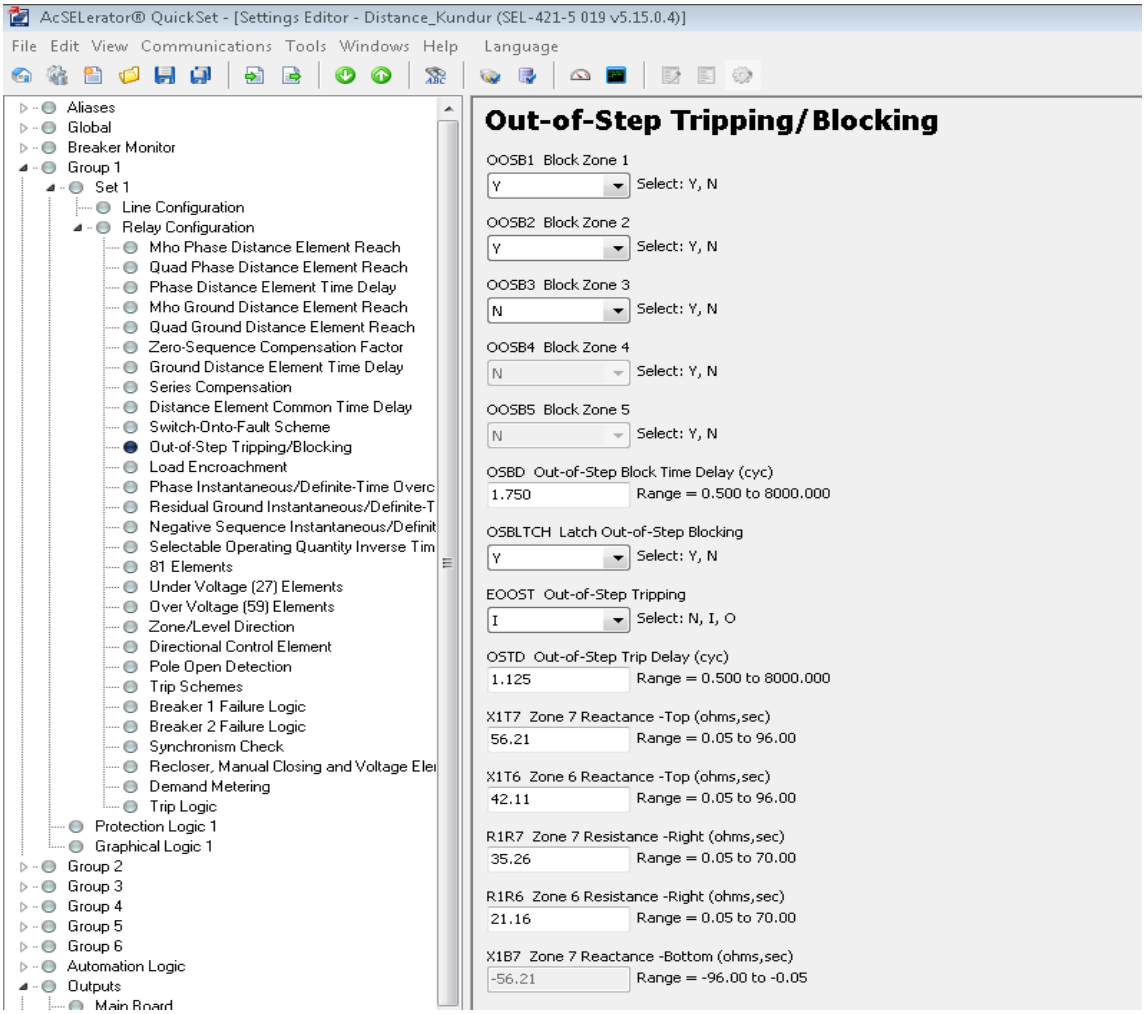

FIGURE 3.17: SEL-421 out-of-step protection settings

The configuration and distance element settings for Relay A and Relay B are shown figures 3.18 and 3.19.

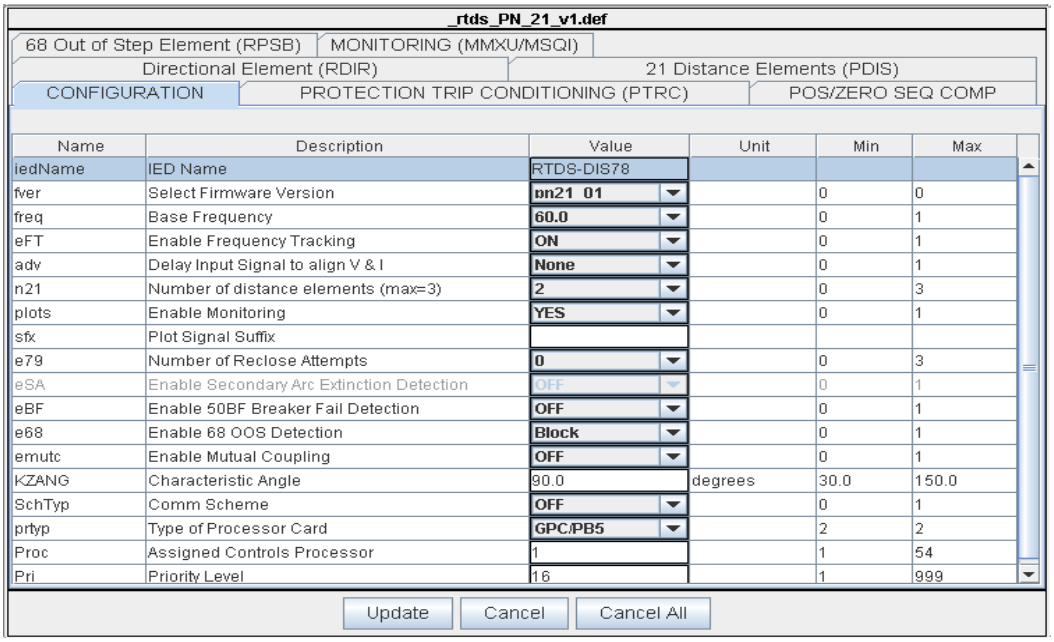

FIGURE 3.18: Configuration settings (21 element)

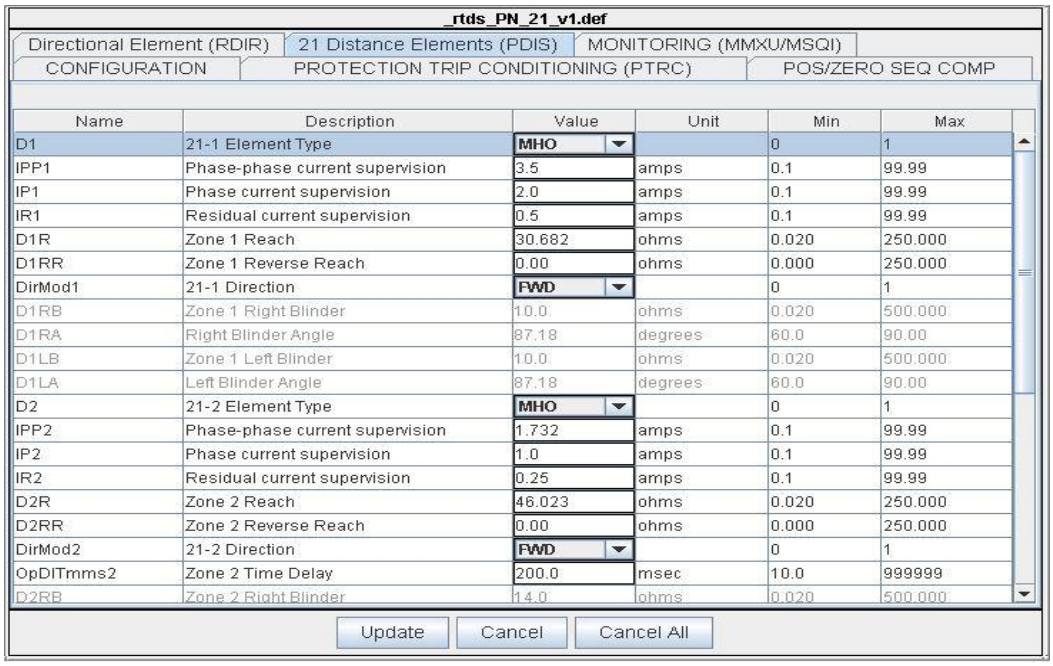

FIGURE 3.19: Distance protection settings (21 element)

3.5. Implementation of Out-of-step Protection using Synchrophasors

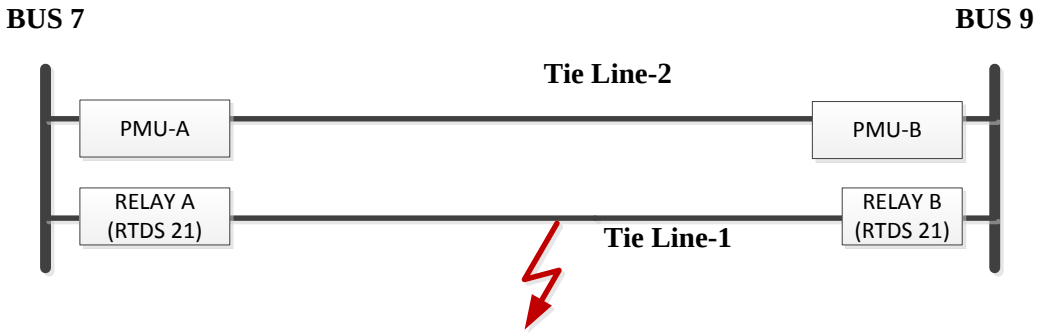

FIGURE 3.20: Test setup for out-of-step protection using synchrophasors

Synchrophasor based scheme require the voltage phasor measurements from the both ends of the tie-line 2. Therefore phasor measurement units PMU-A, PMU-B are located on this line, as shown in figure 3.20. The algorithm is implemented in RTDS and the logic is shown in figure 3.21.

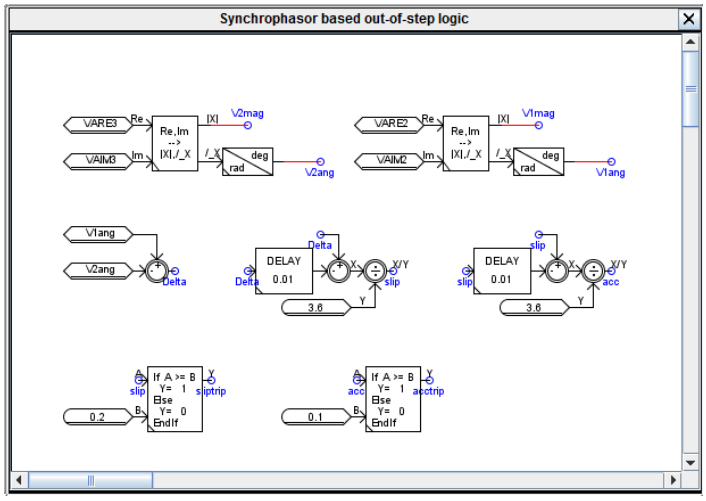

FIGURE 3.21: Synchrophasor based out-of-step scheme logic

3.6. Case Studies

The fault scenarios tabulated in table 3.5 are simulated to compare the out-of-step detection performances of both techniques. In these case the machines present in the test system do not have the power system stabilizers. The plots of machine speeds, line voltages, line currents for all the cases are shown in figures 3.22 to 3.42. The tripping time comparison between dual blinder scheme and synchrophasor based scheme is tabulated in table 3.6.

Table 3.5: Simulated fault scenarios for out-of-step protection

Case	**Description**	**Critical Clearing Time**	**Power Swing**
Case-1	Three phase fault on Bus-7, cleared after 0.2 sec	0.22	Stable
Case-2	Three phase fault on Bus-7, cleared after 0.22sec	0.22	Unstable
Case-3	Three phase fault on Bus-9, cleared after 0.2 sec	0.29	Stable
Case-4	Three phase fault on Bus-9, cleared after 0.3 sec	0.29	Unstable
Case-5	Three phase fault on middle of tie line 2, cleared after 0.5 sec	0.79	Stable
Case-6	Three phase fault on middle of tie line 2, cleared after 0.7 sec	0.79	Stable

Case-7	Three phase fault on middle of tie line 2, cleared after 0.8 sec	0.79	Unstable

Case 1: Three phase fault on bus 7, cleared after 0.2 sec

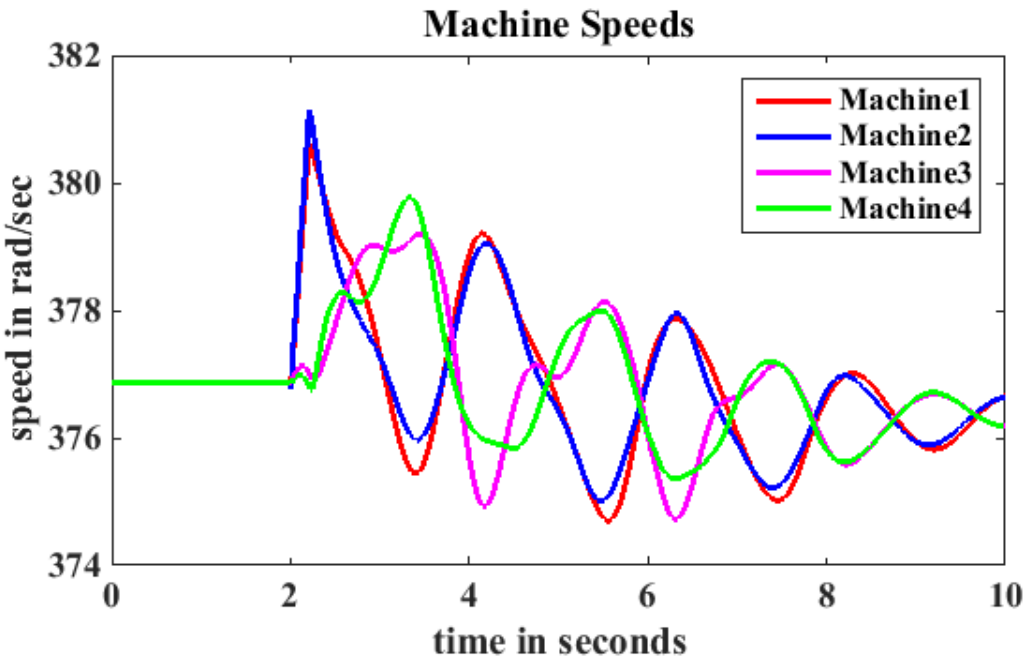

FIGURE 3.22: Machine speeds in Case 1

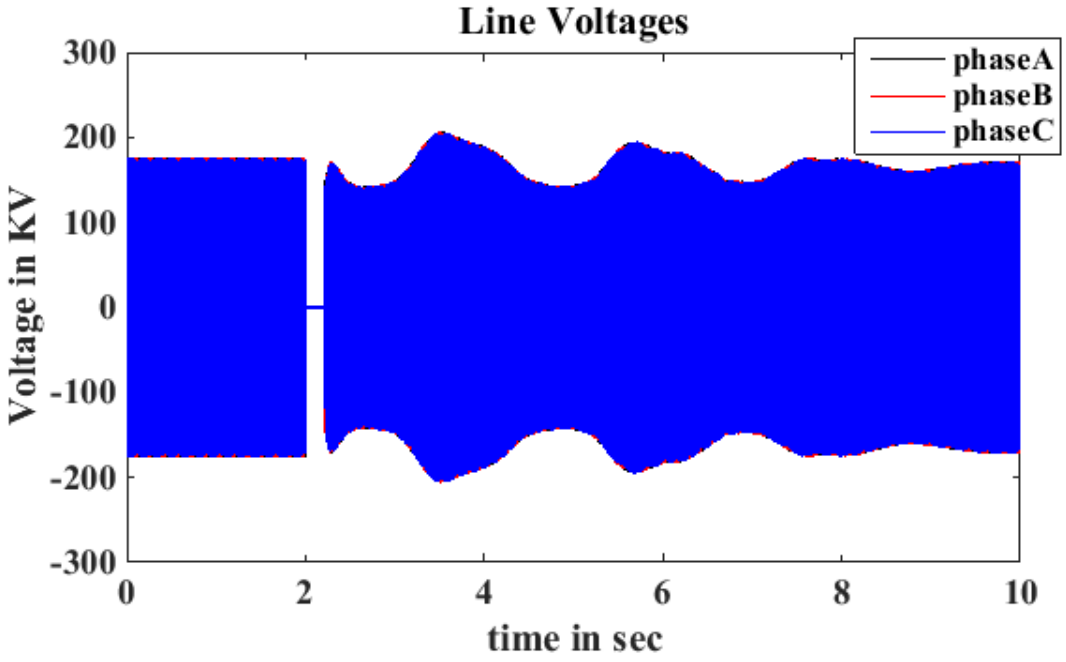

FIGURE 3.23: Tie-line voltages in case 1

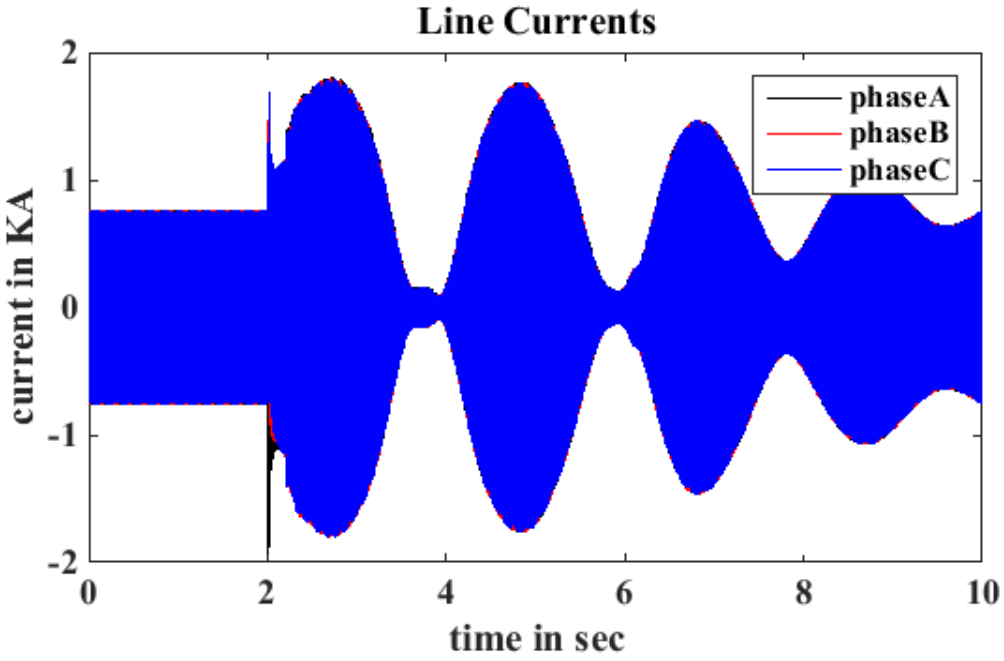

FIGURE 3.24: Tie-line currents in case 1

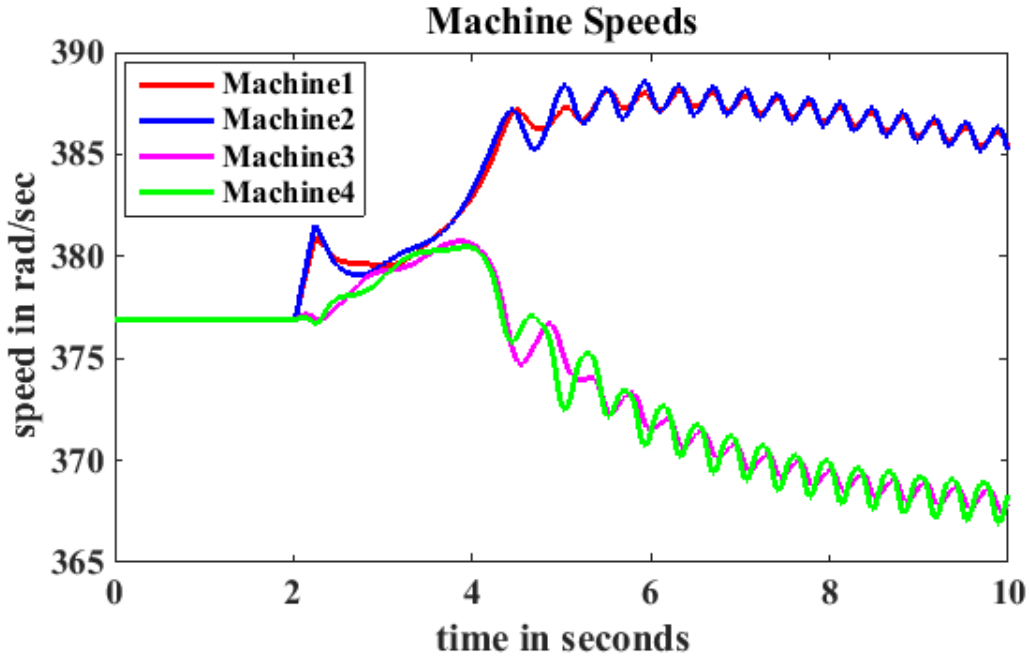

FIGURE 3.25: Machine speeds in case 2

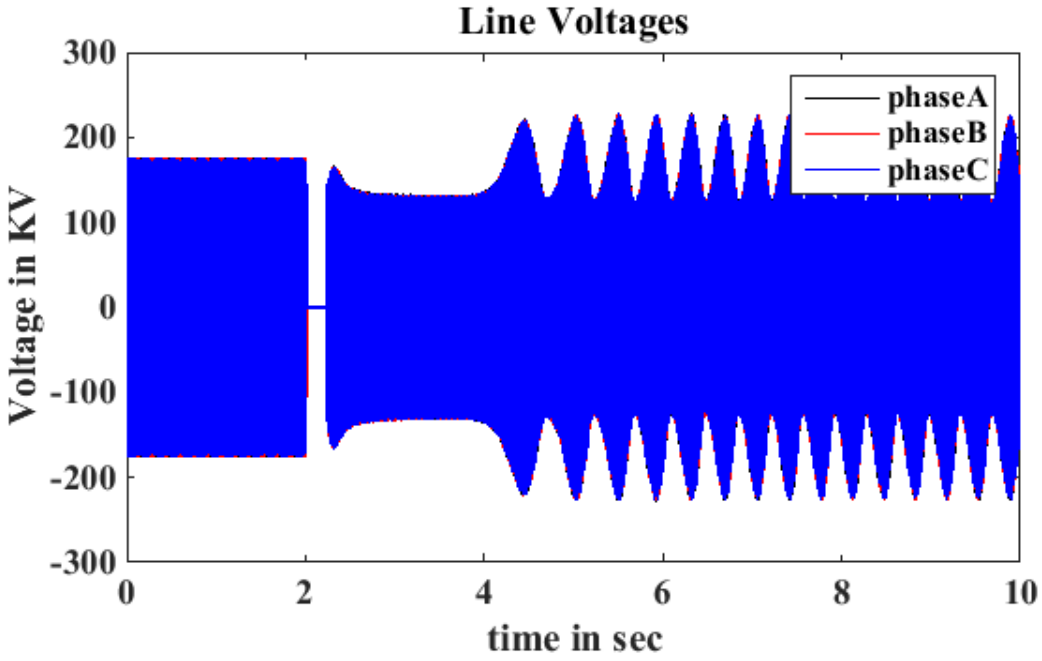

FIGURE 3.26: Tie-line voltages in case 2

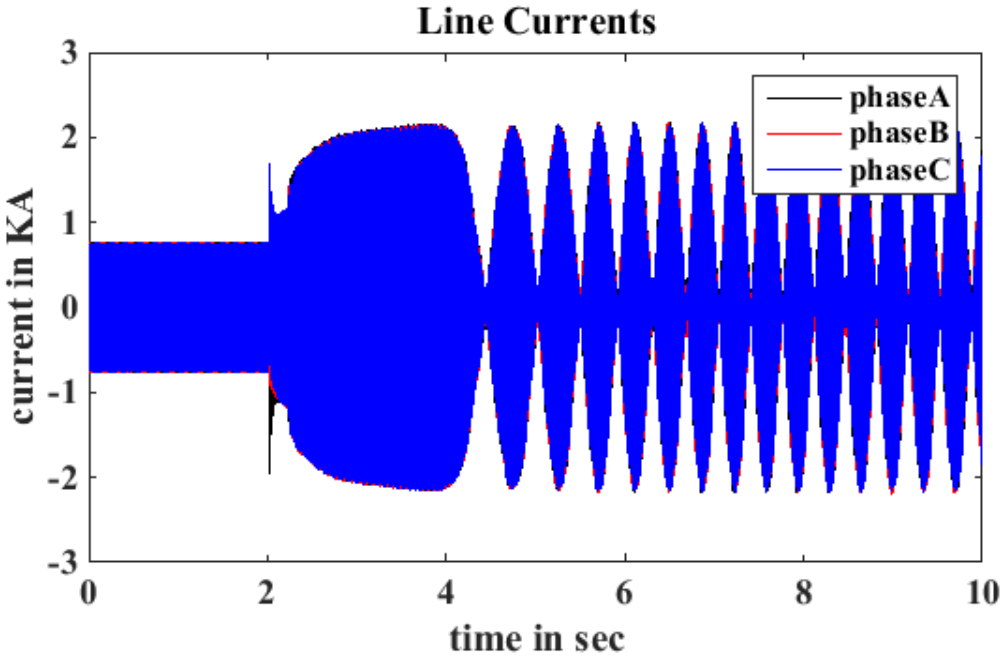

FIGURE 3.27: Tie-line currents in case 2

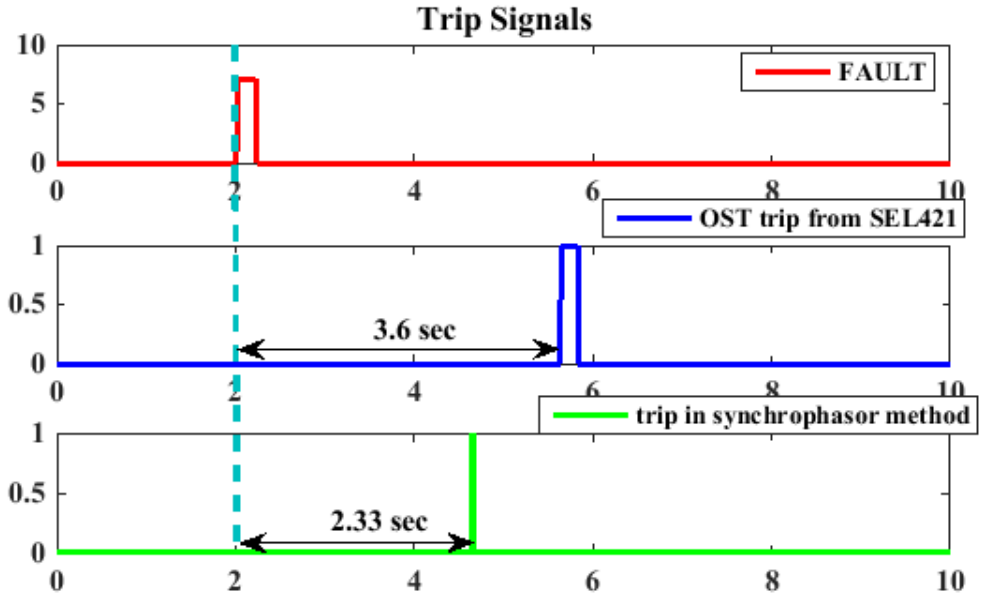

FIGURE 3.28: Trip signals in case 2

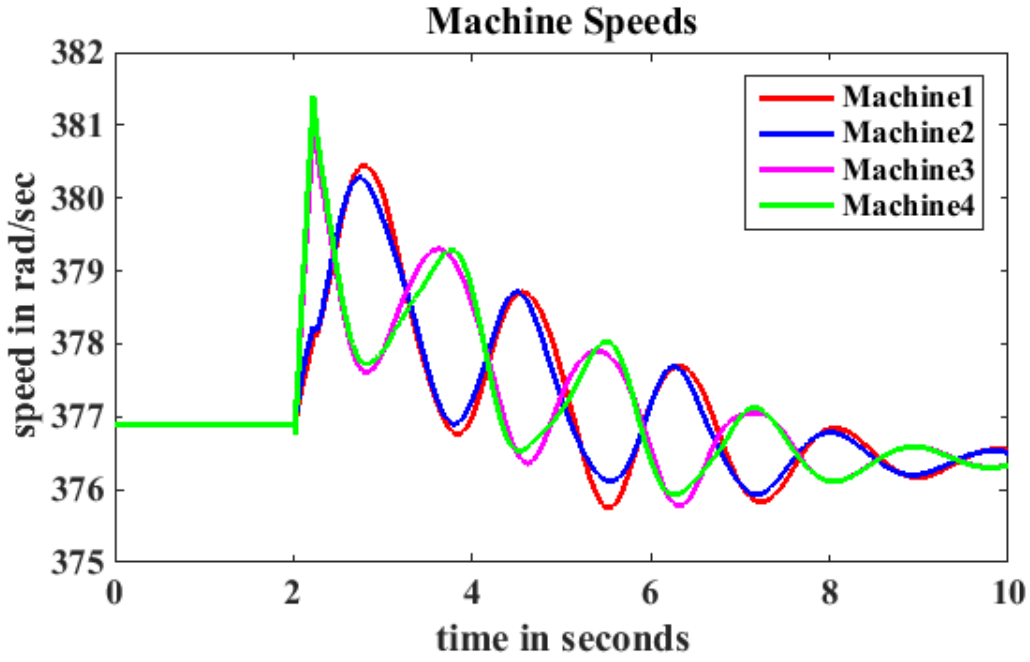

FIGURE 3.29: Machine speeds in case 3

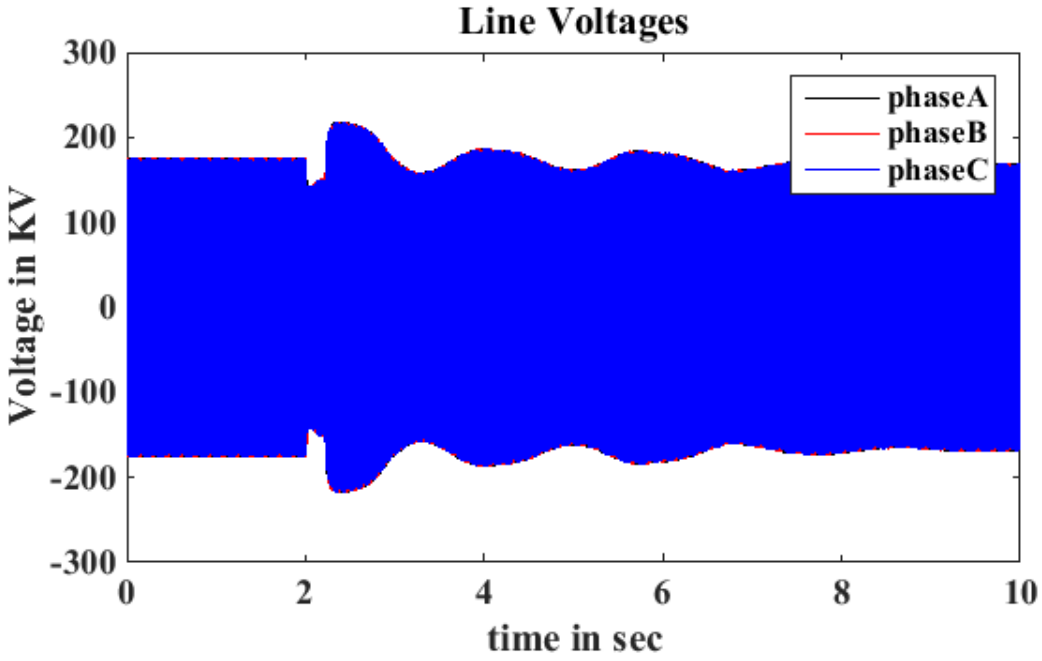

FIGURE 3.30: Tie-line voltages in case 3

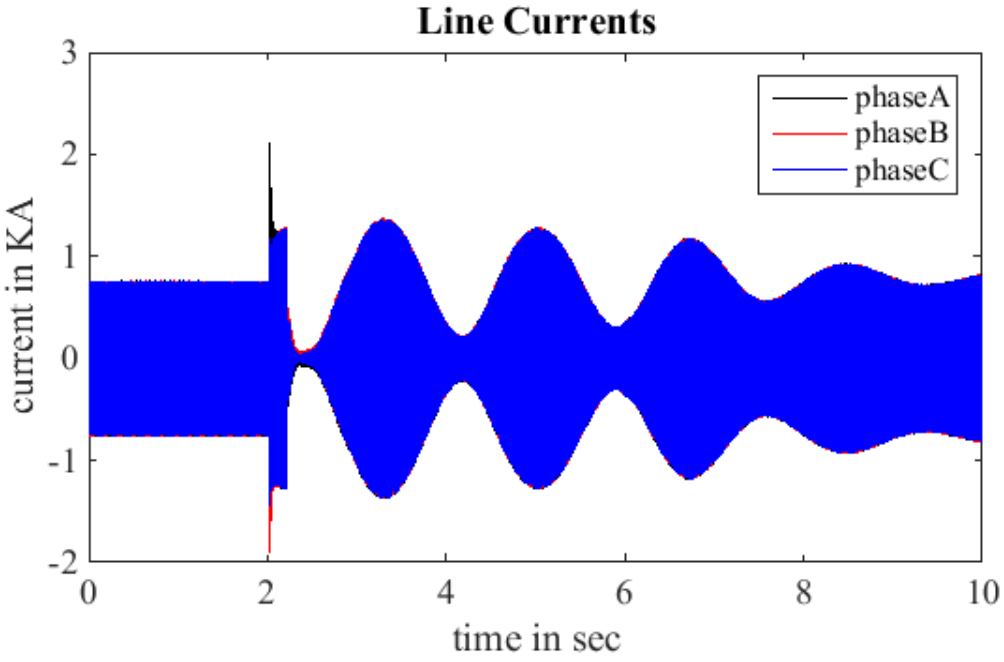

FIGURE 3.31: Tie-line currents in case 3

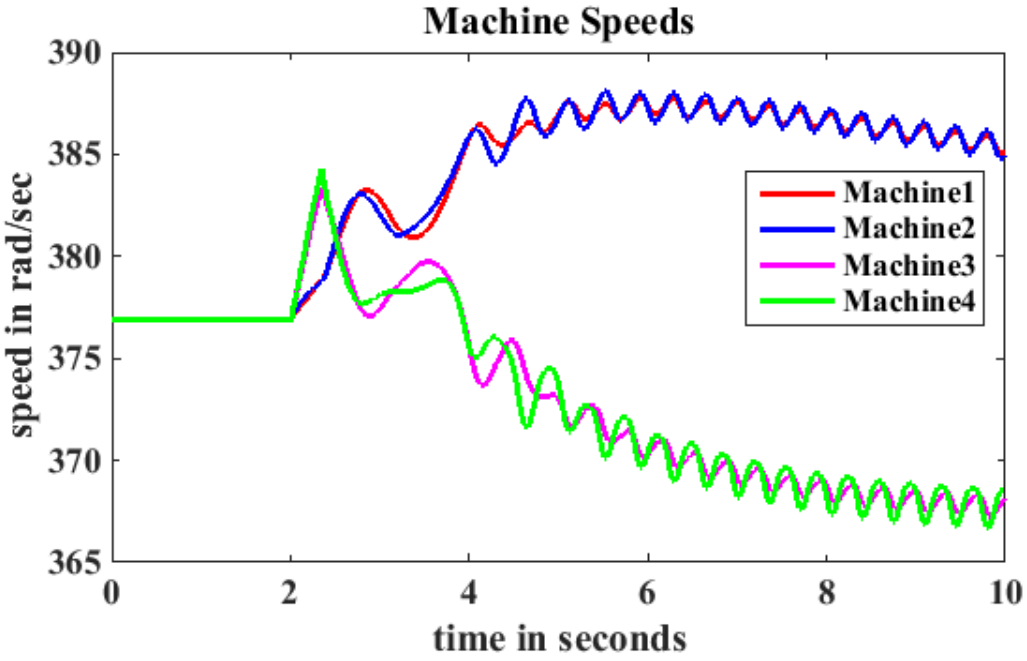

FIGURE 3.32: Machine speeds in case 4

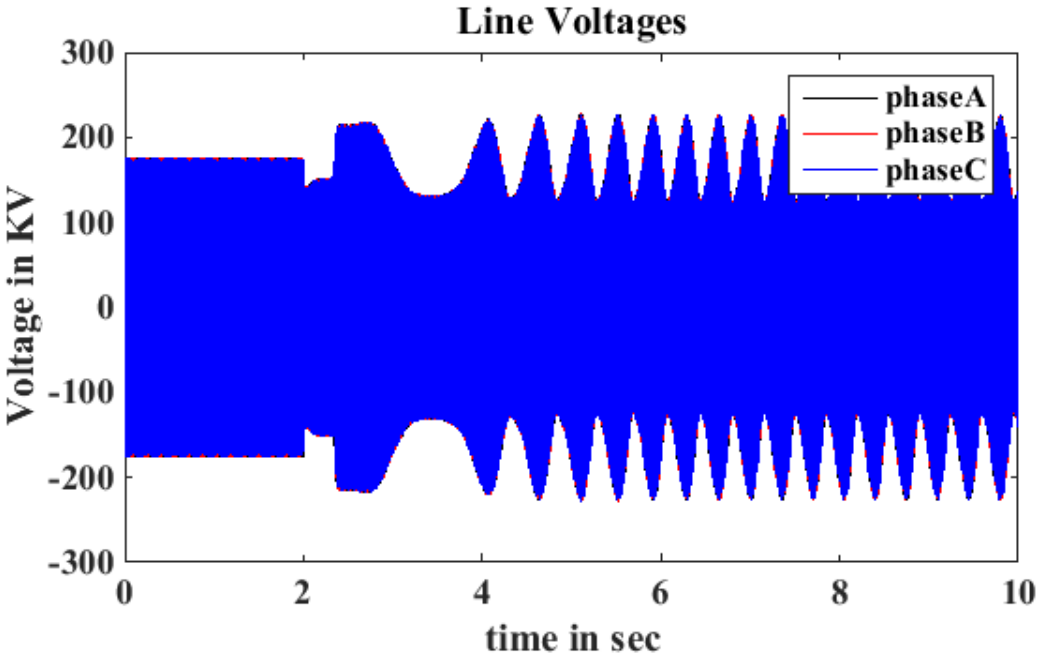

FIGURE 3.33: Tie-line voltages in case 4

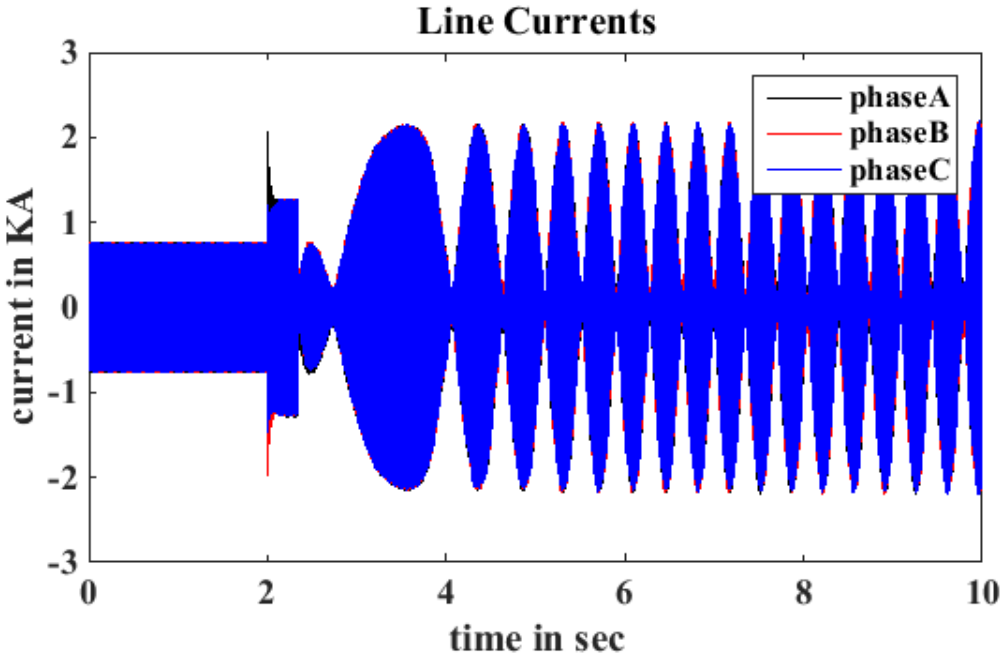

FIGURE 3.34: Tie-line currents in case 4

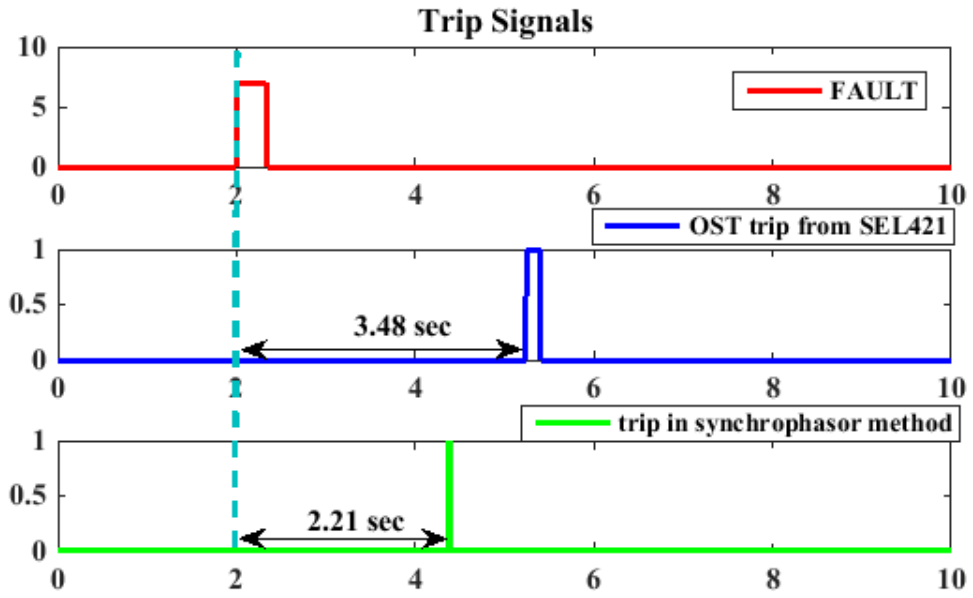

FIGURE 3.35: Trip signals in case 4

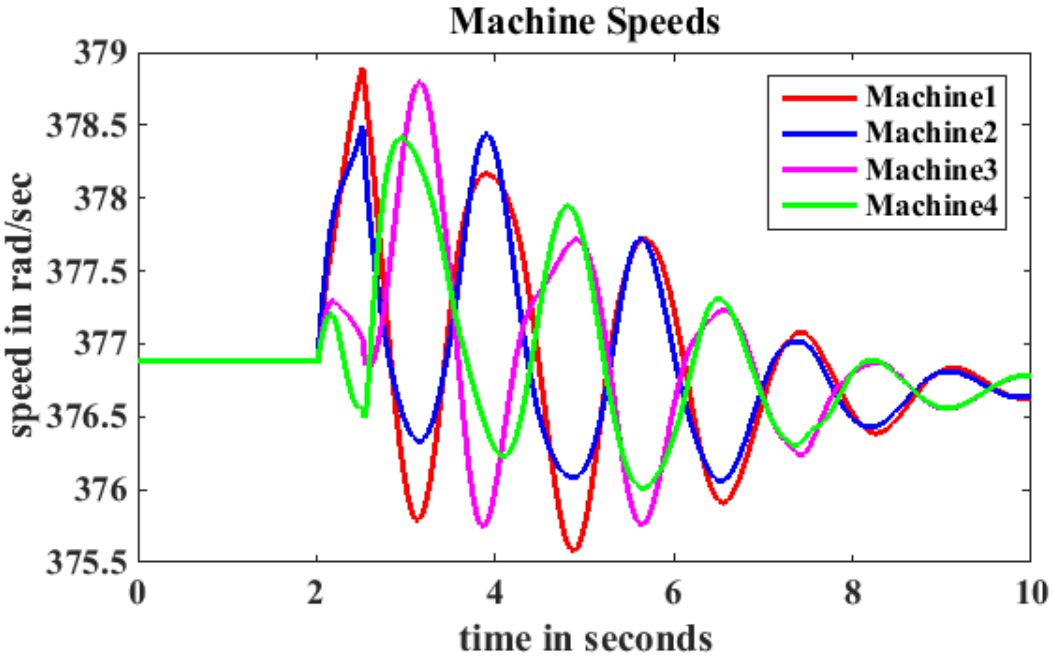

FIGURE 3.36: Machine speeds in case 5

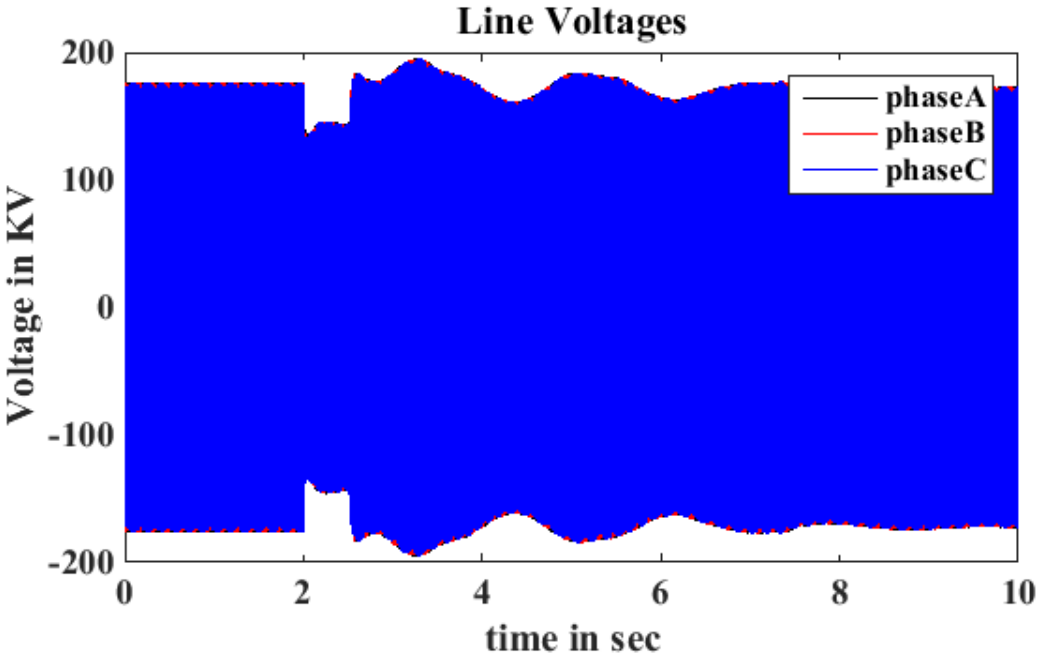

FIGURE 3.37: Tie-line voltages in case 5

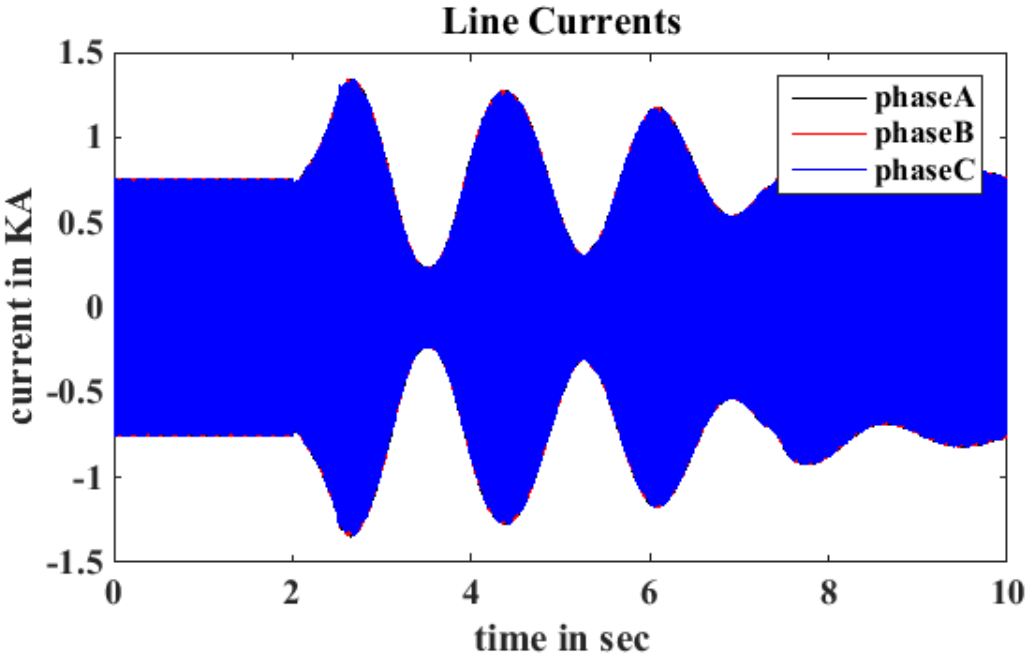

FIGURE 3.38: Tie-line currents in case 5

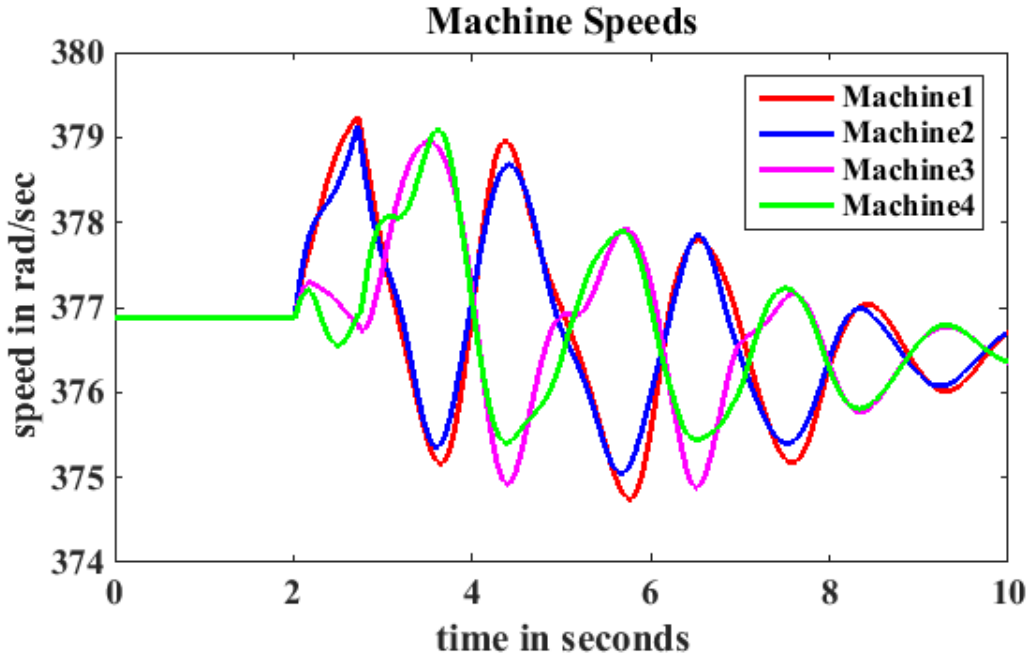

FIGURE 3.39: Machine speeds in case 6

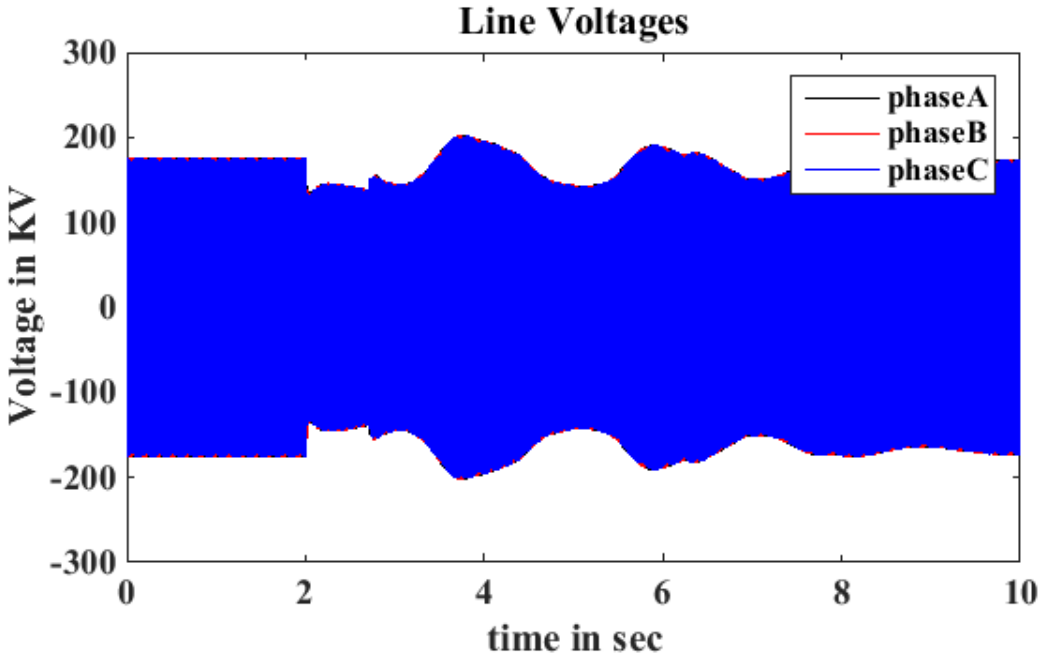

FIGURE 3.40: Tie-line voltages in case 6

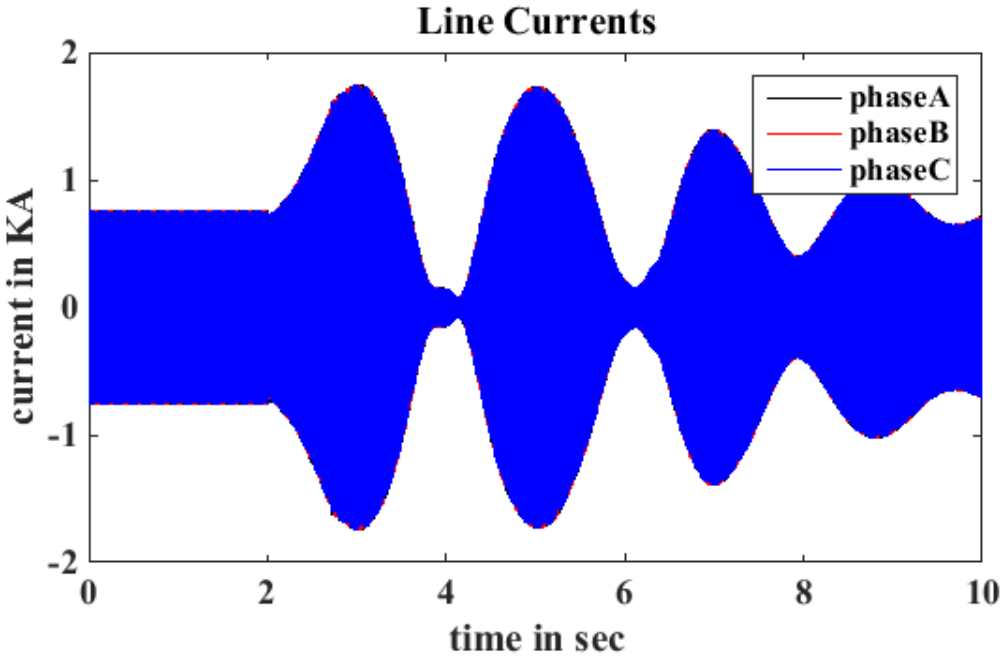

FIGURE 3.41: Tie-line currents in case 6

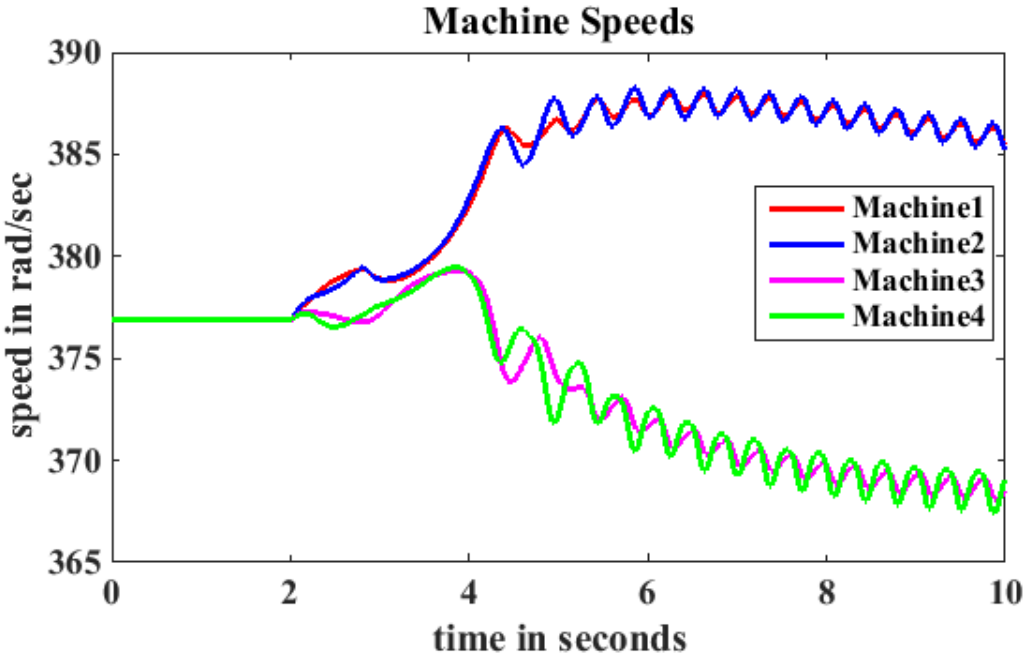

FIGURE 3.42: Machine speeds in case 7

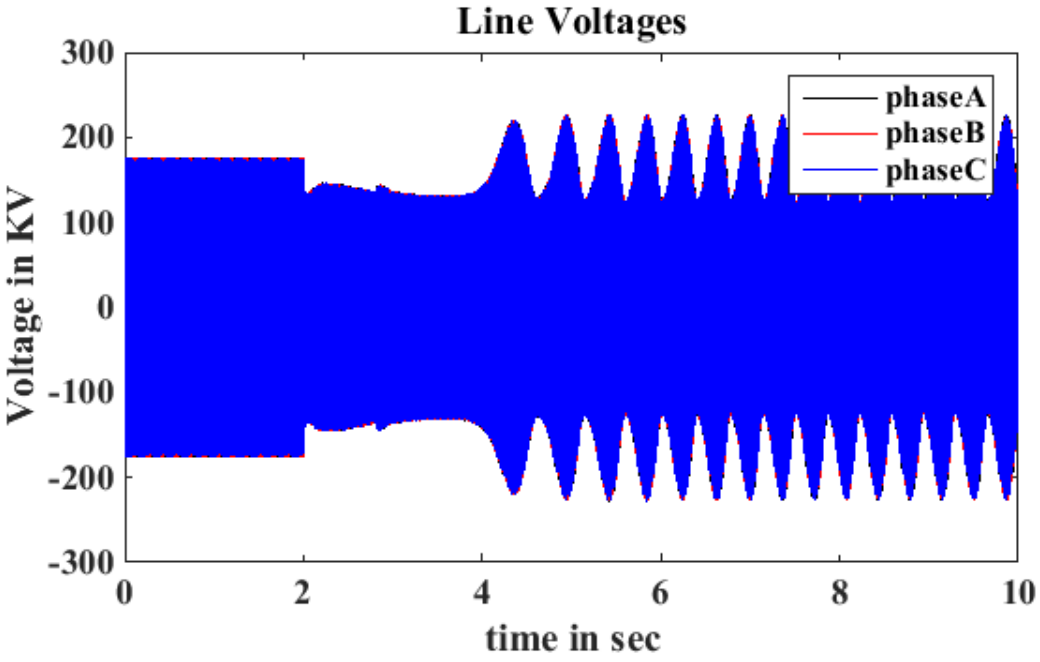

FIGURE 3.43: Tie-line voltages in case 7

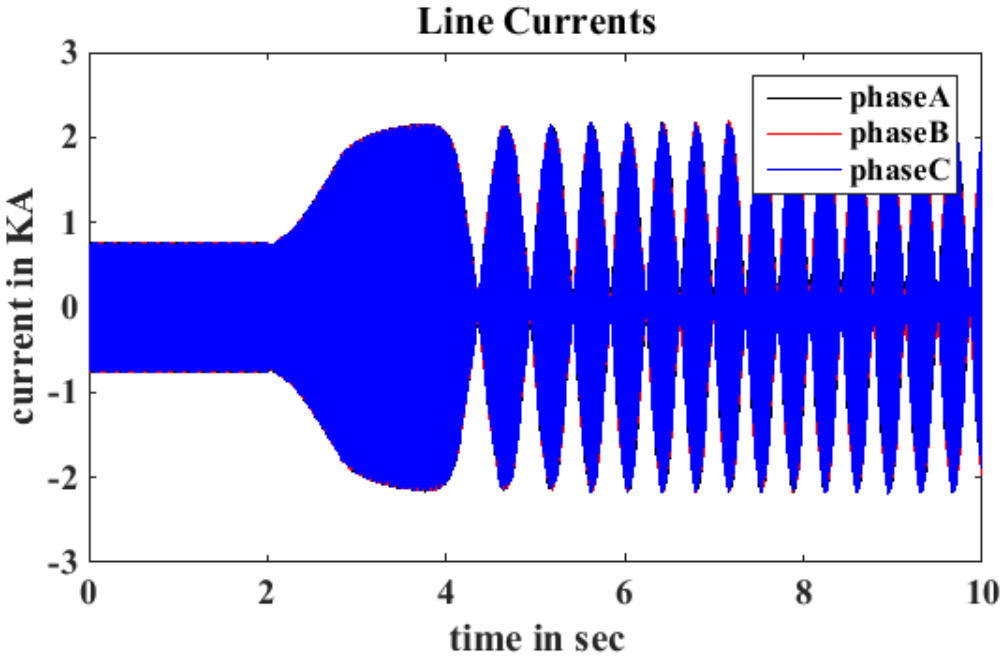

FIGURE 3.44: Tie-line currents in case 7

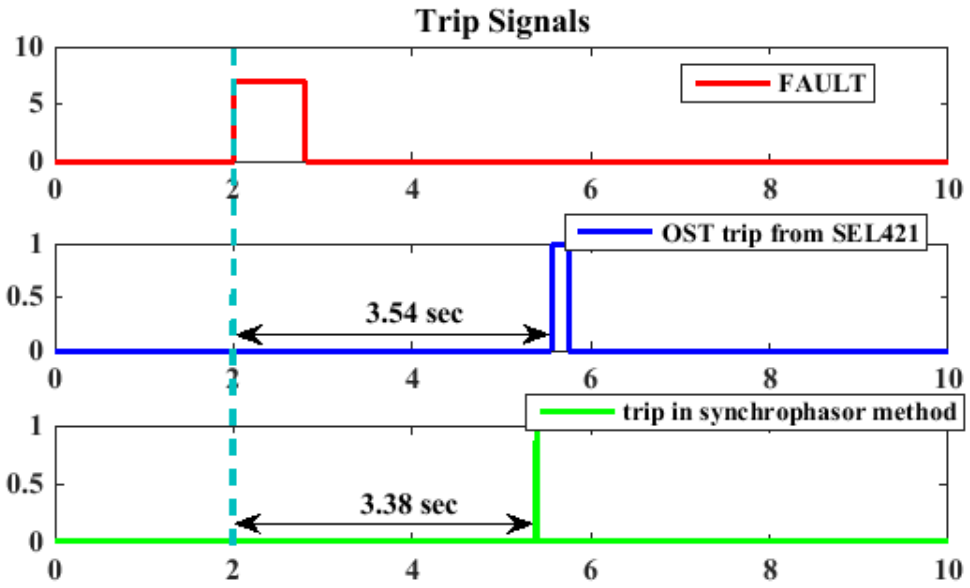

FIGURE 3.45: Trip signals in case 4

Simulation Analysis:

1. Critical clearing time (CCT) is calculated using the time domain simulation analysis. It was observed that CCT in case of bus fault is lower when compared to the line faults.
2. In cases 1, 3, 5 and 6, since the fault clearing time is less than the critical clearing time, the power swings are stable. The machine speeds, Line voltages and Line Currents are eventually going back to the equilibrium position.
3. In cases 2, 4 and 7, the fault is cleared after the CCT and hence the power swings are unstable. The relay trip times using dual blinder method and synchrophasor method are tabulated in table 3.6

Table 3.6: Tripping time comparison between dual blinder method and synchrophasor Method

Case	Tripping Time (Seconds)	
	Dual Blinder Method	Synchrophasor method
Case-1	No trip	No trip
Case-2	3.6	2.33
Case-3	No trip	No trip
Case-4	3.48	2.21
Case-5	No trip	No trip
Case-6	No trip	No trip
Case-7	3.54	3.38

3.7. Summary

In this chapter, the out-of-step protection general design and implementation methodology was described using dual blinder scheme in a two source equivalent power system. The corresponding setting calculations were shown. Moreover, the algorithm for synchrophasor based protection scheme was presented. The performance of these two methods was compared using kundur two area test system using real time digital simulator (RTDS) and SEL-421 numerical relay. The hardware-in-the-loop setup was described with necessary configurations and it is validated by comparing the distance protection scheme using RTDS inbuilt distance component (21). Seven different fault scenarios are simulated in kundur two area test system to compare the performance of the dual blinder scheme and synchrophasor based out-of-step detection scheme. The unstable power swing is the result of transient instability of the system followed by a severe

disturbance like three phase bolted fault. In the next chapter, the transient energy function based out-of-step protection methodology is discussed and implemented in Kundur two area system.

CHAPTER 4 : OUT-OF-STEP PROTECTION USING REAL TIME TRANSIENT STABILITY ANALYSIS

This chapter presents the methodology of out of step protection based on the transient stability assessment techniques using direct methods. The PMUs installed in the power system enables real-time monitoring of the transient swings of the generators and evaluates the total system energy, as a result the dynamic stability of the system is assessed. Section 5.1 presents overview and back ground theory of direct methods and Section 5.2 discusses the out-of-step protection scheme using Transient Energy Function (TEF) method. Further section 5.3 presents the simulation results in Kundur two area test system. Section 5.4 gives the summary of the chapter.

4.1. Theoretical Background of the Direct Methods

Conventional transient stability analysis methods are based on numerical integration of differential equations that represents the power system during and after a disturbance occurrence. Despite the fact that these methods are highly accurate, they cannot be used in online and real-time applications since huge computational effort required. Direct methods are the alternative approaches that do not involve huge number of integrations. A direct method for transient stability is defined as the method that is able to determine the stability without explicitly integrating the differential equations that describe the post fault system. As a result these methods are best suited for real-time applications.

In 1892, A.M. Lyapunov proposed that the stability of the equilibrium point of a non-linear dynamic system of dimension n,

$$\dot{x} = f(x), f(0) = 0 \qquad (4.1)$$

Can be determined without the numerical integration. Lyapunov's theorem states that if there exists a scalar function V(x) for equation 5.1 that is positive definite around the equilibrium point and its derivative $\dot{V}(x) < 0$, then the equilibrium is asymptotically stable. V(x) is the generalization of the concept of energy of the system. This energy based method to determine the stability of the system began with early work of Magnusson [47] and Aylett [48]. Although many different functions have been tried since then, the sum of the kinetic and potential energies of the system has provided the best result. Hence in power literature, the Lyapunov's method is called as Transient Energy Function (TEF) method.

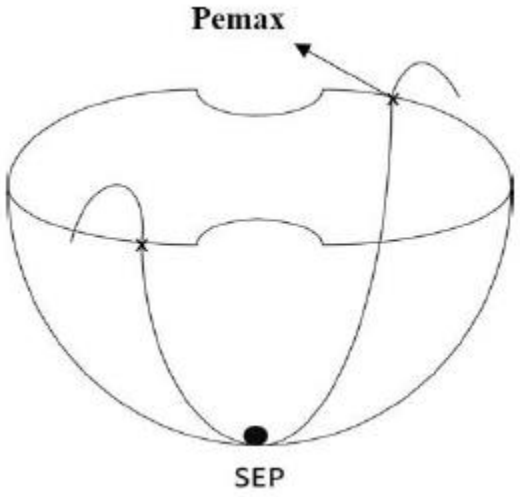

FIGURE 4.1: Rolling ball in a bowl analogy [49].

Transient energy approach can be described by a ball rolling on the inner surface of a bowl as depicted in Figure 4.1. Initially the ball is resting which is equivalent to a power system in its steady state equilibrium. When an external force is applied to the ball, the ball

moves away from the equilibrium point. Equivalently, in power system, a fault occurs on the system which causes the generator rotors to accelerate and gain some kinetic energy causing the system to move away from Stable Equilibrium Point (SEP). If the ball converts all its kinetic energy into potential energy before reaching the rim, then it will roll back and settle down at the SEP eventually. In power systems, after the fault is cleared, the kinetic energy gained during the fault will be converted into potential energy if the system is capable enough to absorb that kinetic energy. Otherwise, the kinetic energy will increase causing the synchronous generators to lose synchronism and become unstable [49].

4.1.1. Mathematical Formulation

The sum of kinetic energy (KE) and the potential energy (PE) for a conservative system is constant. The expression for total energy can be expressed in terms of KE and PE. In case of power systems the total system is represented by classical model i.e. the synchronous generators are modeled as a constant voltage source behind transient reactance and loads are modelled as constant admittances. For this model, the physical motion of the generators is governed by the set of differential equations

$$M_i\dot{\omega}_i + D_i\omega_i = P_i - P_{ei} \qquad (4.2)$$

$$\dot{\delta}_i = \omega_i \qquad (4.3)$$

Where for machine i

δ_i Angle of voltage behind transient reactance, indicative of rotor position

ω_i Rotor speed

M_i Generator inertia constant,

D_i Damping coefficient.

The expressions of P_i and P_{ei} are given by

$$P_i = P_{mi} - E_i^2 G_{ii} \qquad (4.4)$$

$$P_{ei} = \sum_{\substack{j=1 \\ j \neq i}}^{n} \left[C_{ij} \sin\left(\delta_i - \delta_j\right) + D_{ij} \cos\left(\delta_i - \delta_j\right) \right] \qquad (4.5)$$

Where,

$$C_{ij} = E_i E_j B_{ij}$$

$$D_{ij} = E_i E_j G_{ij}$$

P_{mi} mechanical power input,

E_i magnitude of voltage behind reactance,

G_{ii} real part of ith diagonal element of the network's Y-bus matrix,

G_{ij}, B_{ij} real and imaginary components of ijth element of network's Y bus matrix.

Good physical insight into the behavior of the synchronous generators is obtained when their motion is expressed with respect to machines center of inertia (COI). The position of COI is defined by

$$\delta_0 = \frac{1}{M_T} \sum_{i=1}^{n} M_i \delta_i \qquad (4.6)$$

Here $M_T = \sum_{i=1}^{n} M_i$

We define θ_i and $\widetilde{\omega_i}$ by

$$\theta_i = \delta_i - \delta_0$$

$$\omega_i = \dot{\theta}_i = \omega_i - \omega_0$$

Finally we can derive that the equations of motion with respect to center of inertia (COI) reference as in the form

$$M_i\dot{\tilde{\omega}}_i = -D_i\tilde{\omega}_i + P_i - P_{ei} - \frac{M_i}{M_T}P_{COI} \qquad (4.7)$$

$$\dot{\theta}_i = \tilde{\omega}_i, \qquad i = 1, 2, \ldots . n. \qquad (4.8)$$

Furthermore when damping is neglected, the system motion is described by the equations

$$M_i\dot{\tilde{\omega}}_i = P_i - P_{ei} - \frac{M_i}{M_T}P_{COI} \qquad (4.9)$$

$$\dot{\theta}_i = \tilde{\omega}_i, \qquad i = 1, 2, \ldots . n. \qquad (4.10)$$

Next, we develop an expression for individual machine transient energy. Multiplying the i-th post-fault swing equation by $\dot{\theta}_\iota$ and rearranging, we obtain the expression

$$\left[M_i\dot{\tilde{\omega}}_i - P_i + P_{ei} + \frac{M_i}{M_T}P_{COI} \right]\dot{\theta}_i, \qquad i = 1, 2, \ldots, n. \qquad (4.11)$$

Integrating (4.11) with respect to time, using lower limit $t = t_s$, where $\tilde{\omega}(t_s) = 0$ and $\theta(t_s) = \theta^s$ is the stable equilibrium point (SEP), yields

$$V_i = \frac{1}{2}M_i\tilde{\omega}_i^2 - P_i\left(\theta_i - \theta_i^s\right) + \sum_{\substack{j=1 \\ j\neq i}}^{n} C_{ij}\int_{\theta_i^s}^{\theta_i} sin\theta_{ij}\, d\theta_i +$$

$$\sum_{\substack{j=1 \\ j\neq i}}^{n} D_{ij}\int_{\theta_i^s}^{\theta_i} cos\theta_{ij}\, d\theta_i + \frac{M_i}{M_T}\int_{\theta_i^s}^{\theta_i} P_{COI}\, d\theta_i \ , \qquad i = 1, 2, \ldots ., n. \qquad (4.12)$$

This integral is evaluated using the values of $\theta_i, \theta_j, \widetilde{\omega_\iota}$ as obtained from the solution of equation (4.9) and using the values $C_{ij}, D_{ij}\ and\ \theta_i^s$ for the post disturbance network. The first on the right hand side of (4.12) is the kinetic energy of the system inertial center. The remaining terms are considered as the potential energy.

The expression for transient energy is derived for individual machine. The total can be obtained by summing up all the individual machines transient energies and the final expression is derived as

$$V = \frac{1}{2}\sum_{i=1}^{m} M_i \tilde{\omega}_i^2 - \sum_{i=1}^{m} P_i \left(\theta_i - \theta_i^s\right)$$

$$-\sum_{i=1}^{n-1}\sum_{j=i+1}^{n}\left[C_{ij}\left(cos\theta_{ij} - cos\theta_{ij}^s\right) - \int_{\theta_i^s+\theta_j^s}^{\theta_i+\theta_j} D_{ij} cos\theta_{ij}\, d\left(\theta_i - \theta_j\right)\right] \qquad (4.13)$$

Where

M_i Moment of inertia of machine i,

$\widetilde{\omega_i}$ ith generator rotor speed with respect to COI,

θ_i ith generator rotor angle with respect to COI,

θ_s ith generator rotor angle at SEP with respect to COI,

$\theta_{ij} = \theta_i - \theta_j$

The total transient energy of the system V can be expressed as

$$V = V_{KE} + V_{PE} + V_{ME} + V_{DE}$$

where

V_{KE} is the change in kinetic energy relative to COI,

V_{PE} is the change in potential energy with respect to COI,

V_{ME} is the magnetic stored energy in all the branches,

V_{DE} is the dissipated energy in all the branches.

The dissipated energy can be approximated as

$$\sum_{i=1}^{n-1}\sum_{j=i+1}^{n}\left[\int_{\theta_i^s+\theta_j^s}^{\theta_i+\theta_j} D_{ij}cos\theta_{ij}d\left(\theta_i-\theta_j\right)\right]=-\sum_{i=1}^{n-1}\sum_{j=i+1}^{n}\left[D_{ij}\frac{\delta_i+\delta_j-\delta_i^{\,s}-\delta_j^{\,s}}{\delta_i-\delta_j-\left(\delta_i^{\,s}-\delta_j^{\,s}\right)}\right]\left(sin\delta_{ij}-sin\delta_{ij}^{s}\right) \qquad (4.14)$$

4.1.2. Transient Stability Assessment

In a multi machine power system, during a disturbance, transient energy is injected into the system causing the total energy V to increase which causes the machine i to diverge from its equilibrium point. When the fault is cleared, the machine's gained Kinetic energy of the system is converted into PE. This process continues until the initial KE is converted totally into PE causing the system to converge towards a stable equilibrium point. However, if the KE of the machine i is not converted totally into PE, then it loses synchronism and separates from the system. By using the total energy of the system, the boundary of the region of stability is determined by hypersurfaces which passes through the saddle points. These hypersurfaces are from the Potential Energy Boundary Surface (PEBS). At the PEBS, the potential energy is maximum as well as on the boundary of region of instability. The system maintain stability if the total kinetic energy is converted into potential energy before reaching the PEBS.

4.2. Out-of-step Protection Scheme using TEF Methods

As mentioned in the Chapter 2, nowadays, out-of-step protection is based on impedance relays that monitor the impedance trajectory at the terminals of the generator or the transmission line. For the present state-of-the-art out-of-step protection, the most common scheme is a mho relay with single blinder or double blinder set. Specifically, the impedance trajectory is monitored and instability is detected when there is a crossing on the two blinder (right and left). The major disadvantage of this scheme is that the instability

is detected when the unit has already slipped the pole. Furthermore, additional delay of tripping may be needed to avoid breaker overstresses in case of high generator torque angle differences.

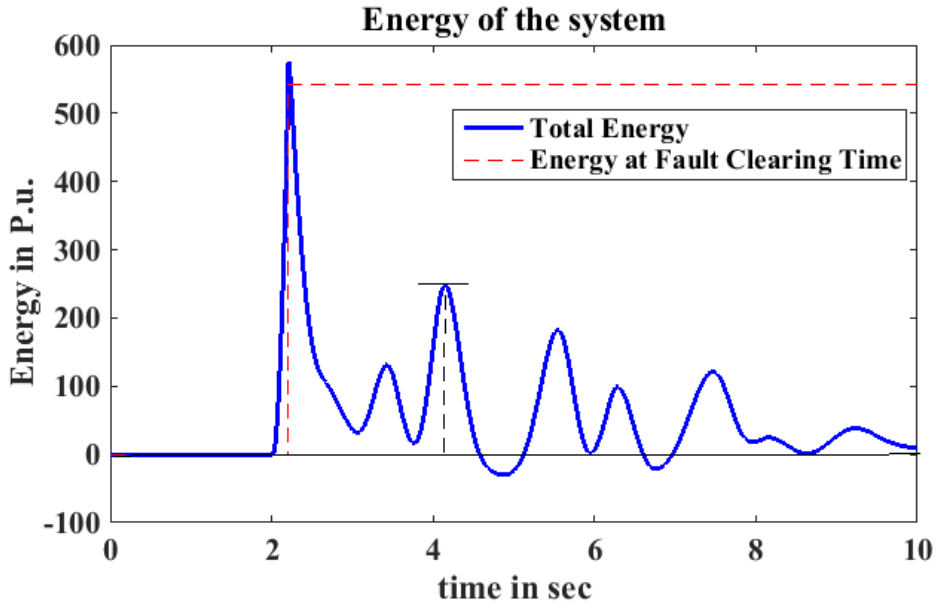

FIGURE 4.2: Typical total energy curve for stable power swing

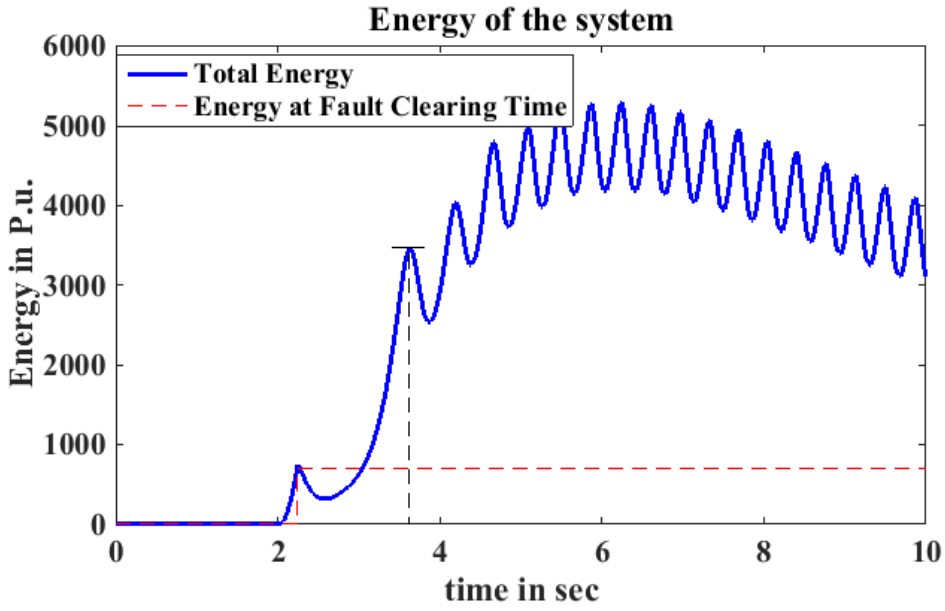

FIGURE 4.3: Typical total energy curve for unstable power swing

Figure 4.2 and 4.3 illustrates total energy trajectory in both stable and unstable power swing situations. The total energy of the generator is computed at each time step using the equations 4.13 and 4.14. The total energy of the system at the fault clearing time is the sum of KE acquired by the system and PE due to the machine rotor angle deviations. If the fault clearing time is less than the critical clearing time (CCT), the energy acquired is absorbed by the system in the successive time steps. The consecutive maxima of the energy curve is observed and it is less than the energy at fault clearing time, then stable power swing is ascertained. If the following maxima of the energy function is more than the energy at fault clearing time, unstable power swing is detected and the corresponding protective and control actions will be taken. The measurements of machine rotor angles and speeds are obtained from the synchrophasor measurements from PMU's located at the machine terminal buses using dynamic state estimation techniques. The Algorithm flowchart is depicted in figure 4.4.

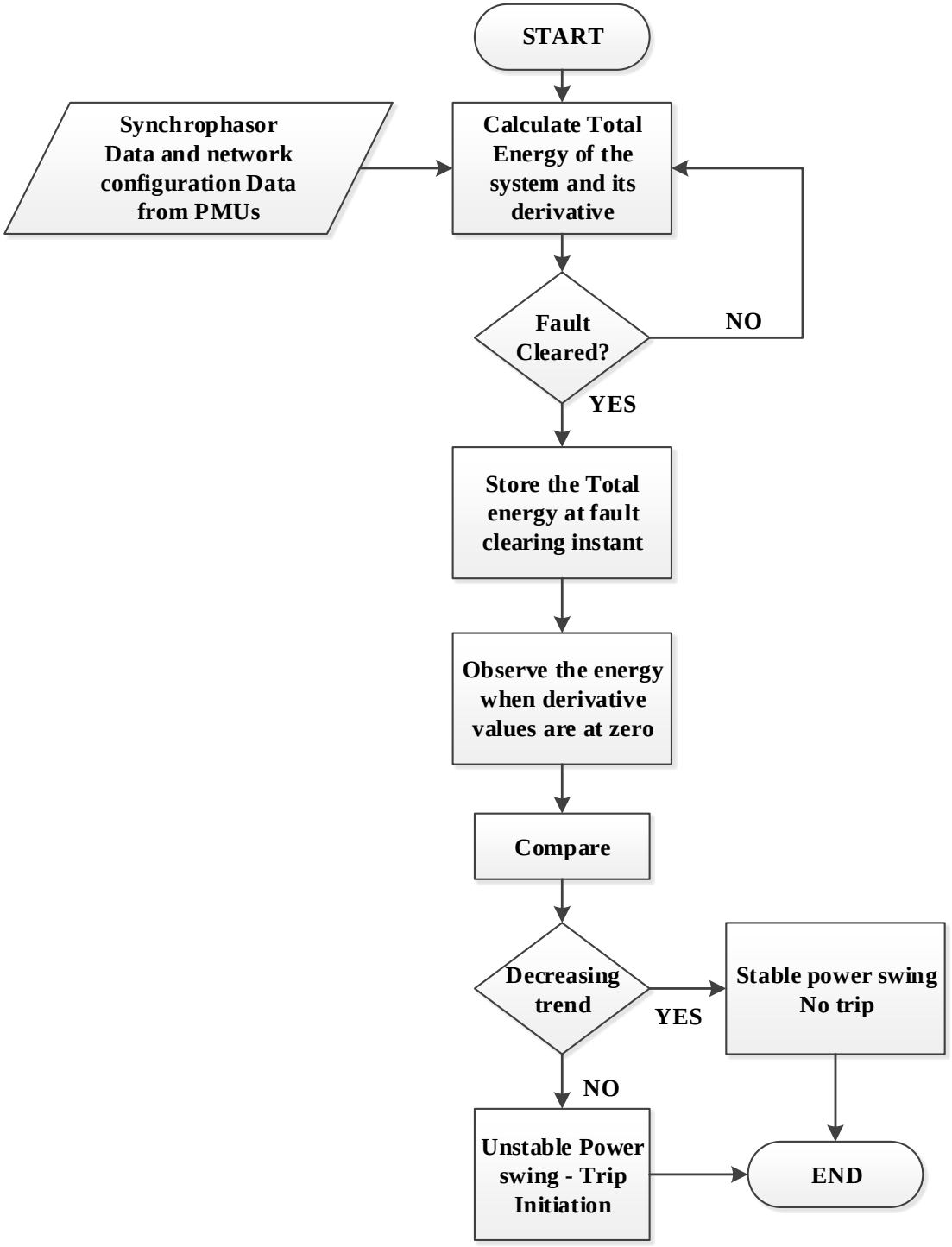

FIGURE 4.4: Algorithm flowchart for TEF Method

4.3. Simulation Results

The proposed out-of-step protection scheme is tested on Kundur two area system which was already described in section 3.2. The same test scenarios in table 3.5 are simulated in RTDS RSCAD and the tripping times are compared with dual blinder method and synchrophasor based method. COI reference frame is used for generators and loads are modeled as constant impedances.

Case 1: Three phase fault on Bus-7 for 0.2 sec

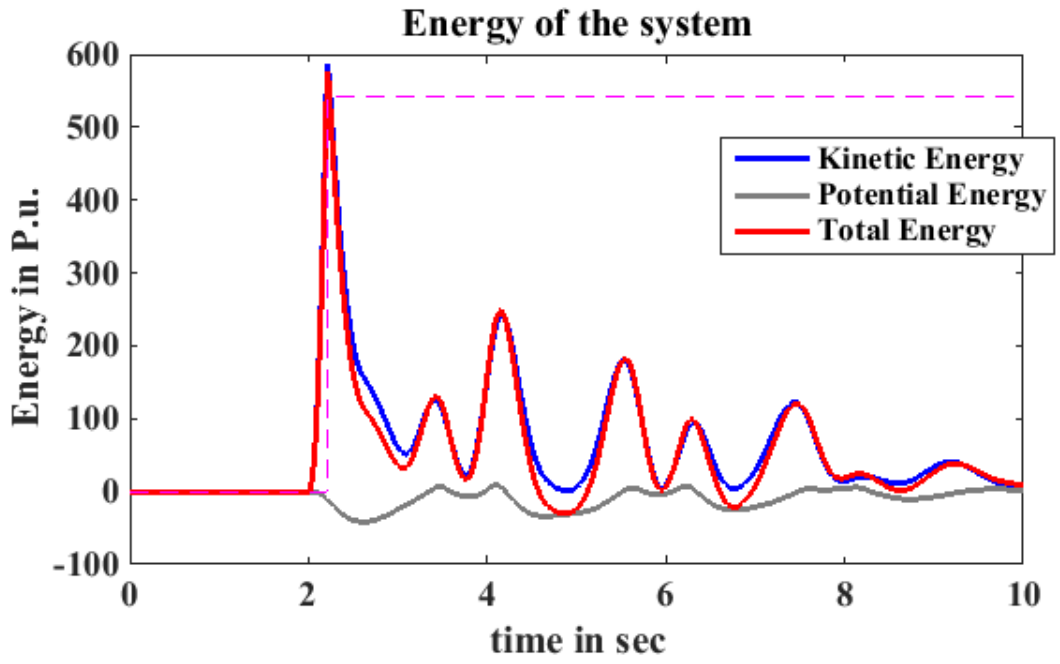

FIGURE 4.5: Energy curves in case 1

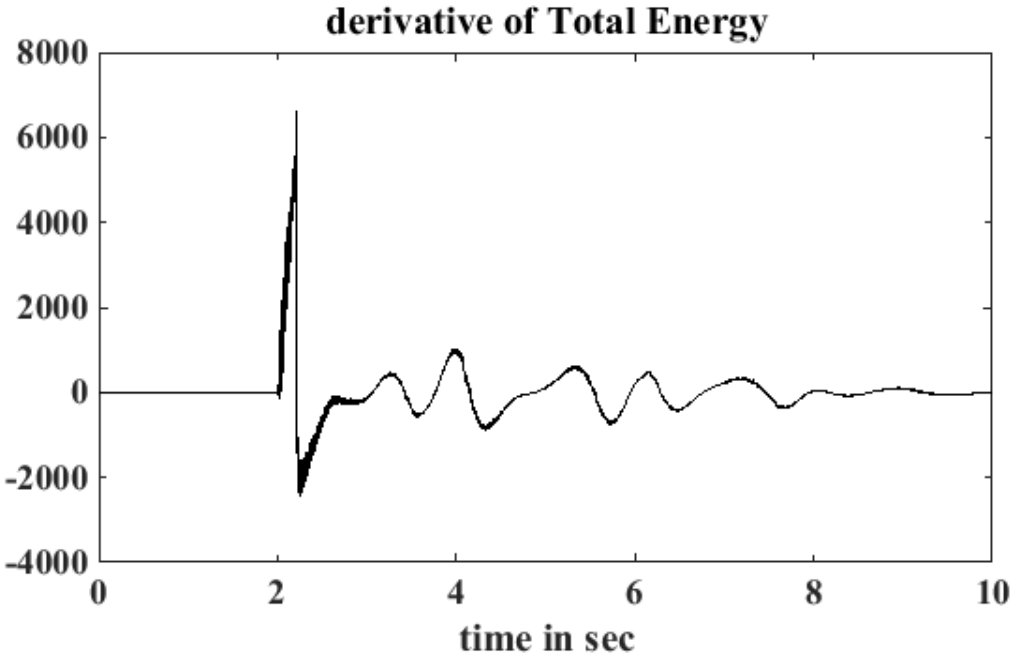

FIGURE 4.6: Derivative of energy in case 1

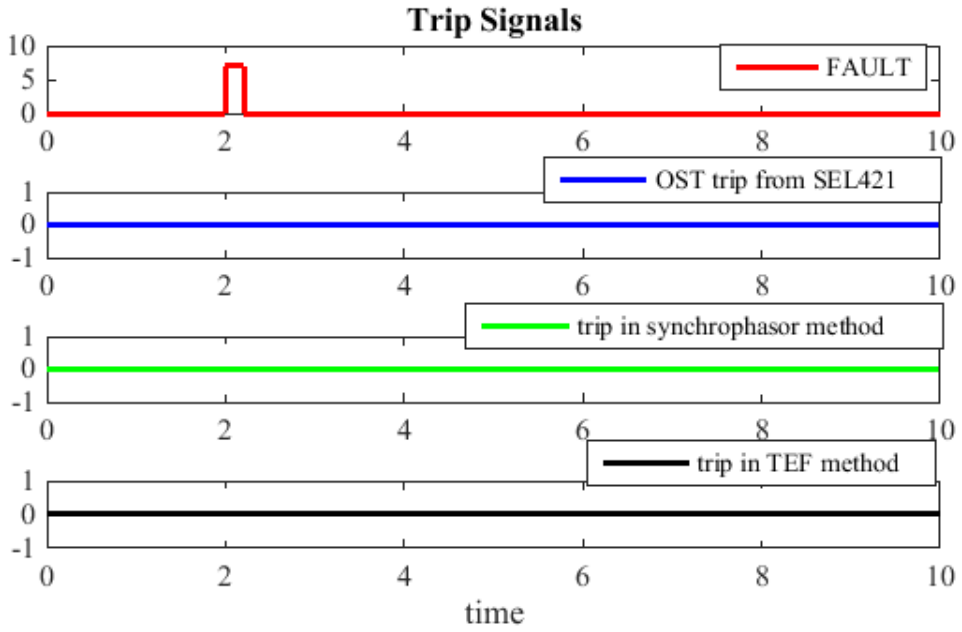

FIGURE 4.7: Trip signals in case 1

Case 2: Three phase fault on Bus-7 for 0.22 sec

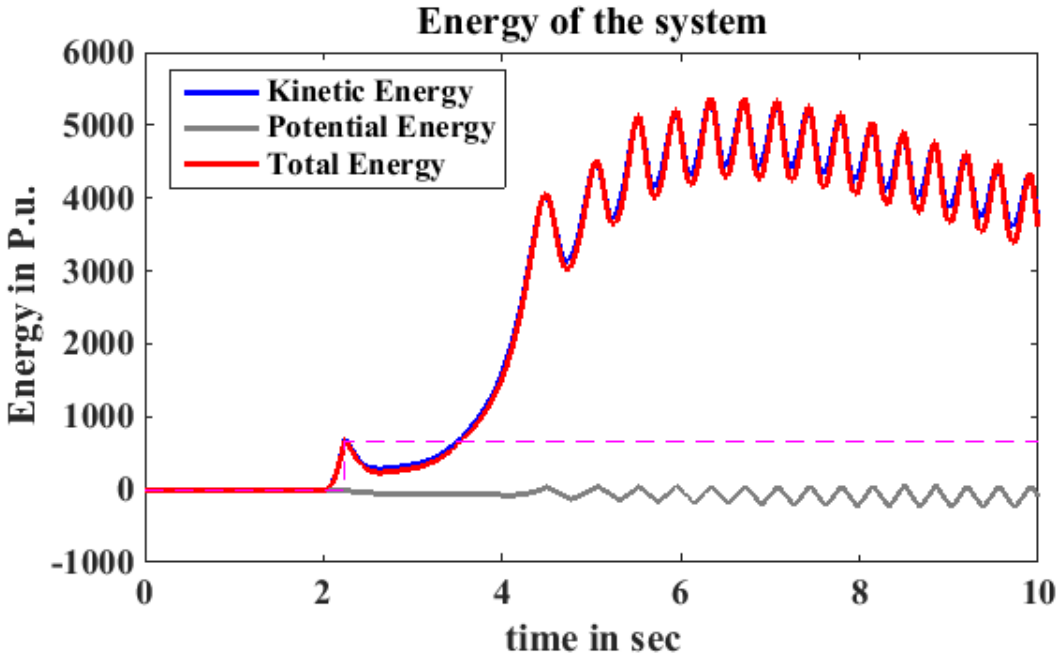

FIGURE 4.8: Energy Curves in case 2

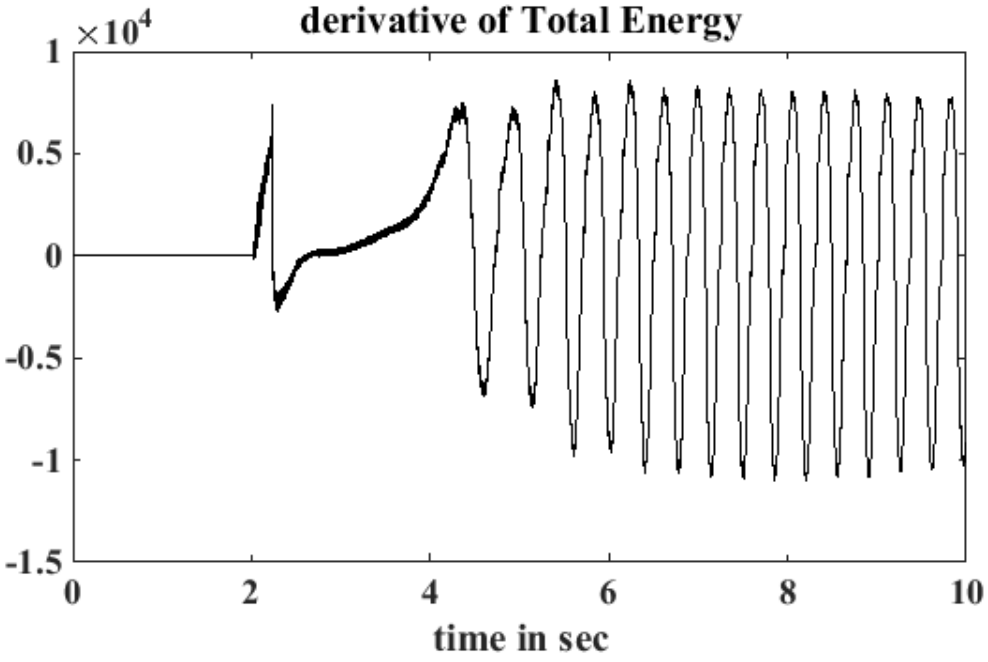

FIGURE 4.9: derivative of energy in case 2

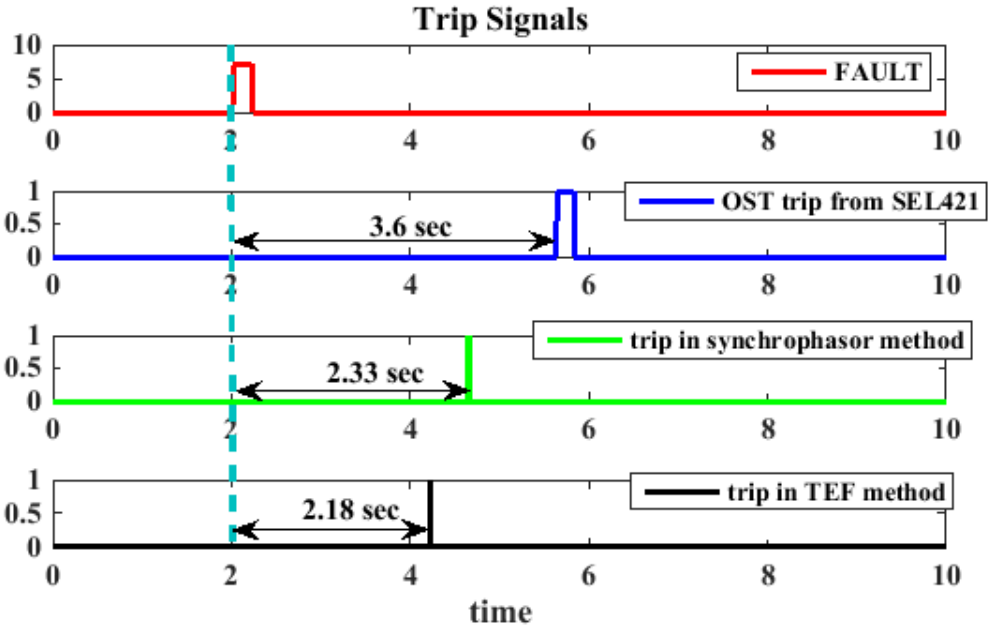

FIGURE 4.10: Trip signals in case 2

Case 3: Three phase fault on Bus-9 for 0.2 sec

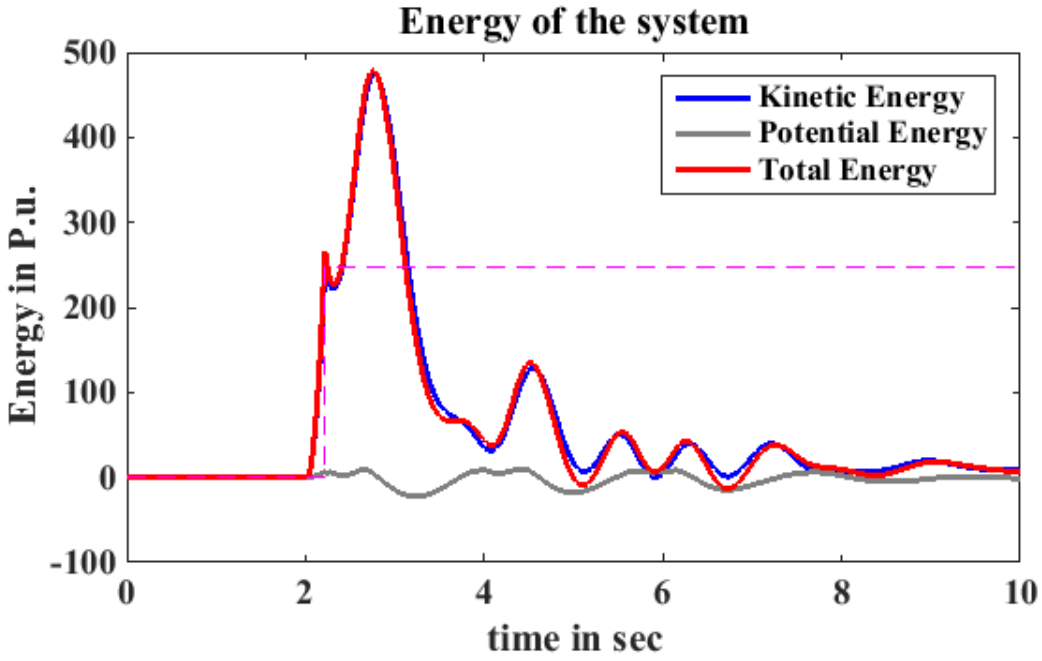

FIGURE 4.11: Energy curves in case 3

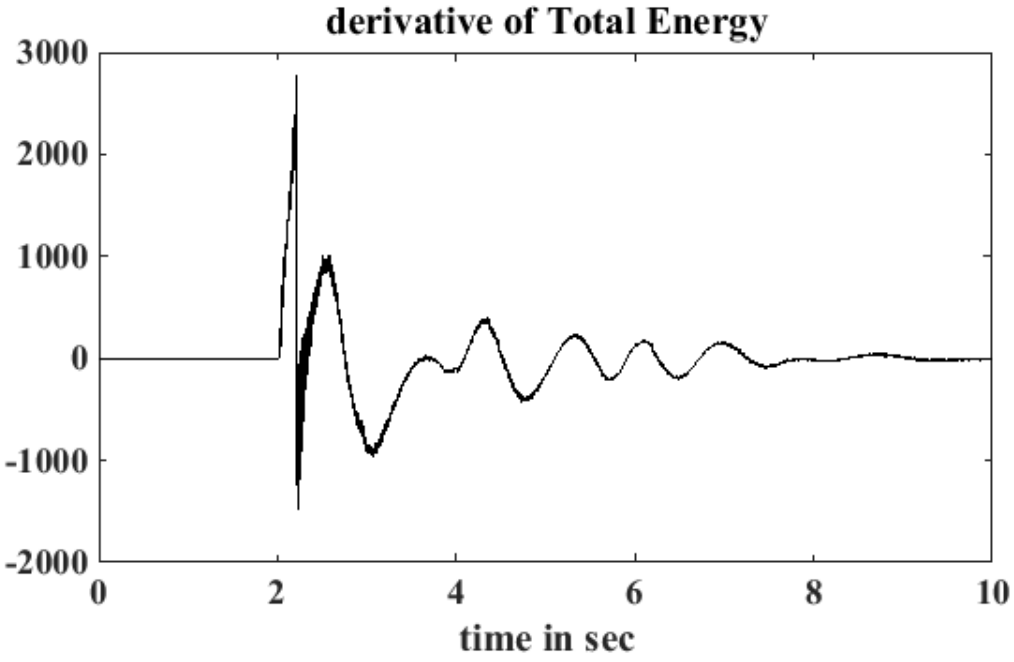

FIGURE 4.12: Derivative of energy in case 3

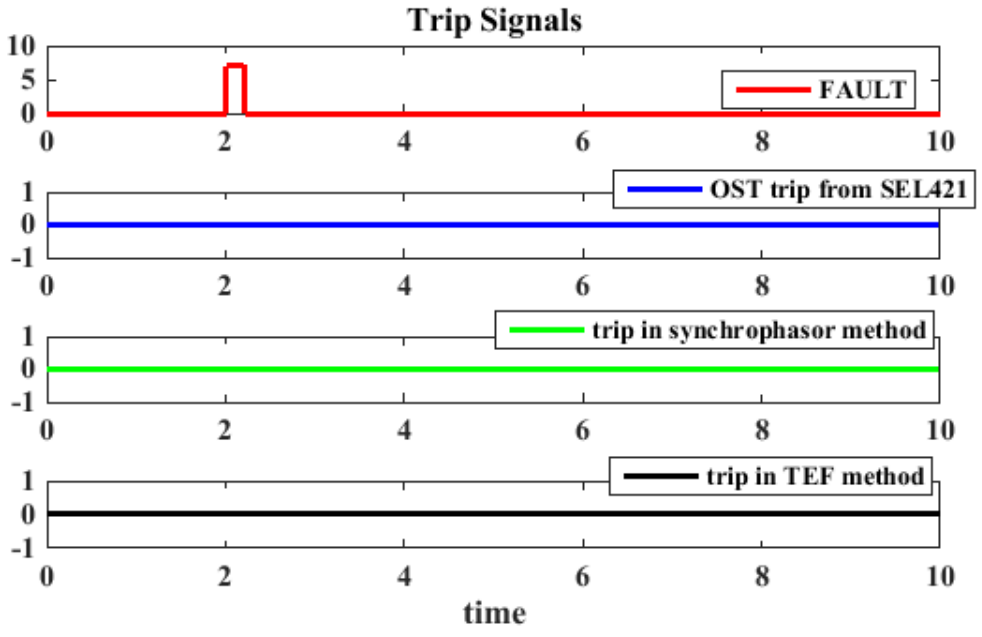

FIGURE 4.13: Trip signals in case 3

Case 4: Three phase fault on Bus-9 for 0.3 sec

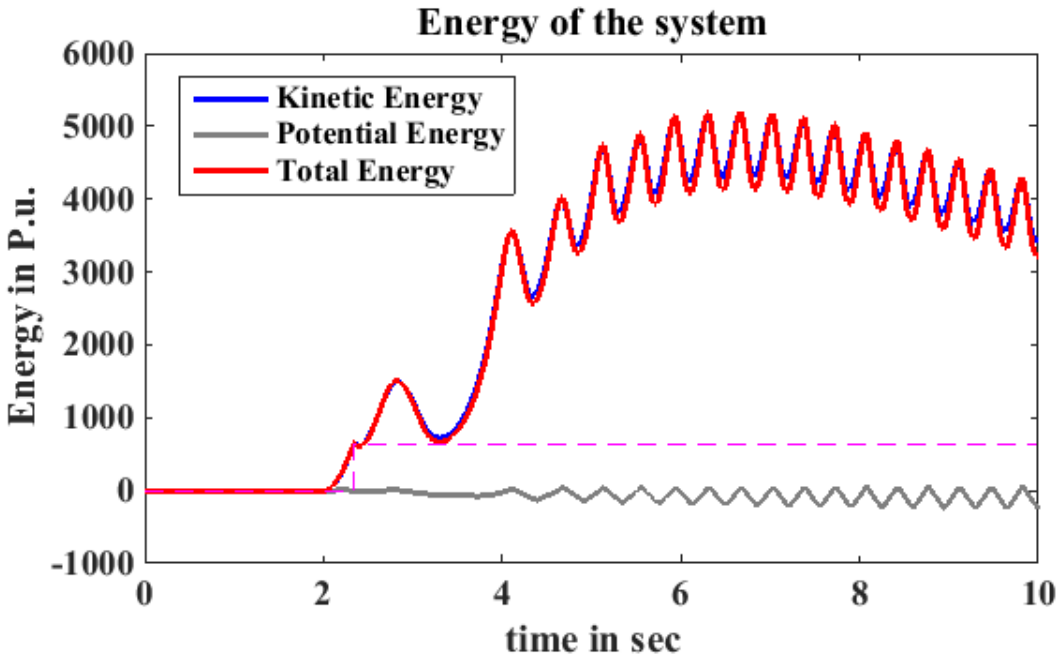

FIGURE 4.14: Energy curves in case 4

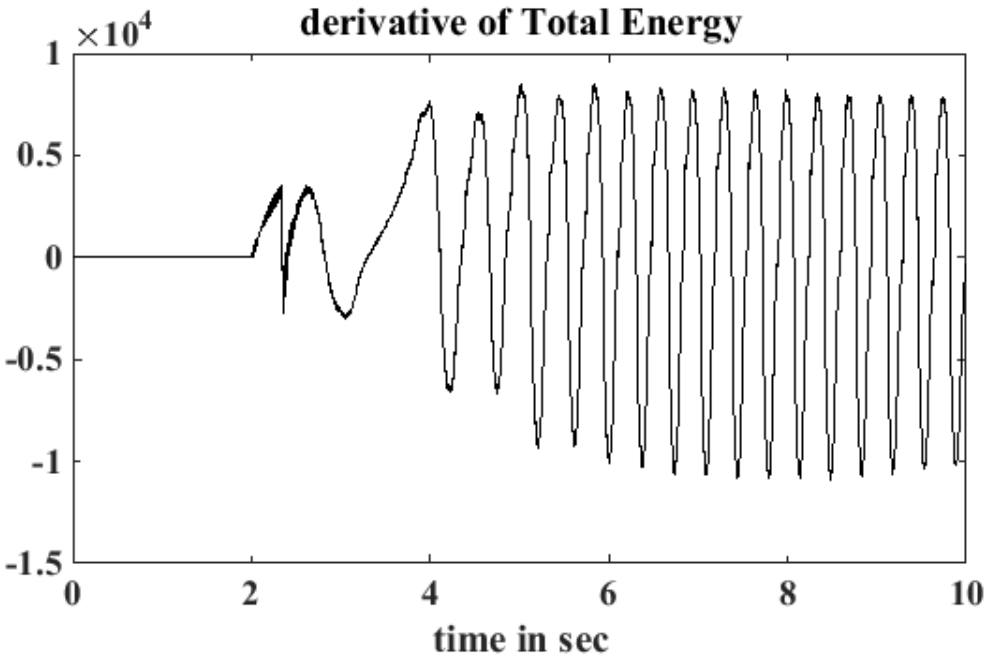

FIGURE 4.15: Derivative of energy in case 4

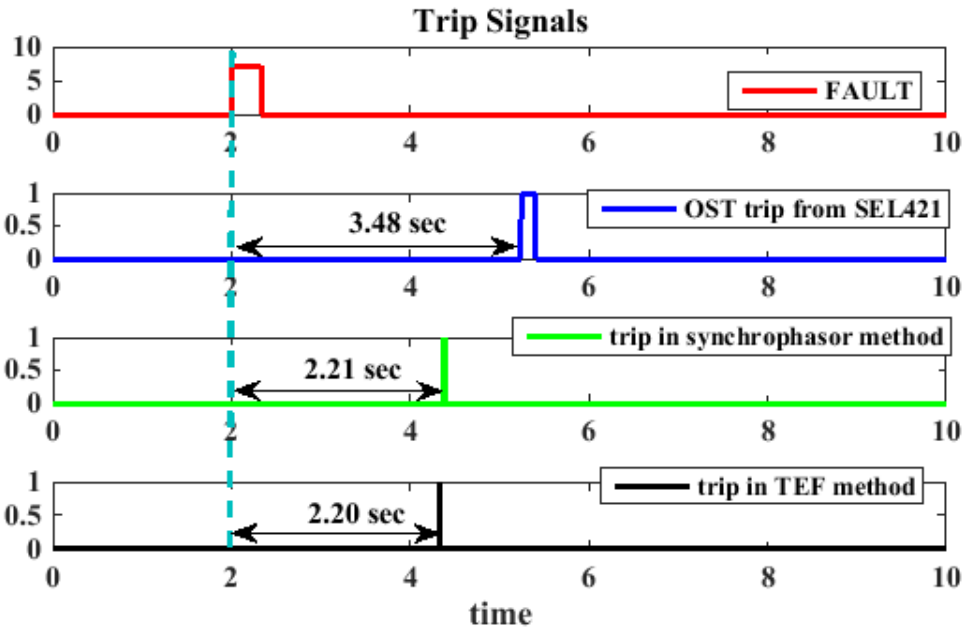

FIGURE 4.16: Trip signals in case 4

Case 5: Three phase fault in middle of tie line for 0.5 sec

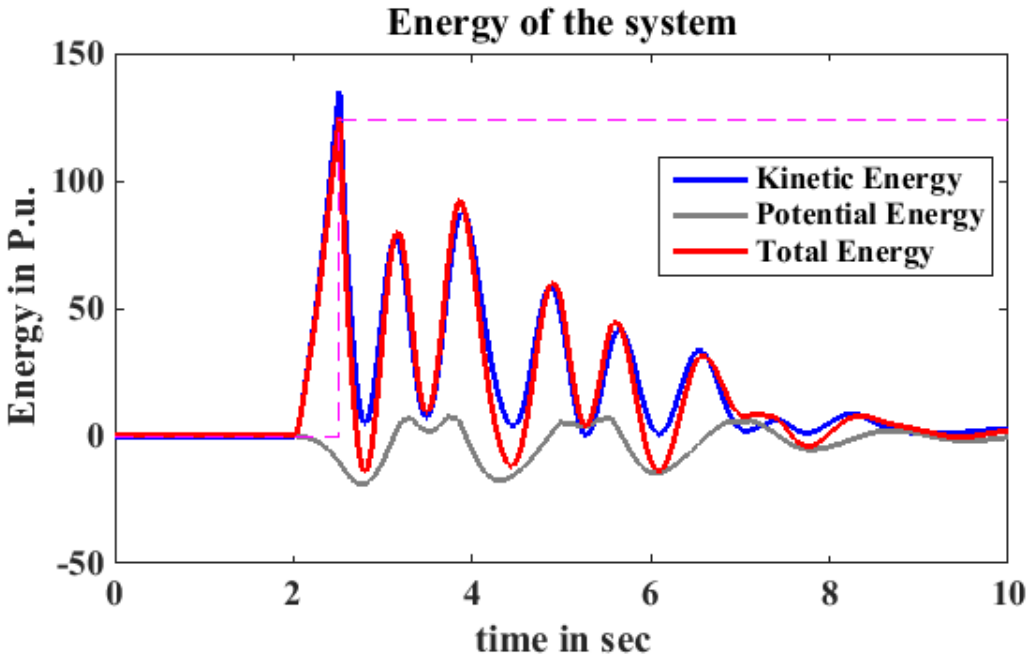

FIGURE 4.17: Energy curves in case 5

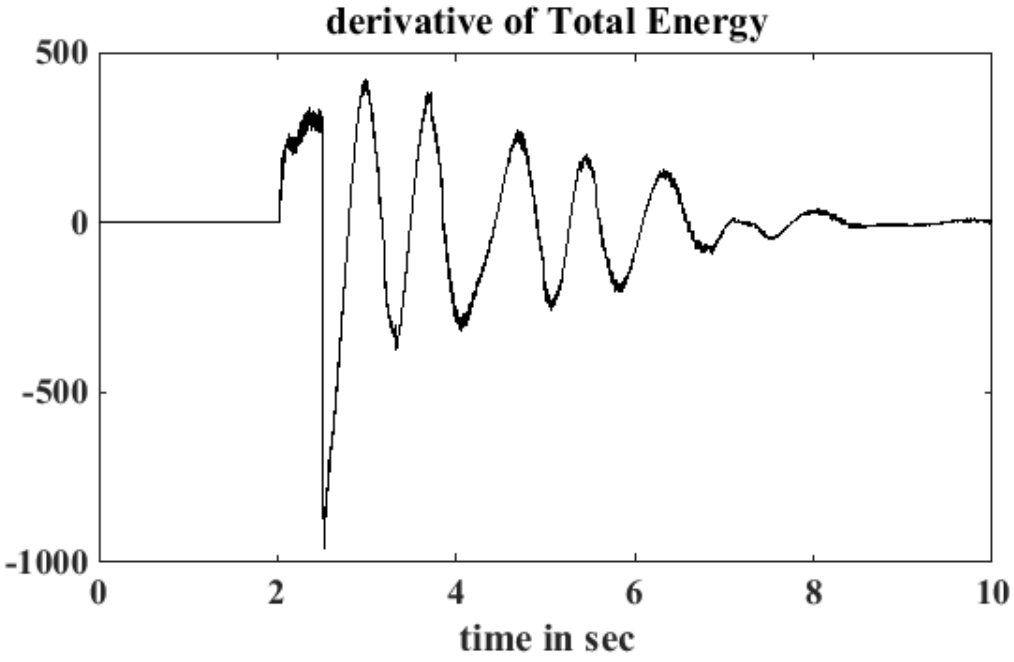

FIGURE 4.18: Derivative of energy in case 5

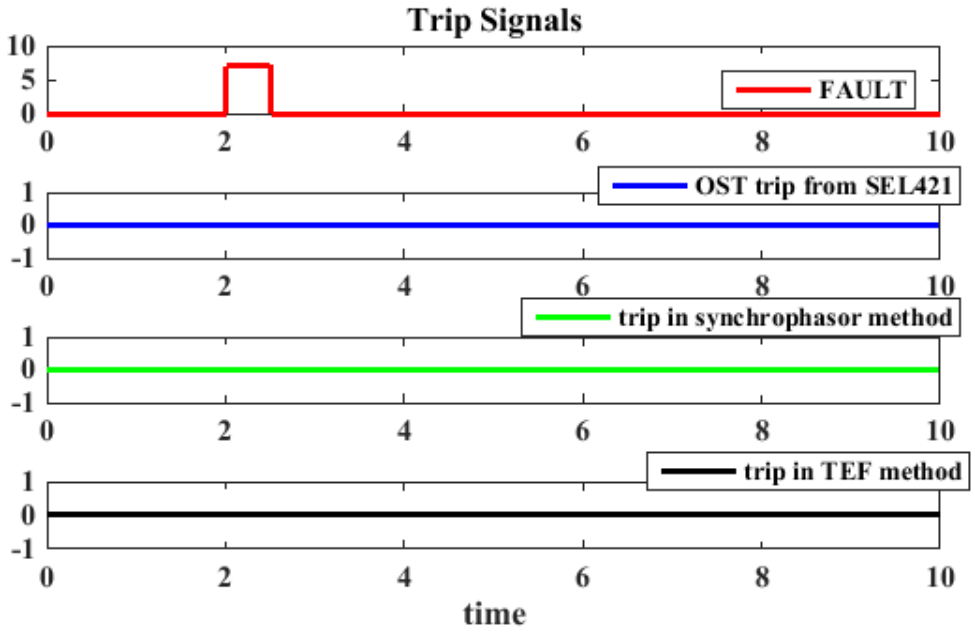

FIGURE 4.19: Trip signals in case 5

Case 6: Three phase fault in middle of tie line for 0.7 sec

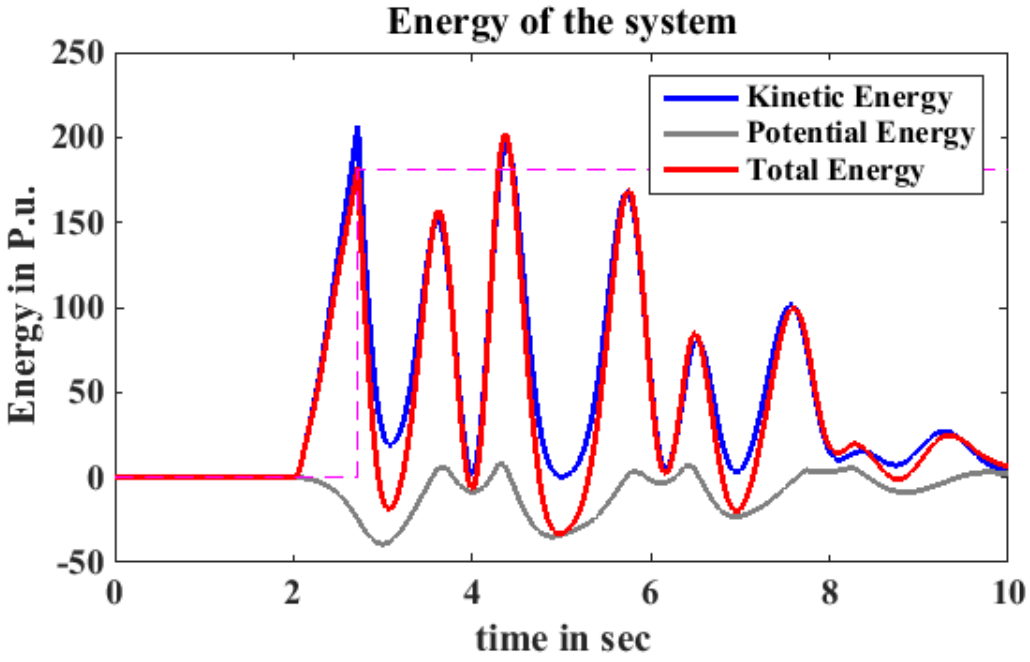

FIGURE 4.20: Energy curves in case 6

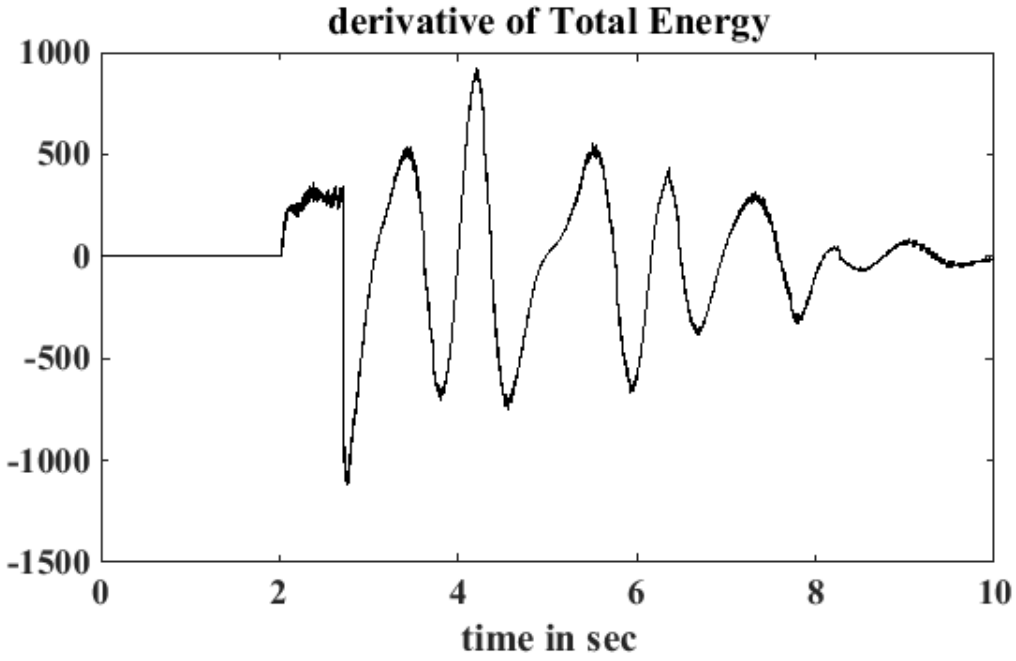

FIGURE 4.21: Derivative of energy in case 6

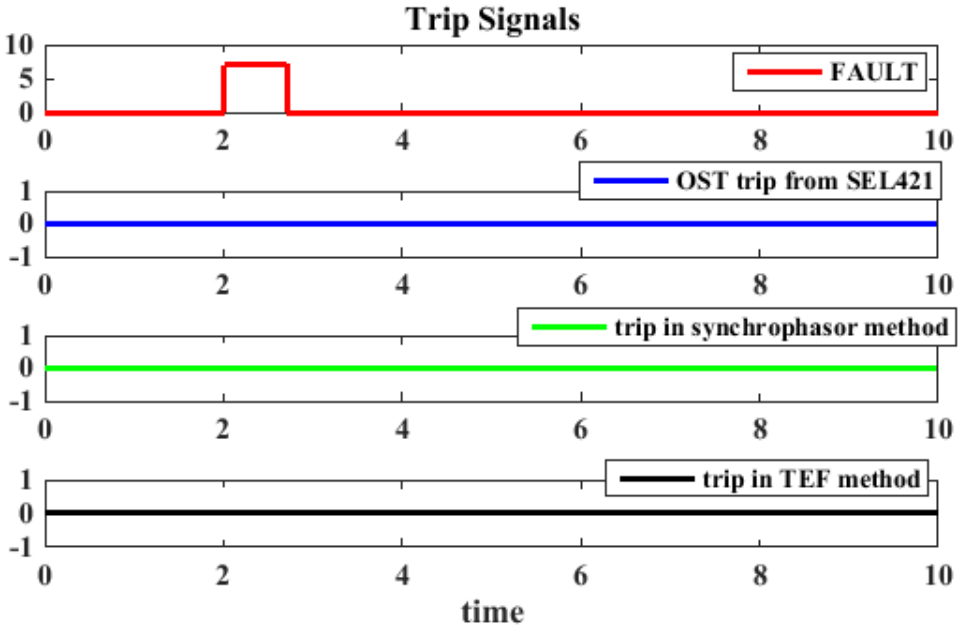

FIGURE 4.22: Trip signals in case 6

Case 7: Three phase fault in middle of tie line for 0.8 sec

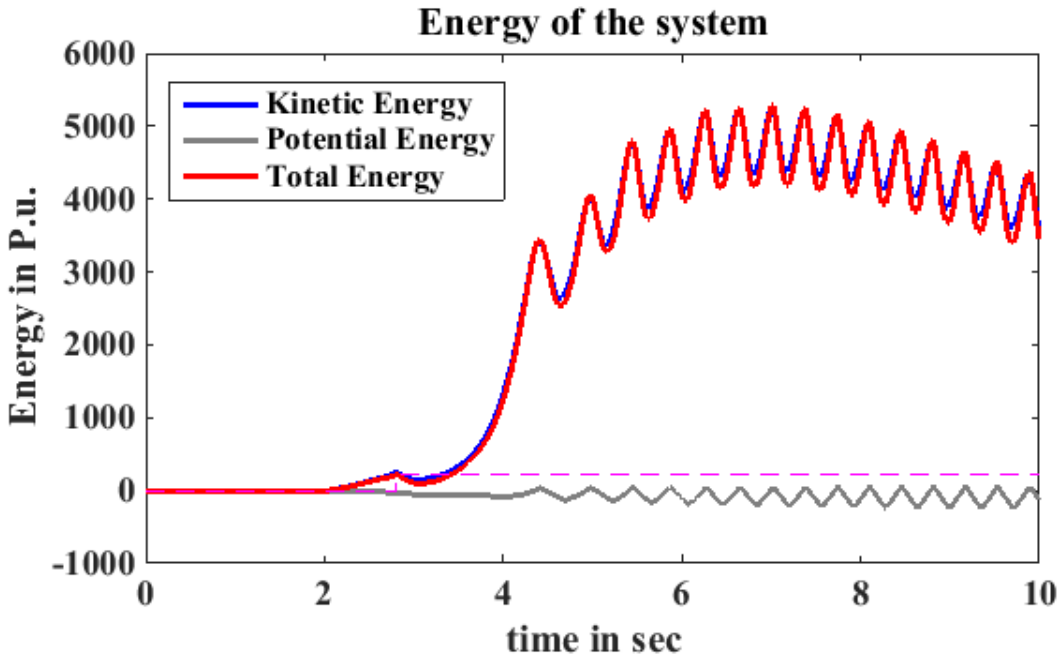

FIGURE 4.23: Energy curves in case 7

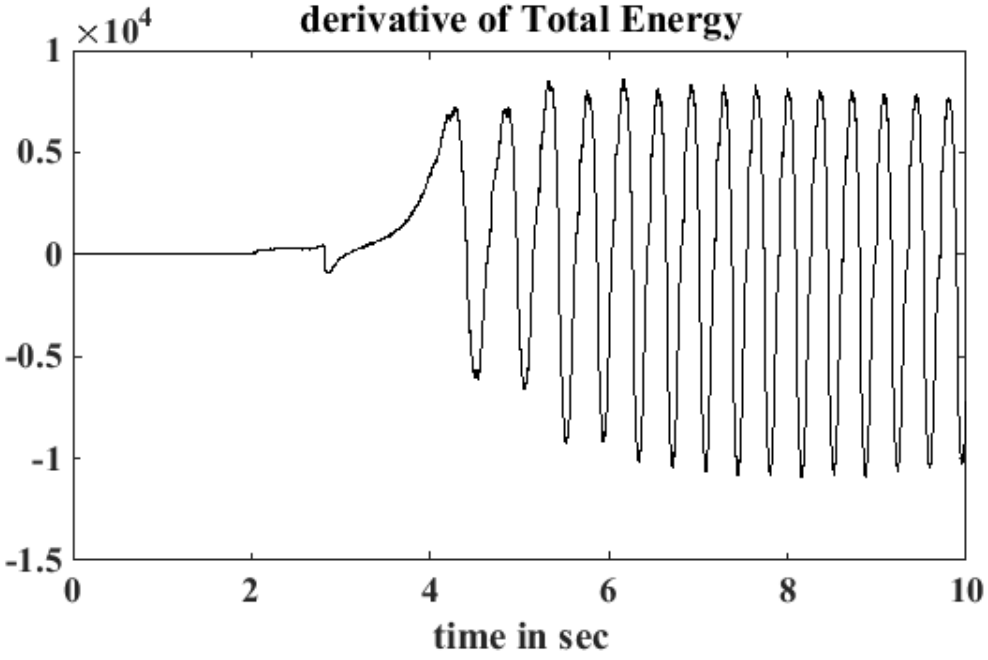

FIGURE 4.24: Derivative of energy in case 7

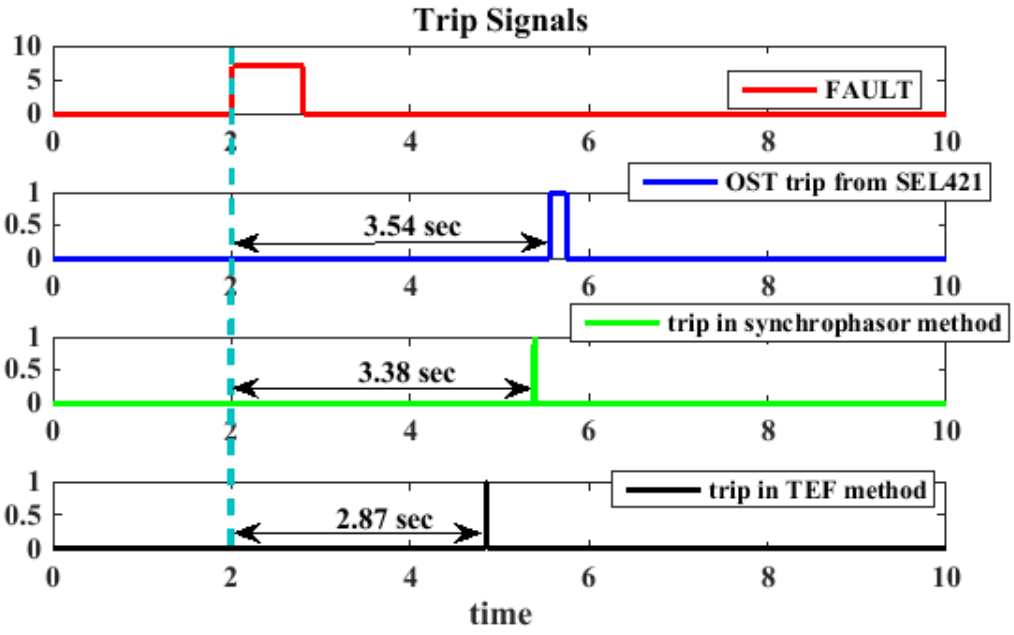

FIGURE 4.25: Trip signals in case 7

Table 4.1: Comparison of trip times –conventional methods vs transient energy based method

Case	Tripping Time (Seconds)		
	Dual Blinder Method	Synchrophasor method	TEF method
Case-1	No trip	No trip	No trip
Case-2	3.6	2.33	2.18
Case-3	No trip	No trip	No trip
Case-4	3.48	2.21	2.20
Case-5	No trip	No trip	No trip
Case-6	No trip	No trip	No trip
Case-7	3.54	3.38	2.87

4.4. Summary

In this chapter, a novel, energy based out-of-step protection scheme is described that is based on real time synchrophasor measurements provided by PMUs in the system. The total system transient energy is computed at each time step using the Transient energy function. An algorithm is identified to detect the unstable power swings and thereby to initiate the out-of-step protection signal. The proposed scheme is advantageous as it can detect the out-of-step conditions faster than the other conventional methods. This was proved by the simulation studies in Kundur two area system. The next chapter is dedicated

to the design of power system stabilizer and to study the impact of PSS on the performance of transient energy function based out-of-step protection scheme.

CHAPTER 5 : INTEGRATED OUT-OF-STEP PROTECTION WITH PSS

This chapter presents the methodology of power system stabilizer design using power system analysis toolbox (PSAT) Eigen value analysis. Section 5.1 discusses about the Heffron-Phillips model of the synchronous machine. Section 5.2 describes the power system stabilizer structure. Section 5.3 outlines the design of power system stabilizer in kundur two area test system. Section 5.5 is dedicated to the implementation of out-of-step protection in presence of PSS at all the generators in the test system.

5.1. Heffron Phillips Model of Synchronous Machine

A valid model for synchronous generator is essential for a reliable analysis of stability and dynamic performance. The Heffron Phillips model of a synchronous machine has been successfully used for investigating low frequency oscillations and designing power system stabilizers. This model is obtained by linearizing the third order non-linear model of synchronous machine around considered operating conditions. The block diagram with field circuit and AVR is shown in figure 5.1.

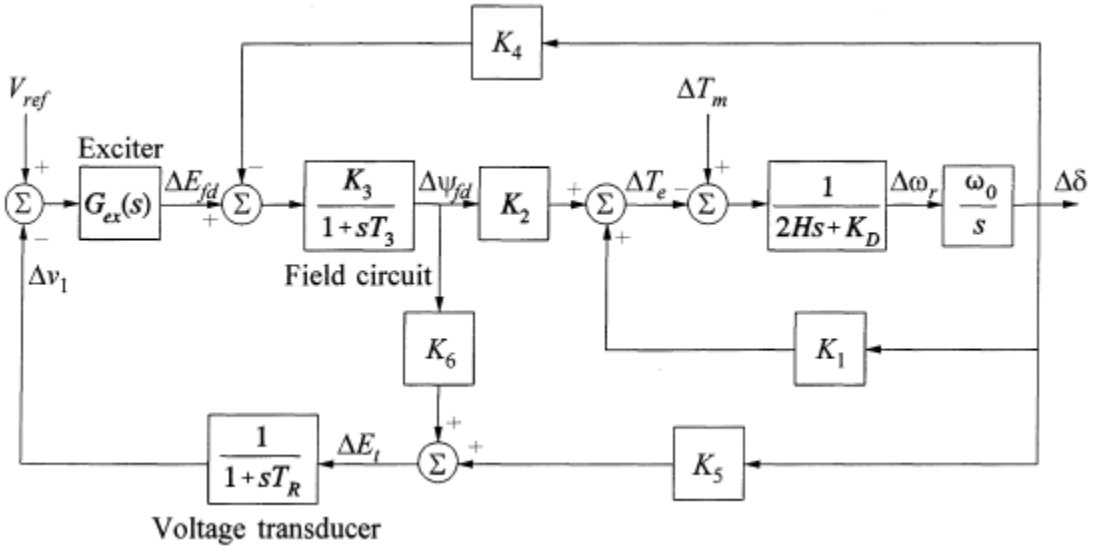

FIGURE 5.1: Heffron Phillips model of synchronous machine [1]

The complete state space model is given by equations

$$\begin{bmatrix} \Delta\dot{\omega}_r \\ \Delta\dot{\delta} \\ \Delta\dot{\psi}_{fd} \\ \Delta\dot{v}_1 \end{bmatrix} = \begin{bmatrix} a_{11} & a_{12} & a_{13} & 0 \\ a_{21} & 0 & 0 & 0 \\ 0 & a_{32} & a_{33} & a_{34} \\ 0 & a_{42} & a_{43} & a_{44} \end{bmatrix} \begin{bmatrix} \Delta\omega_r \\ \Delta\delta \\ \Delta\psi_{fd} \\ \Delta v_1 \end{bmatrix} + \begin{bmatrix} b_1 \\ 0 \\ 0 \\ 0 \end{bmatrix} \Delta T_m$$

Where $a_{11} = -\frac{K_D}{2H}$ (5.1)

$a_{12} = -\frac{K_1}{2H}$ (5.2)

$a_{13} = -\frac{K_2}{2H}$ (5.3)

$a_{21} = \omega_0 = 2\pi f_0$ (5.4)

$a_{32} = -\frac{\omega_0 R_{fd}}{L_{fd}} m_1 L'_{ads}$ (5.5)

$$a_{33} = -\frac{\omega_0 R_{fd}}{L_{fd}}\left[1 - \frac{L'_{ads}}{L_{fd}} + m_2 L'_{ads}\right] \qquad (5.6)$$

$$a_{34} = -\frac{\omega_0 R_{fd}}{L_{adu}} K_A \qquad (5.7)$$

$$a_{42} = \frac{K_5}{T_R} \qquad (5.8)$$

$$a_{43} = \frac{K_6}{T_R} \qquad (5.9)$$

$$a_{44} = -\frac{1}{T_R} \qquad (5.10)$$

The small signal stability can be analyzed by Eigen value analysis of the state matrix. In this thesis work, the state matrices of all the generators are obtained by PSAT Eigen Value analysis.

5.2. Power System Stabilizer

Power system stabilizer is a supplementary excitation controller used to damp the electromechanical oscillations thereby to improve the small signal stability and transient stability. The PSS can be designed in various structures such as [32]:

a) Lead-Lag Structure or conventional structure: The transfer function is in the form

$$u_{PSS} = K_{pss}\left(\frac{sT_w}{1+sT_w}\right)\left(\frac{1+sT_1}{1+sT_2}\right)y \qquad (5.11)$$

Or

$$u_{PSS} = K_{pss}\left(\frac{sT_w}{1+sT_w}\right)\left(\frac{1+sT_1}{1+sT_2}\right)\left(\frac{1+sT_3}{1+sT_4}\right)y \qquad (5.12)$$

Where y is the input signal.

b) Proportional-Integral-Derivative structure: The transfer function is in the form

$$u_{PSS} = \left(\frac{sT_w}{1+sT_w}\right)\left(K_P + \frac{K_I}{s} + K_D s\right) y \qquad (5.13)$$

c) Other structures based on adaptive, optimal, intelligent control, to name a few.

The common input signals used are speed, frequency, electric and accelerating power deviations [32].

FIGURE 5.2: Power system stabilizer structure

In the Heffron-Phillips model, to introduce damping torque component, the logical signal that can be used to control the excitation is $\Delta\omega_r$. The PSS transfer function should have appropriate compensation circuit to compensate for the phase lag between exciter input and electrical torque. The block diagram with power system stabilizer is shown in figure 5.3.

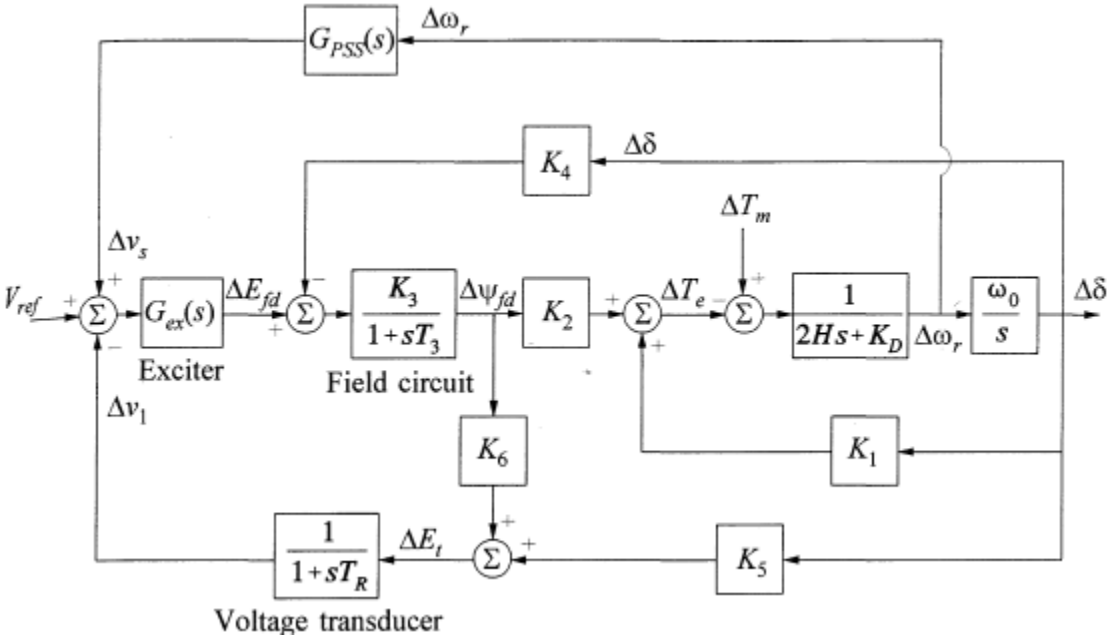

FIGURE 5.3: Heffron Phillips model including PSS [1]

5.3. PSS Design in Kundur Two Area System

The methodology of PSS design using Eigen value analysis is as follows.

Step 1: Run the Eigen value analysis on the test system over and equilibrium point and obtain the system state matrix (A).

Step 2: Obtain the inter area electro mechanical modes using participation factors. Calculate the damped frequency and natural frequency.

Step 3: Obtain the individual synchronous machine state matrices and approximate to the Heffron-Phillips model

Step 4: Calculate the K coefficients form the individual matrices using equations 5.1-5.10

Step 5: Calculate the phase lag in the voltage signal due to Exciter and AVR and the damping factor.

Step 6: Design the Lead-Lag compensator to compensate the phase lag and calculate the gain to introduce additional damping.

Step 7: Implement the designed PSS and perform Eigen value analysis again to confirm the inter area oscillations are damped or not.

In the present test system the Eigen value analysis is performed using MATLAB PSAT software. The plot of Eigen values with only AVR is shown figure.

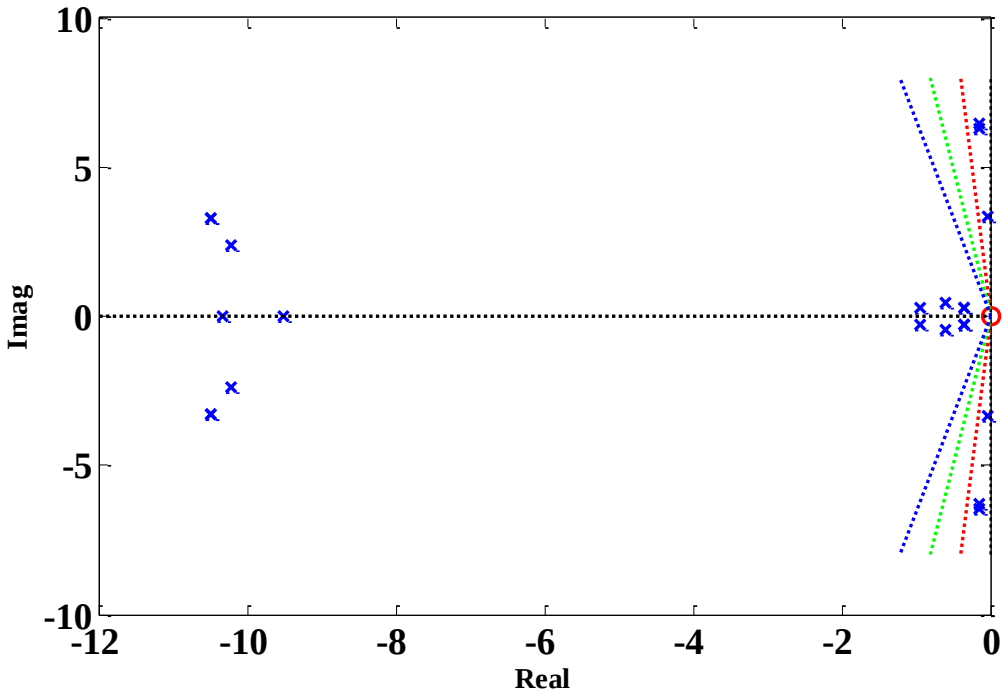

FIGURE 5.4: Eigen value plot for Kundur two area system with AVR only

Table 5.1: Eigen values with AVR only

Eigen Value	Most Associated States	Real part	Imaginary part	Damped frequency	Natural Frequency
1	vm_Exc_3	-1000	0	0	0
2	vm_Exc_2	-1000	0	0	0
3	vm_Exc_4	-1000	0	0	0
4	vm_Exc_1	-1000	0	0	0
5	vf_Exc_3	-10.3237	0	0	0
6	vf_Exc_3	-9.5047	0	0	0
7	vf_Exc_4, vr1_Exc_4	-10.4974	3.27734	0.521603641	1.750238
8	vf_Exc_4, vr1_Exc_4	-10.4974	-3.27734	0.521603641	1.750238
9	vf_Exc_1, vr1_Exc_1	-10.4914	3.26015	0.518867774	1.748519
10	vf_Exc_1, vr1_Exc_1	-10.4914	-3.26015	0.518867774	1.748519
11	vf_Exc_1, vf_Exc_2	-10.2224	2.38304	0.379271709	1.670568
12	vf_Exc_1, vf_Exc_2	-10.2224	-2.38304	0.379271709	1.670568

13	omega_Syn_1, delta_Syn_1	-0.15078	6.47257	1.030139101	1.030419
14	omega_Syn_1, delta_Syn_1	-0.15078	-6.47257	1.030139101	1.030419
15	omega_Syn_2, delta_Syn_2	-0.14835	6.29085	1.001217532	1.001496
16	omega_Syn_2, delta_Syn_2	-0.14835	-6.29085	1.001217532	1.001496
17	omega_Syn_4, delta_Syn_4	-0.02994	3.34651	0.532612363	0.532634
18	omega_Syn_4, delta_Syn_4	-0.02994	-3.34651	0.532612363	0.532634
19	e1q_Syn_2, vr2_Exc_2	-0.94248	0.26333	0.041910173	0.155745
20	e1q_Syn_2, vr2_Exc_2	-0.94248	-0.26333	0.041910173	0.155745
21	e1q_Syn_4, vr2_Exc_4	-0.59354	0.47704	0.075923097	0.121194
22	e1q_Syn_4, vr2_Exc_4	-0.59354	-0.47704	0.075923097	0.121194
23	e1q_Syn_1, vr2_Exc_3	-0.3538	0.3072	0.048892284	0.074573

24	e1q_Syn_1, vr2_Exc_3	-0.3538	-0.3072	0.048892284	0.074573
25	e1q_Syn_3, vr2_Exc_1	-0.36286	0.30982	0.049309269	0.075938
26	e1q_Syn_3, vr2_Exc_1	-0.36286	-0.30982	0.049309269	0.075938
27	delta_Syn_2	0	0	0	0
28	omega_Syn_2	0	0	0	0

From the Table 5.1, the Eigen values 17, 18 corresponds to the inter area electro mechanical oscillation modes. The natural frequency $f_n = 0.532634\ Hz$

$$\omega_n = 3.3466\ rad/sec$$

Damping Ratio $KD = 4 * H * \xi * \omega_n = 0.777$

The state matrix of generator 1 is obtained as

$$\begin{array}{c} \\ \Delta\omega \\ \Delta\delta \\ \Delta e1q \\ \Delta v_m \\ \Delta v_{r1} \\ \Delta v_{r2} \\ \Delta v_f \end{array} \begin{bmatrix} 0 & -0.074 & -0.102 & 0 & 0 & 0 & 0 \\ 376.99 & 0 & 0 & 0 & 0 & 0 & 0 \\ 0 & -0.143 & -0.289 & 0 & 0 & 0 & 0 \\ 0 & 73.841 & 150.877 & -1000 & 0 & 0 & 0 \\ 0 & 0 & 0 & -363.63 & -18.181 & -363.63 & -25.25 \\ 0 & 0 & 0 & 0 & 0 & -0.556 & -0.0386 \\ 0 & 0 & 0 & 0 & 2.778 & 0 & -2.8164 \end{bmatrix}$$

From Equations 5.1 to 5.10

The K values are calculated and tabulated in table

Table 5.2: Calculated K Values for the four generators

Value	Generator 1	Generator 2	Generator 3	Generator 4
K1	0.9649	0.8167	0.6062	0.7398
K2	1.3357	1.2257	1.0225	1.1538
K3	0.0361	0.0384	0.0376	0.0369
K4	13.6998	13.4931	13.9594	14.4020
K5	0.0738	0.01	-0.0541	-0.0242
K6	0.1509	0.687	0.0555	0.644
KD	0	0	0	0
T3	3.4594	3.2554	3.3234	3.3880

From the Heffron Phillips Model shown in figure 5.6, the transfer function of ΔT_e due to PSS with respect to Δv_s is given by

$$\frac{\Delta T_{pss}}{\Delta v_s} = \frac{(K2 * K3 * KA)}{sT3 + 1 + (K3 * K6 * KA)}$$

Substituting the all values at $s = j\omega_n = j3.3466$

$$\frac{\Delta T_{pss}}{\Delta v_s} = 0.0818\angle - 94.9658^0$$

If ΔT_{pss} has to be in phase with $\Delta\omega$, the $\Delta\omega$ signal should be processed through a phase-lead network, so that the signal advanced by 94.9658 degrees at frequency of oscillation 3.3466 rad/sec. The gain of the PSS depends on the required damping value.

In this test case, the angle to be compensated is more than 45 degrees. So we need two Lead-Lag structures in PSS. From the equation (3.34) let T2= T4 = 0.05, Tw =10

Then T1 and T3 can be calculated as T1 = T3 = 0.4598.

Let the required damping Kpss = 20.

The Lead-Lag structure of PSS for Generator 1 is $20 * \frac{10s}{1+10s} * \frac{1+0.4598s}{1+0.05s} * \frac{1+0.4598s}{1+0.05s}$

Similarly for Generator 2 PSS $20 * \frac{10s}{1+10s} * \frac{1+0.4386s}{1+0.05s} * \frac{1+0.4386s}{1+0.05s}$

For Generator 3 PSS $20 * \frac{10s}{1+10s} * \frac{1+0.4608s}{1+0.05s} * \frac{1+0.4608s}{1+0.05s}$

For Generator 4 PSS $20 * \frac{10s}{1+10s} * \frac{1+0.4433s}{1+0.05s} * \frac{1+0.4433s}{1+0.05s}$

After Implementing PSS in the system the plot Eigen value is

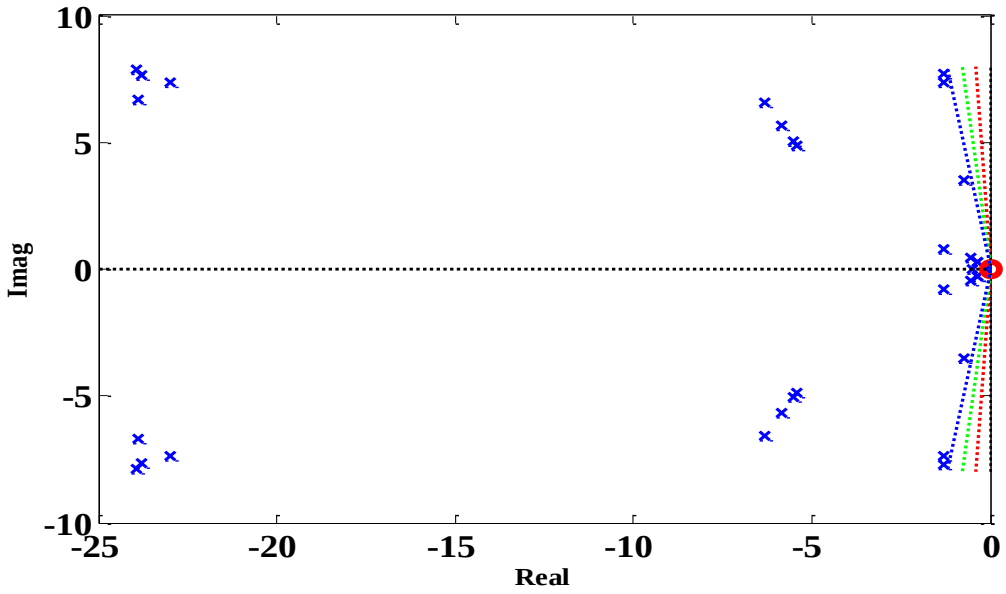

FIGURE 5.5: Eigen value plot for Kundur two area system with AVR and PSS

Table 5.3: Eigen values with AVR and PSS

Eigen Value	Most Associated States	Real part	Imaginary part	Damped frequency	Natural Frequency
1	vm_Exc_3	-1000	0	0	0
2	vm_Exc_2	-1000	0	0	0
3	vm_Exc_4	-1000	0	0	0
4	vm_Exc_1	-1000	0	0	0
5	v2_Pss_3, v3_Pss_3	-23.8667	6.66315	1.060471	3.943746161
6	v3_Pss_3, v2_Pss_3	-23.8667	-6.66315	1.060471	3.943746161
7	vr1_Exc_3, v3_Pss_3	-23.9143	7.84956	1.249293	4.005858698
8	vr1_Exc_3, v2_Pss_3	-23.9143	-7.84956	1.249293	4.005858698
9	vr1_Exc_2, v2_Pss_2	-23.7727	7.67011	1.220733	3.975588724
10	vr1_Exc_2, v2_Pss_2	-23.7727	-7.67011	1.220733	3.975588724
11	v3_Pss_3, v2_Pss_3	-22.9966	7.34056	1.168284	3.841946684

12	v2_Pss_3, v3_Pss_3	-22.9966	-7.34056	1.168284	3.841946684
13	omega_Syn_1, omega_Syn_4	-1.30528	7.72654	1.229714	1.247138064
14	omega_Syn_1, omega_Syn_4	-1.30528	-7.72654	1.229714	1.247138064
15	omega_Syn_2, delta_Syn_2	-1.28543	7.38297	1.175033	1.192710092
16	omega_Syn_2, delta_Syn_2	-1.28543	-7.38297	1.175033	1.192710092
17	vf_Exc_1, vf_Exc_3	-6.30671	6.60021	1.050454	1.452910938
18	vf_Exc_1, vf_Exc_3	-6.30671	-6.60021	1.050454	1.452910938
19	vf_Exc_4, vf_Exc_1	-5.84386	5.65494	0.90001	1.294241273
20	vf_Exc_4, vf_Exc_1	-5.84386	-5.65494	0.90001	1.294241273
21	vf_Exc_2, vf_Exc_1	-5.49616	5.03485	0.801319	1.186288777
22	vf_Exc_2, vf_Exc_1	-5.49616	-5.03485	0.801319	1.186288777

23	vf_Exc_3, v3_Pss_3	-5.43575	4.87874	0.776474	1.162476601
24	vf_Exc_3, v2_Pss_3	-5.43575	-4.87874	0.776474	1.162476601
25	omega_Syn_4, delta_Syn_4	-0.72638	3.4951	0.556261	0.568147309
26	omega_Syn_4, delta_Syn_4	-0.72638	-3.4951	0.556261	0.568147309
27	e1q_Syn_2, e1q_Syn_3	-1.3073	0.79343	0.126278	0.243384988
28	e1q_Syn_2, e1q_Syn_3	-1.3073	-0.79343	0.126278	0.243384988
29	e1q_Syn_4, vr2_Exc_4	-0.55766	0.47439	0.075501	0.116523598
30	e1q_Syn_4, vr2_Exc_4	-0.55766	-0.47439	0.075501	0.116523598
31	vr2_Exc_3	-0.48566	0	0	0
32	e1q_Syn_1, vr2_Exc_3	-0.34418	0.29507	0.046962	0.072152717
33	e1q_Syn_1, vr2_Exc_3	-0.34418	-0.29507	0.046962	0.072152717

34	e1q_Syn_3, vr2_Exc_1	-0.35316	0.2979	0.047412	0.073533269
35	e1q_Syn_3, vr2_Exc_1	-0.35316	-0.2979	0.047412	0.073533269
36	v1_Pss_4	-0.10165	0	0	0
37	v1_Pss_2	-0.10153	0	0	0
38	v1_Pss_4	-0.10132	0	0	0
39	delta_Syn_1	0	0	0	0
40	delta_Syn_1	0	0	0	0

From the Table 5.3, the Eigen values 25, 26 corresponds to the inter area electro mechanical oscillation modes. The natural frequency $f_n = 0.5681\ Hz$

$$\omega_n = 3.57\ rad/sec$$

Damping Ratio $KD = 4 * H * \xi * \omega_n = 18.56$

The damping increased due to the implementation of power system stabilizer. Now the simulation cases are re simulated in presence of PSS. The eigen values of the system before the simulation of fault are calculated using PSAT. And after the application of fault the eigen values are calculated using the machine speed signal data. These results are tabulated in Table 5.4.

Table 5.4: Eigen value comparison before and after the fault

State	Eigen values before fault		Eigen values after fault	
	without PSS	with PSS	without PSS	with PSS
W1	-0.151+6.47i	-1.305+7.727i	-0.3+0.46i	-1.3+0.43i
W2	-0.148+6.29i	-1.285+7.38i	-0.6+0.39i	-1.3+0.37i
W3	-0.029+3.34i	-0.729+3.48i	-0.5+0.47i	-1.0+0.46i
W4	-0.029+3.34i	-0.729+3.495i	-0.1+0.42i	-1.8+0.39i

5.4. Out-of-step Protection Integrated with PSS

The power system stabilizers are implemented with calculated parameters in all the machines in Kundur two area test system. The three simulation scenarios are re-simulated and the results are tabulated in table 5.5.

Table 5.5: Tripping time comparison in presence of PSS

Case	Description	Critical Clearing Time	Tripping Time (Seconds)		
			Dual Blinder Method	Synchro-phasor method	Energy based Method
Case-1	Three phase Fault on Bus 7 , cleared in 0.22 sec	0.25	No trip	No trip	No trip

Case-2	Three phase Fault on Bus 7, cleared in 0.25 sec	0.25	3.65	2.37	2.20
Case-3	Three phase Fault on Bus 9 , cleared in 0.3 sec	0.32	No trip	No trip	No trip
Case-4	Three phase Fault on Bus 9 , cleared in 0.32 sec	0.32	3.62	2.24	2.21
Case-5	Three phase Fault on middle of tie line2 , cleared in 0.8 sec	0.84	No trip	No trip	No trip
Case-6	Three phase Fault on middle of tie line2 , cleared in 0.84 sec	0.84	3.61	3.32	2.85

5.5. Summary

In this chapter, Heffron-Phillips model of synchronous machine with exciter and power system stabilizer was described. Then a methodology to design the power system stabilizer was presented using PSAT eigenvalue analysis. The PSS was incorporated in Kundur two area test system and the six scenarios were re-simulated. From the results it was observed that the critical clearing time in the presence of PSS is more than the cases without the PSS. This indicates that we get more time before the system goes out of step

and become unstable. This time can be used to implement necessary control actions like load shedding or generator tripping to restore the power system to another equilibrium point. The performance of out-of-step protection schemes is not affected in the presence of power system stabilizer.

CHAPTER 6 : CONCLUSIONS AND FUTURE WORKS

In this chapter, the conclusion and the potential future works are presented. Section 6.1 outlines the conclusions of the research work and Section 6.2 presents the potential future works.

6.1. Conclusions

From the present research work, the following conclusions can be drawn.

1. Synchrophasor based protection schemes are superior to the conventional schemes in terms of tripping times and their wide area orientation.
2. The proposed energy function based scheme takes the advantage of direct transient stability analysis methods by computing the overall energy of the system. As a result the out-of-step conditions are identified faster than the conventional methods.
3. Energy based approach can be expanded to the larger systems by aggregating them into equivalent two area system as the total energy computed remains the same.
4. Because of the real time stability assessment, adaptive protection techniques can be applied using the energy based approach.

6.2. Future Works

Following directions could be explored for future work.

1. Applications to the larger power systems by preserving the network structure.
2. Dynamic stability assessment in multiple contingency situations.
3. Impact of the Renewable energy sources on the out-of-step protection schemes.

BIBLIOGRAPHY

[1] Prabha Kundur. Power System Stability and Control. McGraw-Hill Inc, 1994.

[2] M. M. Adibi. Controlled Islanding in Power Systems, IRD Corp., 2002.

[3] J. M. Haner, T. D. Laughlin, C.W.Taylor "Experience with R-RDOT Out-of-Step Relay" IEEE Transactions on Power Systems, Vol. PWRD-1, No.2, April 1986.

[4] Mustafa A. Saad, Ahmed H. Eltom, Gary L. Kobet, Raga Ahmed "Performance Comparison between Dual-Blinder and Phasor-Based Out-of-Step Detection Functions Using Hardware-in-the Loop Simulation" Industry Applications Society Annual Meeting, 2015 IEEE.

[5] Virgilio Centeno, Jaime De La Ree, A.G. Phadke, Gary Michel, J. Murphy, and R. Burnett, "Adaptive Out-of-Step Relaying using Phasor Measurement Techniques".

[6] Divya Asija, Pallavi Choudekar, K. M. Soni, S. K. Sinha, "Power Flow Study and Contingency status of WSCC 9 Bus Test System using MATLAB", 2015 International Conference on Recent Developments in Control, Automation and Power Engineering (RDCAPE).

[7] Jonas Persson, "Kundur's Two Area System" SRI AB, July, 1996 and revised September, 2004.

[8] V. Centeno, A. G.Phadke, A. Edris, J. Benton, M. Gaudi, G. Michel, "An Adaptive Out-of-Step Relay", IEEE Transactions on Power Delivery, Vol. 12, No. 1, January 1997.

[9] Dawei Fan, Virgilio Centeno, "Adaptive Out-of-Step Protection Schemes Based On Synchrophasors",

[10] J. H. Chow, J. J. Sanchez-Gasca, "Pole-Placement Designs of Power System Stabilizers", IEEE Transactions on Power Systems, Vol No. 4, No. 1, February 1989.

[11] "Power Swing and Out-of-Step Considerations on Transmission Lines", IEEE PSRC WG D6, A report to the Power System Relaying Committee OF the IEEE Power Engineering Society.

[12] Norman Fischer, Gabriel Benmouyal, Daqing Hou, Demetrios Tziouvaras, John Byrne-Finley, and Brian Smyth, "Do System Impedances Really Affect Power Swings – Applying Power Swing Protection Elements Without Complex System Studies".presented at the 2012 Texas A&M Conference for Protective Relay Engineers.

[13] Evangelos Farantatos, Renke Huang, George J. Cokkinides, A. P. Meliopoulos, “A predictive Out of Step protection Scheme based on PMU enabled Dynamic state estimation”..

[14] C. W. Taylor, J. M. Haner, L. A. Hill, W. A. Mittelstadt, R. L. Cresap, “A New Out-of-Step Relay With Rate of Change of Apparent Resistance Augmentation”, IEEE Transactions on Power Apparatus and Systems, Vol. PAS-102, No . 3, March 1983.

[15] Michael J. Thompson, Amit Somani, “A Tutorial on Calculating Source Impedance Ratios for Determining Line Length”, http://dx.doi.org/10.119/CPRE.2015.7102207.

[16] Joe Mooney, P. E. and Normann Fischer, “Application Guidelines for Power Swing Detection on Transmission Systems”, presented at WPRC 2005 and Power System Conference 2006.

[17] Daqing Hou, Shaojun Chen, Steve Turner, “SEL-321-5 Relay Out-of-Step Logic”, Application Guide, Volume 1, AG97-13.

[18] Jinyu Xiao, Xiaorong Xie, Yingduo Han, Jingtao Wu, “Dynamic Tracking of Low Frequency Oscillations with Improved Prony Method in Wide-Area Measurement System”.

[19] Miroslav Begovic, Damir Novosel, and Mile ilisavljevic, “Trends in Power System Protection and Control”, Proceedings of 32nd Hawaii International Conference on System Sciences - 1999.

[20] Ian Hiskens, “IEEE PES Task Force on Benchmark Systems for Stability Controls”, IEEE 10-generator, 39 bus system, November 19, 2013.

[21] D S Ouellette, W J Geisbrecht, R P Wierckx, P A Forsyth, “Modelling an Impedance Relay Using a Real Time Digital Simulator”, RTDS Technologies Inc., Canada.

[22] Sukumar M. Brahma, Adly A. Girgis, “Fault Location on a Transmission Line Using Synchronized Voltage Measurements”, IEEE Transactions on Power Deliver, Vol. 19, NO. 4, October 2004.

[23] Srinu Babu, Matta, Seethlekshmi. K., “Out of Step Detection Using Wide Area Measurements”, 2013 colloquium, November 13-15, 2013, Mysore – Karnataka, India.

[24] Chenfeng Zhang, Vamsi K Vijapurapu, Anurag K Srivastava, Noel N. Schulz, Jimena Bastos, Rudi Wierckx, "Hardware-in-the-Loop Simulation of Distance Relay Using RTDS", SCSC 2007, ISBN # 1-56555-316-0

[25] Gurunath Gurrala, Indraneel Sen, "Power System Stabilizers Design for Interconnected Power Systems", IEEE Transactions on Power Systems, Vol. 25, No. 2, May 2010.

[26] Ali Reza Sobbouhi and Mohammad Reza Aghamohammadi, "A new algorithm for predicting out-of-step condition in large-scale power systems using rotor speed-acceleration", Int. Trans. Electr. Energ. Syst. 2016; 26:486-508.

[27] J. Krata, P. Balcerek, Z. Gajic, "The new Frequency Difference based Out of Step protection for Multiterminal Transmission System", Conference paper –January 2014, DOI:10.1049/cp.2014.0055.

[28] Ching-Shan Chen, Chih-Wen Liu, and Joe-Air Jiang, "A New Adaptive PMU Based Protection Scheme for Transposed / Untransposed Parallel Transmission Lines", IEEE Transactions on Power Delivery, Vol. 17, No. 2, April 2002.

[29] Jie Yan, Chen-Ching Liu, Umesh Vaidya, "PMU-Based Monitoring of Rotor Angle Dynamics", IEEE Transactions on Power Systems, Vol. 26, No. 4, November 2011.

[30] H. Hashim, I. Z. Abidin, H. A. A. Rashid, N. Z. Zulkapli, S. H. Ibrahim, Sheik Kamar, Nik Sofizan, "An Out-of-Step Detection Based on Stability Index", Australian Journal of Basic and Applied Sciences, 7(4): 353-365, 203 ; ISSN 1991-8178.

[31] Demetrios A. Tziouvaras, Daqing Hou, "Out-of-Step Protection Fundamentals and Advancements", 30th Annual Western Protective Relay Conference, Spokane, Washington, October 21-23, 2003.

[32] Ahmed A. Ba-muqabel, Dr. Mohammad A. Abido, "Review of Conventional Power System Stabilizer Methods".

[33] Joe-Air Jiang, Ching-shan Chen, "A Novel Adaptive PMU-Based Transmission-Lone Relay – Design and EMTP Simulation Results", IEEE Transactions on Power Delivery, Vol. 17, No. 4, October 2002.

[34] Fan Chunju, Li Shenfang, Yu Weiyong, K. K. Li, "Study on Adaptive Relay Protection Scheme Based on Phasor Measurement Unit (PMU)" ©2004 The institution of Electrical Engineers.

[35] Yuan-Yih Hsu, Chung-Yu Hsu, “A proportional-Integral Power System Stabilizer”, IEEE Transactions on Power Systems, Vol. PWRS-1, No. 2, May 1986.

[36] Ali Feliachi, Xiaofan Zhang, Craig S. Sims, “Power System Stabilizers Design Using Optimal Reduced Order Models Part1: Model Reduction”, IEEE Transactions on Power Systems, Vol. 3, No. 4, November 1988.

[37] Ali Feliachi, Xiaofan Zhang, Craig S. Sims, “Power System Stabilizers Design Using Optimal Reduced Order Models Part2: Design”, IEEE Transactions on Power Systems, Vol. 3, No. 4, November 1988.

[38] M. A. Abido, “Optimal Design of Power-System Stabilizers Using Particle Swarm Optimization”, IEEE Transactions on Energy Conversion, Vol. 17, No. 3, September 2002.

[39] Yuan-Yih Hsu, Chern-Lin Chen, “Identification of optimum location for stabilizer appliations using participation factors”, IEE Proceedings, Vol. 134, Pt. C, No. 3, May 1987.

[40] Y. Zhang, G. P. Chen O. P. Malik, G. S. Hope, “An Artificial Neural network Based Adaptive Power System Stabilizer”, IEEE Transactions on Energy Conversion, Vol. 8, No. 1, March 1993.

[41] Arthur R. Bergen and Vijay Vittal. Power System Analysis. 2nd Edition, Prentice Hall, 2000.

[42] J. Machowski, J.W. Bialek, S.Robak, J.R. Bumby, “Excitation control system for use with synchronous generators,” IEE Proc.- Gener. Transm. Distrib., Vol. 145, No. 5, September 1998.

[43] Jerkovic, Vedrana; Miklosevic, Kresimir; Spoljaric Zeljko, “Excitation System Models of Synchronous Generator”.

[44] Schweitzer Engineering Laboratories, “Instruction Manual SEL-421-4, -5 Relay Protection and Automation System”.

[45] C. R. Mason, “The Art and Science of Protective Relaying”, John Wiley & Sons, New York, 1956.

[46] Mania Pavella, Damien Ernst, and Daniel Ruiz-Vega, “Transient Stability of Power Systems: A Unified Approach to Assessment and Control”, Kluwer's Power Electronics and Power Systems Series.

[47] Magnusson, P.C., “Transient Energy Method of Calculating Stability,” AIEE Trans., Vol. 66, pp. 747-755, 1947.

[48] Da-Zhong Fang, Chung, T.S., Yao Zhang, Wennan Song, "Transient Stability Limit Conditions Analysis Using a Corrected Transient Energy Function Approach," Power Systems, IEEE Transactions on, vol.15, no.2, pp.804-810, May 2000.

[49] Ravi Shankar Buyyanapragada, “An investigation towards structure preserving transient stability analysis using energy functions”, thesis submitted to the faculty of university of North Carolina at charlotte 2015.

[50] Evangelos Farantatos, “A predictive out-of-step protection scheme based on PMU enabled distributed dynamic state estimation”, dissertation presented to the faculty of Georgia Institute of Technology 2012.

APPENDIX A : MATLAB CODES

PSS deign Code:

```
%after running eigen analysis in PSAT
fm_abcd;
% clc;
A_MAT=LA.a;
GEN1_A=A_MAT([2 1 3 13:16],[2 1 3 13:16]);
num2str(GEN1_A)
GEN2_A=A_MAT([5 4 6 17:20],[5 4 6 17:20]);
GEN3_A=A_MAT([8 7 9 21:24],[8 7 9 21:24]);
GEN4_A=A_MAT([11 10 12 25:28],[11 10 12 25:28]);
H1=6.5;
H2=6.5;
H3=6.125;
H4=6.125;

[PSS_T1,PSS_T2,phaselead ]=PSS_DESIGN(GEN1_A,H1)
[PSS_T1,PSS_T2,phaselead ]=PSS_DESIGN(GEN2_A,H2)
[PSS_T1,PSS_T2,phaselead ]=PSS_DESIGN(GEN3_A,H3)
[PSS_T1,PSS_T2,phaselead ]=PSS_DESIGN(GEN4_A,H4)

function [ PSS_T1,PSS_T2,phaselead ] = PSS_DESIGN(GEN1_A,H)
%PSS Design
Kd=-GEN1_A(1,1)*2*H;
K1=-GEN1_A(1,2)*2*H;
K2=-GEN1_A(1,3)*2*H;
T3=-(1/GEN1_A(3,3));
K5=-GEN1_A(4,2)/GEN1_A(4,4);
K6=-GEN1_A(4,3)/GEN1_A(4,4);
Td0=8;
K3=-(1/Td0*GEN1_A(3,3));
K34=GEN1_A(3,2)/GEN1_A(3,3);
K4=K34/K3;
KA=20;
TA=0.055;
num=K2*K3*KA;
den=[(T3*TA) (T3+TA) (1+(K3*KA*K6))];
TransTeVpss=tf(num,den);
mode=-0.15078+6.47257i;
mode_naturalfreq=abs(mode);

value=evalfr(TransTeVpss,mode_naturalfreq*1i);

phaselead=-angle(value)*(180/pi);
PSS_T2=0.05;
temp=-(angle(value)/2)+atan(mode_naturalfreq*PSS_T2);
PSS_T1=tan(temp)/mode_naturalfreq;


End
```

APPENDIX B: LOGICS IN RSCAD

Total Transient Energy Calculation logic in RTDS :

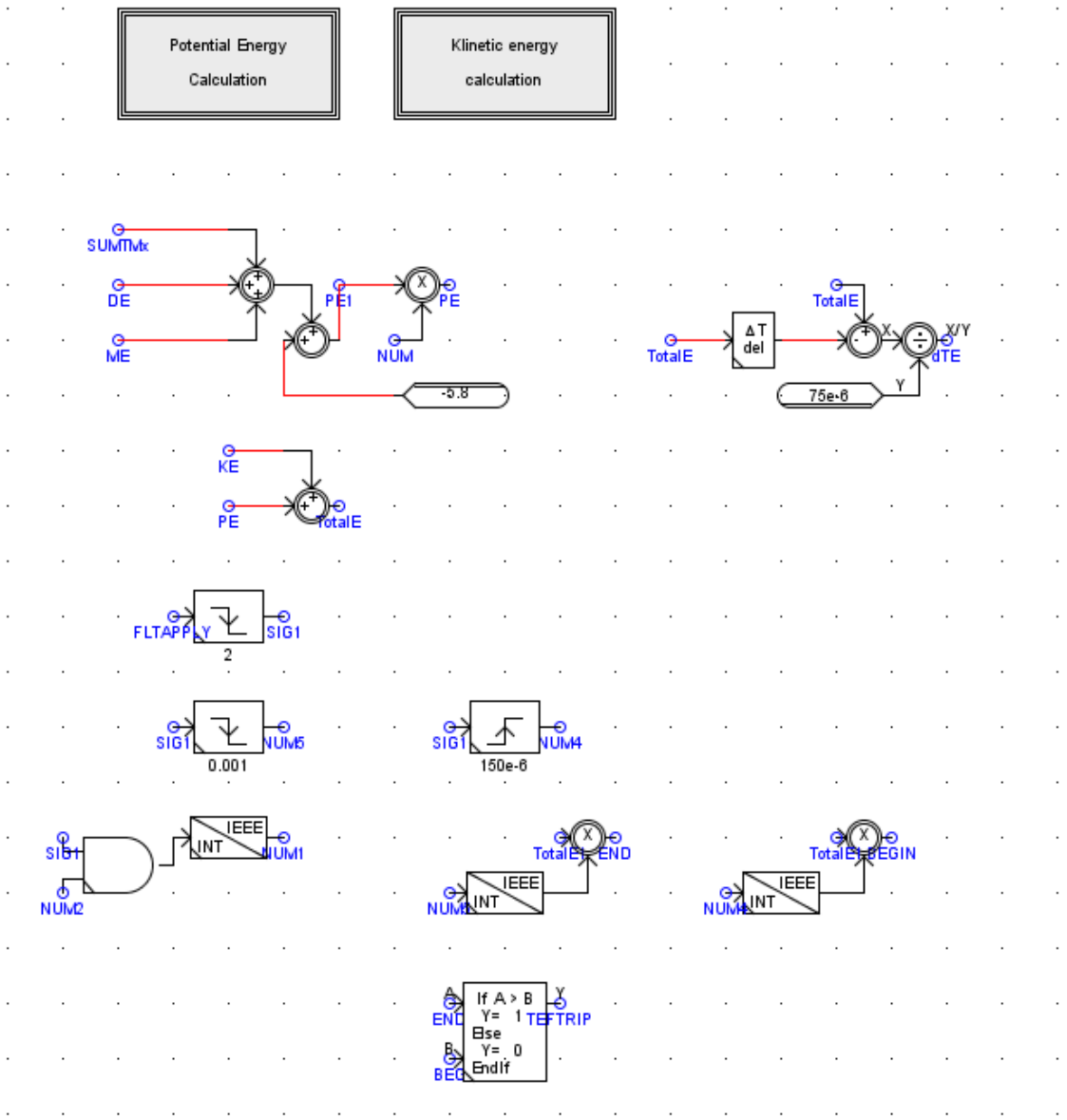

Potential Energy Calculation logic in RTDS-RSCAD:

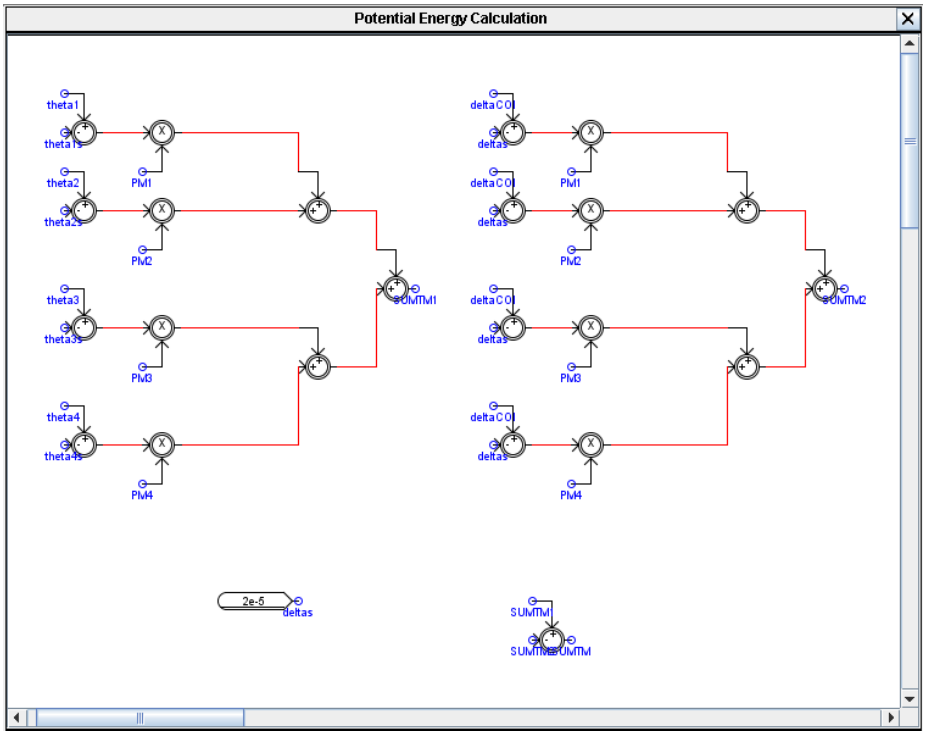

Kinetic Energy Calculation logic in RTDS-RSCAD: